Technical Report Documentation Page

1. Report No. FHWA/TX-05/0-4185-3	2. Government Accession No.	3. Recipient's Catalog No.
4. Title and Subtitle PERFORMANCE ASSESSMENT BY USING NONDESTRUCTIVE TESTING		5. Report Date June 2003 Rev. February 2004 Second Rev. August 2005 Third Rev. February 2006
		6. Performing Organization Code
7. Author(s) Yetkin Yildirim, Mehmet Sait Culfik, Jeffrey Lee, Andre Smit, Kenneth H. Stokoe II		8. Performing Organization Report No. 0-4185-3
9. Performing Organization Name and Address Center for Transportation Research The University of Texas at Austin 3208 Red River, Suite 200 Austin, TX 78705-2650		10. Work Unit No. (TRAIS)
		11. Contract or Grant No. 0-4185
12. Sponsoring Agency Name and Address Texas Department of Transportation Research and Technology Implementation Office P.O. Box 5080 Austin, TX 78763-5080		13. Type of Report and Period Covered Technical Report
		14. Sponsoring Agency Code

15. Supplementary Notes
Project performed in cooperation with the Texas Department of Transportation and the Federal Highway Administration.

16. Abstract
This project was conducted to determine the correlation of field performance to Hamburg Wheel Tracking Device (HWTD) testing results. HWTD measures the combined effects of rutting and moisture damage by rolling a steel wheel across the surface of an asphalt concrete specimen that is immersed in hot water. The test results from this laboratory equipment have been promising in regard to evaluating the moisture susceptibility of hot mix asphalt mixtures. While there is some information on the relationship between the laboratory results from this test and the field performance, it is quite limited. This 5-year research project will be an important step in validating the test and ensuring that the test results could be reliably used to predict performance. Three designs (Superpave, CMHB-C, and Type C) and three aggregate sources (siliceous gravel, sandstone, and quartzite) were used for this study. The test sections including nine different mixture designs were constructed on IH-20 in Harrison County to observe the performance of the overlays under real traffic conditions. Field performance will be observed through visual pavement condition surveys and nondestructive tests for four years. This research report summarizes the nondestructive test results and visual pavement condition surveys in the third year of this study.

17. Key Words Hamburg Wheel Tracking Device (HWDT), Pavement Performance, Nondestructive Testing	18. Distribution Statement No restrictions. This document is available to the public through the National Technical Information Service, Springfield, Virginia 22161. www.ntis.gov

19. Security Classif. (of report) Unclassified	20. Security Classif. (of this page) Unclassified	21. No. of pages 138	22. Price

Form DOT F 1700.7 (8-72) Reproduction of completed page authorized

PERFORMANCE ASSESSMENT BY USING NONDESTRUCTIVE TESTING RESULTS

Yetkin Yildirim
Mehmet Sait Culfik
Jeffrey Lee
Andre Smit
Kenneth H. Stokoe II

CTR Research Report: 0-4185-3
Report Date: June 2003, Revised February 2004, Second Revision August 2005, Third Revision 2006
Research Project: 0-4185
Research Project Title: *Correlation of Field Performance to Hamburg Wheel Tracking Results*
Sponsoring Agency: Texas Department of Transportation
Performing Agency: Center for Transportation Research at The University of Texas at Austin

Disclaimers

The contents of this report reflect the views of the authors, who are responsible for the facts and the accuracy of the data presented herein. The contents do not necessarily reflect the official views or policies of the Texas Department of Transportation (TxDOT) or the Federal Highway Administration. This report does not constitute a standard, specification, or regulation.

There was no invention or discovery conceived or first actually reduced to practice in the course of or under this contract, including any art, method, process, machine, manufacture, design or composition of matter, or any new and useful improvement thereof, or any variety of plant, which is or may be patentable under the patent laws of the United States of America or any foreign country.

NOT INTENDED FOR CONSTRUCTION, BIDDING, OR PERMIT PURPOSES
Yetkin Yildirim, P.E. (Texas No. 92787)
Kenneth H. Stokoe II P.E. (Texas No. 49095)
Research Supervisors

Preface

This is the third report from the Center for Transportation Research (CTR) on Project 0-4185. To evaluate the laboratory-field correlation for the Hamburg Wheel Tracking Device (HWTD), nine test sections are being constructed on IH-20 in Harrison County. This research includes monitoring the construction of these test sections, collection of construction data, performance data through a 5-year period, performance of laboratory tests using the HWTD, and analysis of the collected information. This report presents the results and findings of the information collected from the test sections for the third year of a 5-year project.

Acknowledgments

This project has been initiated and sponsored by the Texas Department of Transportation (TxDOT). The financial support of TxDOT is greatly appreciated. The authors would like to thank TxDOT Project Director Miles Garrison for his guidance. Special thanks are extended to Richard Izzo and Dale Rand of TxDOT for their great assistance in conducting the laboratory tests. The assistance of the Atlanta District personnel is greatly appreciated. We are also grateful to John Bilyeu and Deren Yuan for their perseverance in carrying forward and conducting the nondestructive tests.

Table of Contents

1. Introduction 1
1.1 Background 1
1.2 Objective 2
1.3 Scope 2

2. Experimental Program 3
2.1 Test Sections 3
2.2 Materials and Mixture Designs 3
2.2.1 Superpave Mixes 3
2.2.2 CMHB-C Mixes 4
2.2.3 Type C Mixes 4
2.2.4 Test Results of Mixtures 4

3. Visual Pavement Condition Survey for 0-4185 5
3.1 Classification of Distresses According to SHRP Distress Identification Manual 5
3.1.1 Transverse Cracking 5
3.1.2 Fatigue Cracking 5
3.1.3 Longitudinal Cracking 6
3.1.4 Reflection Cracking at Joints 6
3.1.5 Patching 6
3.1.6 Potholes 6
3.2 Westbound Outside Lane 7
3.3 Eastbound Outside Lane 7
3.4 Comparison of Changes in the Number of Cracks for Different Test Sections 7

4. PSI Measurements 17
4.1 Statistical Analysis of Data 17
4.2 Comparison of PSI Values Test Results with the Results of Visual Pavement Survey 20

5. FWD Measurements 23
5.1 Introduction 23
5.1.1 FWD Testing Completed 23
5.2 FWD Testing 24
5.2.1 Overview 24
5.2.2 Back-Calculation of Layer Moduli 25
5.2.3 Normalization of FWD Deflections 25
5.3 FWD Deflection Results 27
5.3.1 Outliers 27
5.3.2 Summary Means of FWD Deflection Parameters 29
5.3.3 Standard Deviations 32
5.4 Discussion of Deflection Results 36
5.4.1 Deflection Parameters 36

5.4.2 Paired Student's t-Test Analyses (January 2002–November 2002) 37
5.5 Summary 39
6. RDD Measurements: Overview of the Rolling Dynamic Deflectometer 41
6.1 Introduction 41
6.2 RDD Continuous Deflection Profiles 41
7. PSPA Measurements 55
8. Conclusions 59
References 61
Appendix A: Crack Pictures on Westbound Lane 63
Appendix B: PSI Values 77
Appendix C: Aggregate and Mix Design Properties of the Specimens 95
Appendix D: Orientation of the Test Sections 99
Appendix E: FWD Measurements 103

List of Tables

Table 3.1 Severity levels of potholes 7
Table 3.2 Visual pavement condition survey results at westbound outside lane 9
Table 3.3 Beginning and ending of the test sections at westbound outside lane 9
Table 3.4 Visual pavement condition survey results at eastbound outside lane 10
Table 3.5 Beginning and ending of the test sections at eastbound outside lane 10
Table 3.6 Changes in the number of transverse cracks for different test sections 11
Table 3.7 Existing number of cracks on CRCP 11
Table 4.1 PSI values of test sections 19
Table 4.2 t_α , t-statistics and p-values for each test section 20
Table 5.1 Summary of FWD testing 24
Table 5.2 Number of FWD deflection records after and before eliminating outliers 28
Table 5.3 Mean W1 deflections 29
Table 5.4 Mean W7 deflections 30
Table 5.5 Mean SCI deflections 30
Table 5.6 Mean BCI deflections 30
Table 5.7 Standard deviation of W1 deflections 33
Table 5.8 Standard deviation of W7 deflections 33
Table 5.9 Standard deviation of SCI deflections 33
Table 5.10 Standard deviation of BCI deflections 34
Table 5.11 Student's t-analyses of W1 deflections 37
Table 5.12 Student's t-analyses of W7 deflections 37
Table 5.13 Student's t-analyses of SCI deflections 37
Table 5.14 Student's t-analyses of BCI deflections 37
Table 6.1 Schedule of the RDD testing along Interstate Highway 20 42
Table 6.2 Station limits for overlay mix design on Interstate Highway 20 near Marshall, TX 43
Table 6.3 Summary statistics for the RDD deflection profile on Interstate Highway 20 53
Table 7.1 Summary of PSPA measurements on sections of IH-20 56
Table 7.2 Statistical analyses results to determine the significance difference in PSPA modulus means between January and November 2002 57

Table B.1 PSI values on westbound IH-20 outside lane 79
Table B.2 PSI values on westbound IH-20 inside lane 80
Table B.3 PSI values on eastbound IH-20 outside lane 81
Table B.4 PSI values on eastbound IH-20 inside lane 82

Table C.1 Sources of the materials used in this research project 96
Table C.2 Aggregate gradations for superpave mixes....96
Table C.3 Summary of design mixture properties for superpave mixes 96
Table C.4 Aggregate gradations for CMHB-C mixes 97
Table C.5 Summary of design mixture properties for CMHB-C mixes....97
Table C.6 Aggregate gradations for Type C mixes 97
Table C.7 Summary of stability, TSR, and HWTD tests results 98
Table D.1 Summary of test section, westbound 101
Table D.2 Summary of test section, eastbound....101

List of Figures

Figure 3.1 Low-level transverse crack 12
Figure 3.2 Moderate-level transverse crack 13
Figure 3.3 High-level transverse crack 13
Figure 3.4 Number of transverse cracks on asphalt pavement detected on January 2002 survey 14
Figure 3.5 Number of transverse cracks on asphalt pavement detected on November 2002 survey 14
Figure 3.6 Number of transverse cracks on asphalt pavement for each section at different surveys 15
Figure 3.7 Number of cracks on the CRCP 15
Figure 5.1 FWD configuration 25
Figure 5.2 Mean air temperatures during FWD testing 26
Figure 5.3 Standard deviation of air temperatures during FWD testing 26
Figure 5.4 Number of outliers identified on the nine sections 28
Figure 5.5 Number of outliers identified on the nine sections between January and November 2002 29
Figure 5.6 Mean W1 FWD deflections for sections evaluated 31
Figure 5.7 Mean W7 FWD deflections for sections evaluated 31
Figure 5.8 Mean SCI for sections evaluated 32
Figure 5.9 Mean BCI for sections evaluated 32
Figure 5.10 Standard deviations of W1 FWD deflections of sections as evaluated 34
Figure 5.11 Standard deviations of W7 FWD deflections of sections as evaluated 35
Figure 5.12 Standard deviations of SCI of sections as evaluated 35
Figure 5.13 Standard deviations of BCI of sections as evaluated 36
Figure 6.1 Schematic diagram of the major components of the RDD (after Bay 1997) 41
Figure 6.2 RDD deflection profile for Section 3 along Interstate Highway 20 44
Figure 6.3 RDD deflection profile for Section 8 along Interstate Highway 20 45
Figure 6.4 RDD deflection profile for Section 5 along Interstate Highway 20 46
Figure 6.5 RDD deflection profile for Section 2 along Interstate Highway 20 47
Figure 6.6 RDD deflection profile for Section 7 along Interstate Highway 20 48
Figure 6.7 RDD deflection profile for Section 3 along Interstate Highway 20 49
Figure 6.8 RDD deflection profile for Section 1 along Interstate Highway 20 50
Figure 6.9 RDD deflection profile for Section 9 along Interstate Highway 20 51
Figure 6.10 RDD deflection profile for Section 6 along Interstate Highway 20 52
Figure 6.11 Summary statistics of the RDD continuous deflection profile 54
Figure 7.1 PSPA measurements on the concrete pavement, eastbound on IH-20 55

Figure 7.2 PSPA measurements on the concrete pavement, westbound on IH-20 56
Figure 7.3 Mean January and November 2002 PSPA measurements on IH-20 sections 57

Figure A.1 WBP1TC 65
Figure A.2 WBP2ATC 65
Figure A.3 WBP3ARC 66
Figure A.4 WBP4AP 66
Figure A.5 WBP5ATC 67
Figure A.6 WBP6ATC 67
Figure A.7 WBP7ATC 68
Figure A.8 WBP8ATC 68
Figure A.9 WBP9ATC 69
Figure A.10 WBP10ATC 69
Figure A.11 WBP11TC 70
Figure A.12 WBP12TC 70
Figure A.13 WBP13TC 71
Figure A.14 WBP14AP 71
Figure A.15 WBP15BTC 72
Figure A.16 WBP16TC 72
Figure A.17 WBP17ATC 73
Figure A.18 WBP18CTC 73
Figure A.19 WBP19TC 74
Figure A.20 WBP20TC 74
Figure A.21 WBP21TC 75
Figure A.22 WBP22TC 75
Figure A.23 WBP23TC 76
Figure B.1 PSI values on westbound outside lane measured on November 2002 and just after construction 83
Figure B.2 PSI values on westbound inside lane measured on November 2002 and just after construction 84
Figure B.3 PSI values on eastbound outside lane measured on November 2002 and just after construction 85
Figure B.4 PSI values on eastbound inside lane measured on November 2002 and just after construction 86
Figure B.5 d(average) values and their standard deviations for eastbound inside and outside lanes 87
Figure B.6 d(average) values and their standard deviations for westbound inside and outside lanes 88

Figure B.7 Comparison of t-statistics and t_α values for sections on eastbound outside and inside lanes 89
Figure B.8 Comparison of t-statistics and t_α values for sections on westbound outside and inside lanes 90
Figure B.9 p-values for sections on eastbound outside and inside lanes 91
Figure B.10 p-values for sections on westbound outside and inside lanes 92
Figure B.11 Number of transverse cracks on asphalt pavement for each section at different surveys....93
Figure B.12 Number of cracks on the CRCP....94
Figure D.1 Layout of the test sections....102
Figure E.1 Section 1 normalized W1 deflections 105
Figure E.2 Section 1 normalized W7 deflections 105
Figure E.3 Section 1 normalized SCI 106
Figure E.4 Section 1 normalized BCI....106
Figure E.5 Section 2 normalized W1 deflections 107
Figure E.6 Section 2 normalized W7 deflections 107
Figure E.7 Section 2 normalized SCI 108
Figure E.8 Section 2 normalized BCI....108
Figure E.9 Section 3 normalized W1 deflections 109
Figure E.10 Section 3 normalized W7 deflections 109
Figure E.11 Section 3 normalized SCI 110
Figure E.12 Section 3 normalized BCI....110
Figure E.13 Section 4 normalized W1 deflections 111
Figure E.14 Section 4 normalized W7 deflections 111
Figure E.15 Section 4 normalized SCI 112
Figure E.16 Section 4 normalized BCI....112
Figure E.17 Section 5 normalized W1 deflections 113
Figure E.18 Section 5 normalized W7 deflections 113
Figure E.19 Section 5 normalized SCI 114
Figure E.20 Section 5 normalized BCI....114
Figure E.21 Section 6 normalized W1 deflections 115
Figure E.22 Section 6 normalized W7 deflections 115
Figure E.23 Section 6 normalized SCI 116
Figure E.24 Section 6 normalized BCI....116
Figure E.25 Section 7 normalized W1 deflections 117
Figure E.26 Section 7 normalized W7 deflections 117
Figure E.27 Section 7 normalized SCI 118
Figure E.28 Section 7 normalized BCI....118
Figure E.29 Section 8 normalized W1 deflections 119

Figure E.30 Section 8 normalized W7 deflections 119
Figure E.31 Section 8 normalized SCI 120
Figure E.32 Section 8 normalized BCI 120
Figure E.33 Section 9 normalized W1 deflections 121
Figure E.34 Section 9 normalized W7 deflections 121
Figure E.35 Section 9 normalized SCI 122
Figure E.36 Section 9 normalized B 122

1. Introduction

1.1 Background

This project was conducted to determine the correlation of field performance to Hamburg Wheel Tracking testing results. Three mix design methods (Superpave, CMHB-C, and Type C) and three aggregate sources (siliceous gravel, sandstone, and quartzite) were used for this study. The test sections, including all mixture designs, were constructed on IH-20 in Harrison County to observe the performance of the overlays under real traffic conditions. Type B mixture was used for all overlays as a base layer. Field performance will be observed through visual pavement condition surveys and nondestructive tests (NDT) for 4 years.

In the first year of Project 0-4185, specimens were prepared and tested using the Hamburg Wheel Tracking Device (HWTD). The results of the tests were analyzed and included in Research Report 0-4185-1 (Yildirim and Kennedy 2001). In the second year of this project, samples from the plant mixes and cores from the test sections were taken for each mixture type. The samples were tested using the HWTD in the Texas Department of Transportation (TxDOT) asphalt laboratory. The results of these tests were summarized in Research Report 0-4185-2 (Yildirim and Kennedy 2002).

The HWTD is a wheel-tracking device used to simulate field traffic effects on hot mix asphalt pavement (HMA) in terms of rutting and moisture-induced damage (Yildirim and Kennedy 2002). This equipment measures the combined effects of rutting and moisture damage by rolling a steel wheel across the surface of an asphalt concrete slab that is immersed in hot water. The HWTD was developed in the 1970s by Esso A.G. of Hamburg, Germany. Originally, only cubical-shaped specimens could be tested. The test now can be performed on both cubical and cylindrical specimens. The cubical specimens are approximately 320 mm long, 260 mm wide, and 40 mm thick. The cylindrical specimens are 150 to 300 mm in diameter and about 40 mm thick. The sample is typically compacted to 7±1 percent air voids. The plate type compactor has been proposed for compacting the specimens. However, use of cylindrical specimens makes it possible to obtain compacted specimens very easily with the aid of the gyratory compactors. The test temperature can vary between 25°C (77°F) and 70°C (158°F). Approximately 6.5 hours are required for a test, but in many cases the samples have failed in a much shorter period of time (Yildirim and Kennedy 2001). The device operates two steel wheels simultaneously. Each wheel, making about fifty passes per minute, applies 705 ± 22 N force on specimens. Two samples are required for every single wheel. Because the device has two wheels, it can test four samples (two couples) at the same time and provides a single report for each couple. The test results from the HWTD include post-compaction consolidation, creep slope, stripping slope, stripping inflection point, and final rut depth (Aschenbrener and Currier 1993). The post-compaction consolidation is the deformation (mm) at about 1,000 wheel passes. It is called post-compaction consolidation because it is assumed that the wheel is densifying the mixture within the first 1,000 wheel passes. The creep slope relates to rutting from plastic flow. It measures the accumulation of permanent deformation primarily owing to mechanisms other than moisture damage. The stripping slope is the inverse of the rate of deformation in the linear region of the deformation curve, after stripping begins and until the end of the test. This slope measures the accumulation of permanent deformation owing

primarily to moisture damage. The stripping point is the number of passes at the intersection of the creep slope and the stripping slope. It is related to the resistance of the HMA to moisture damage. After this point, moisture damage starts to dominate performance. The Colorado Department of Transportation (CDOT) reports that an inflection point below 10,000 wheel passes indicates moisture susceptibility (Yildirim and Kennedy 2002). To report the creep slope and the stripping slope in terms of wheel passes, inverse slopes are used. Higher creep slopes, stripping inflection points, and stripping slopes indicate less damage (Hines 1991).

This research report summarizes the visual pavement condition survey and nondestructive test results in the third year of this study. Chapter 3 reviews the visual pavement condition survey, Chapter 5 the falling weight deflectometer (FWD) measurements, Chapter 6 the rolling dynamic deflectometer (RDD) measurements, and Chapter 7 the portable seismic pavement analyzer (PSPA) measurements.

1.2 Objective

The objective of this study is to determine the relationship between the HMA field performance and the Hamburg Wheel Tracking Device test results. Three mix design methods (12.5 mm Superpave, CMHB-C, and Type C) and three different coarse aggregate sources (siliceous gravel, sandstone, and quartzite) were studied in this project.

1.3 Scope

The project will be completed in 5 years. Test sections were built on IH-20 in Harrison County and nine different types of overlay were placed in December 2001. Test sections will be monitored for 4 years by the Center for Transportation Research (CTR) at The University of Texas at Austin. The HWTD was utilized to determine the laboratory performances of the samples. The HWTD results and the field performance of the overlays on continuously reinforced concrete pavement (CRCP) will be gathered and compared at the end of the project. The field performance will be observed using NDTs. Falling weight deflectometer (FWD), portable seismic pavement analyzer (PSPA), and rolling dynamic deflectometer (RDD) are the types of NDT devices that will be utilized. In addition, visual pavement condition surveys will be performed at the end of each year. Field performance will be monitored every year until 2005. At the end of the project, the field and laboratory data will be compared to determine the behavior of the mixture types and a guideline will be developed to correlate the HWTD results and field performance.

2. Experimental Program

2.1 Test Sections

Nine hot mix asphalt (HMA) mixture types were prepared for this project using three mix designs: Type C, 12.5 mm Superpave, and CMHB-C mixture. Each mix design uses three different coarse aggregate sources: siliceous gravel, quartzite, and sandstone. Overlays were placed on test sections constructed on IH-20 in Harrison County. Test sections include all nine different types of surface mixtures shown in Tables D.1 and D.2. Base course, which is the same for all surface mixtures, was designed with 90 percent limestone and 10 percent local field sand. PG 76-22 binder was used for all mixtures including the base course.

2.2 Materials and Mixture Designs

Siliceous gravel is made mostly of quartz-rich sand and sandstone. It shows high thermal expansion. Sandstone is a sedimentary rock that has quartz-rich varieties. If it is cemented by silica or iron oxides (feldspar, calcite, or clay), it shows excellent quality. Sandstone is mostly porous and permeable. Pore water pressure plays a significant role in the compressive strength and deformation characteristics. It can reduce the unconfined compressive strength by 30 to 60 percent. Sandstone is resistant to surface wearing. It shows variable toughness, hardness, and durability, good crushed shape, and excellent chemical stability and surface characteristics. It has a relatively low density of 2.54 g/cm^3. Quartzite is a metamorphic rock. It is made of quartz (silicon dioxide) and sandstone. It is one of the hardest, toughest, and most durable rocks known. Because it contains high quartz content, it requires an anti-stripping agent when used with bituminous materials. Quartzite is excellent in toughness, hardness, durability, and chemical stability; fair in crushed shape; and fair to good in surface characteristics. Its density is 2.69 g/cm^3, which is medium (Roberts et al. 1991). The source of the binder was the same for all mixtures. Aggregate location data are provided in Table C.1.

2.2.1 Superpave Mixes

A nominal maximum aggregate size of 12.5 mm was used for all three Superpave mixes designed for this project. The first Superpave mix is composed of 67 percent siliceous gravel, 32 percent limestone screenings, and 1 percent lime. The design asphalt binder content for this mix is 5.0 percent. The second Superpave mix is composed of 91 percent sandstone, 8 percent igneous screenings, and 1 percent lime. The design asphalt binder content for this mix is 5.1 percent. The third Superpave mix is composed of 89 percent quartzite, 10 percent igneous screenings, and 1 percent lime. The design asphalt binder content is 5.1 percent. All three Superpave mix design gradations are passing below the Superpave restricted zone. Table C.2 shows the aggregate gradations for these mixes.

All of the Superpave mixes satisfy Superpave mixture design requirements. Specimens were prepared by using a Superpave press. Because all of the Superpave mixes are 12.5 mm, a minimum of 14.0 percent voids in mineral aggregate (VMA) value was used as a criterion. Based on the expected traffic level, specification for voids filled with asphalt (VFA) was selected between 65 and 75 percent. Densification requirements at the

initial number of gyrations and maximum number of gyrations are a maximum of 89.0 percent and 98.0 percent, respectively and Ndesign was 96.0 percent. The numbers of gyrations were 9 for N (initial), 125 for N (design) and 205 for N (max). An acceptable dust portion (DP) ranges from 0.6 to 1.2 for all Superpave mixtures. Table C.3 summarizes the design mixture properties for Superpave mixes at design binder contents.

2.2.2 CMHB-C Mixes

The first CMHB-C mix is composed of 79 percent siliceous gravel, 20 percent igneous screenings, and 1 percent lime. The second CMHB-C mix is composed of 87 percent quartzite, 12 percent igneous screenings, and 1 percent lime. The third CMHB-C mix is composed of 87 percent sandstone, 12 percent igneous screenings, and 1 percent lime. The design asphalt binder content is 4.7 percent for the first mix and 4.8 percent for the second and the third mixes. The aggregate gradations for these mixes are shown in Table C.4. For these mixes target air void content was 3.5 percent. Table C.5 shows the volumetric properties for CMHB-C mixes. For these mixes a Texas Gyratory Press was utilized.

2.2.3 Type C Mixes

The first Type C mix is composed of 61 percent siliceous gravel, 30 percent limestone screenings, 8 percent igneous screenings, and 1 percent lime. The second Type C mix is composed of 91 percent quartzite, 8 percent igneous screenings, and 1 percent lime. The third Type C mix is composed of 99 percent sandstone and 1 percent lime. For these mixes target air void content was 4 percent. The design asphalt binder contents for the mixtures are 4.4 percent, 4.6 percent, and 4.5 percent, respectively. Gradation for Type C mixtures is shown in Table C.6. For these mixes a Texas Gyratory Press was utilized.

2.2.4 Test Results of Mixtures

The results of stability, tensile strength ratio (TSR), and the HWTD tests are given in Table C.7. The lowest stability value was recorded as 41 on the Superpave mix with quartzite (A 0113 (H 01-09)), and the highest value was recorded as 51 on the Superpave mix with sandstone (A 0112 (H 01-08)). Stability tests were not conducted on the CMHB-C mixes with quartzite and sandstone (A 0115 (H 01-16) and A 0116 (H 01-17), respectively). The highest TSR value was recorded as 1.06 on the Type C mix with quartzite (A 0118 (H 01-19)), and the lowest value was recorded as 0.90 on the Type C mix with sandstone (A 0119 (H 01-20)). HWTD tests were conducted for 20,000 passes. The deformations recorded after 20,000 passes are also shown in Table C.7. The highest deformation observed was 3.1 on the Superpave mix with siliceous gravel (A 0111 (H 01-07)), and the lowest deformation recorded was 1.4 on the CMHB-C mix with sandstone (A 0116 (H 01-17)).

3. Visual Pavement Condition Survey for 0-4185

The second visual pavement condition survey was conducted on the east- and westbound test sections on IH-20 in the Atlanta District on the 13th and 14th of November 2002, respectively. The survey was conducted according to the Distress Identification Manual for the Long-Term Pavement Performance Studies (SHRP-LTPP/FR-90-001).

3.1 Classification of Distresses According to SHRP Distress Identification Manual

The manual classifies distresses in pavements into four general modes: cracking, joint deficiencies, surface defects, and miscellaneous distresses. Cracking distresses include corner breaks, longitudinal cracking, and transverse cracking. Joint deficiencies consider joint seal damage of transverse joints, longitudinal joints, and transverse joints. Surface defects include map cracking and scaling, polished aggregate, and popouts. Finally, miscellaneous distresses include blowups, faulting of transverse joints and cracks, lane-to-shoulder drop-off and separation, patch/patch deterioration, water bleeding, and pumping.

In this survey, observed distress types were described with the associated severity levels. In addition, photographs of distresses occurred are provided to aid in quantifying their severity levels. The severity levels of transverse cracks are recorded. Detected distresses are mostly transverse cracks, which are the cracks relatively perpendicular to pavement centerline. In addition to transverse cracks, longitudinal cracks, fatigue cracks, potholes, and patching were rarely observed, which are defined, classified, and measured according to the SHRP distress identification manual as follows.

3.1.1 Transverse Cracking

Transverse cracks are relatively perpendicular to pavement centerline.

Low: Cracks with low severity or no spalling; mean unsealed as width of ¼" or less. (See Figure 3.1)

Moderate: Cracks with moderate severity spalling; mean unsealed crack width of greater than ¼"; low severity random cracking near the crack. (See Figure 3.2)

High: Cracks with high severity spalling; moderate or high severity random cracking near the crack. (See Figure 3.3)

How to measure: Number and linear feet of transverse cracks at each severity level.

3.1.2 Fatigue Cracking

Fatigue cracking is a series of interconnected cracks. Fatigue cracks are many-sided, sharp-angled pieces, and are usually less than 1" on the longest side. They occur in chicken wire/alligator pattern. Fatigue cracks occur only in areas subjected to repeated traffic loadings (usually in wheelpaths). They initially appear as longitudinal cracks.

Low: Longitudinal disconnected hairline cracks running parallel to each other; may be a single crack in wheel path; crack not spalled.

Moderate: A pattern of articulated pieces formed by cracks that may be lightly spalled; cracks may be sealed.

High: Pieces more severely spalled at edges and loosened until the pieces rock under traffic; pumping may exist.

How to measure: Square feet of surface area at each severity level. If different severity levels existing within an area can not be distinguished, rate entire area at highest severity present.

3.1.3 Longitudinal Cracking

Longitudinal cracks are relatively parallel to pavement centerline.

Low: Cracks with low severity or no spalling; mean unsealed crack width of ¼" or less; sealant material in good condition.

Moderate: Cracks with moderately severe spalling; mean unsealed crack width of greater than ¼"; sealant material in bad condition; low severity random cracking near the crack.

High: Cracks with high severity spalling; moderate or high severity random cracking near the crack.

How to measure: Linear feet at each severity level.

3.1.4 Reflection Cracking at Joints

Cracks in asphalt concrete (AC) overlay surfaces over jointed concrete pavements at original joints. Knowing slab dimensions beneath AC surface helps identify these cracks.

Low: Cracks with low severity or no spalling; mean unsealed crack width of ¼" or less; sealant material in good condition.

Moderate: Cracks with moderate severity spalling; mean unsealed crack width of greater than ¼"; sealant material in bad condition; low severity random cracking near the crack.

High: Cracks with high severity spalling; moderate or high severity random cracking near the crack.

How to measure: Number and linear feet of longitudinal and transverse cracks at each severity level. Measurements for longitudinal and transverse cracks shall be recorded separately.

3.1.5 Patching

Patching is a portion of pavement surface that has been removed or replaced.

Low: Patch is in very good condition or has low severity distress of any type.

Moderate: Patch has moderate severity distress of any type.

High: Patch has high severity distress of any type.

How to measure: Square feet of surface area and number of patches at each severity level.

3.1.6 Potholes

Potholes are bowl-shaped holes of various sizes in the pavement surface.

Table 3.1 Severity levels of potholes

	Area (Square Feet)		
Depth (Inches)	<1	1-3	>3
<1	Low	Low	Moderate
1-2	Moderate	Moderate	High
>2	Moderate	High	High

How to measure: Number of potholes at each severity level.

3.2 Westbound Outside Lane

The visual pavement condition survey was conducted on the westbound outside lane on the 13th of November 2002. Mostly transverse cracks were detected. In addition to transverse cracks, three reflection cracks, one fatigue crack and one pothole were detected. Visual condition survey results on the westbound outside lane are given in Table 3.2. Beginning and end of the test sections and corresponding mixture and aggregate types are given in Table 3.3. Pictures of each distress are included in Appendix A.

3.3 Eastbound Outside Lane

The visual pavement condition survey was conducted on the eastbound outside lane on the 14th of November 2002. Distresses detected were mostly transverse cracks. Cracks were at low and moderate levels, so they were considered to be insignificant. In addition to transverse cracks, one patch and one longitudinal crack were recorded. Distresses are summarized in Table 3.4. Beginning and end of the test sections and corresponding mixture and aggregate types are given in Table 3.5. Pictures for every distress are available in Appendix B.

3.4 Comparison of Changes in the Number of Cracks for Different Test Sections

Table 3.6 shows the changes in the number of transverse cracks for different test sections between December 2001, January 2002, and November 2002. Since the estimated time for this project is five years and these data are collected before the end of the first year of the pavement construction, it should be emphasized that these data are premature. The data that will be collected in the coming periods will help us make better recommendations about the performance of the pavement and the reasons of the distresses that might occur.

In Figures 3.4 and 3.5, the numbers of transverse cracks on asphalt concrete overlay on January 2002 and November 2002 are shown. The comparison of these figures clearly shows that for all sections except Section 3, the number of distresses increased from January 2002 to November 2002.

The aggregate type that was used in different sections is expected to affect the pavement performance. The aggregate types that were used in different sections are as follows:

- Sections 2, 5, and 8 – sandstone
- Sections 3, 6, 9 – quartzite
- Sections 1, 4, 7 - gravel

In both Figures 3.5 and 3.6 it is seen that the maximum number of cracks occurred on the asphalt sections that include sandstone and the minimum number of cracks occurred on the sections that include quartzite. The total number of cracks that occurred in the sections with gravel aggregate is in between the total number of cracks that occurred in the sections with sandstone and quartzite aggregates. These observations show that the type of aggregate used in the test sections seems to affect the crack formation on the pavement with time, and that the best results are achieved on the sections where quartzite was used. In Figure 3.6 it can be seen that until November 2002 the best performance in terms of transverse cracking was seen in Section 3 (Superpave with quartzite aggregate), where no cracking was observed so far.

In addition to the effect of aggregate type on the performance of the asphalt pavement, it is observed that the initial condition of the CRCP can affect the formation of distresses on asphalt pavement. Table 3.6 shows the existing number of cracks that include both transverse cracks and patchings on the CRCP before the asphalt pavement was placed on it. The existing transverse cracks and the edges of the patchings on the CRCP are expected to affect the crack formation in asphalt pavement. Figures 3.6 and help us to observe the last condition of asphalt pavement in comparison with the initial condition of the CRCP. The comparison shows us a possible effect of the distresses on the CRCP on the crack formation in asphalt pavement. Figure 3.6 shows us that the maximum number of distresses occurred at Sections 2, 5, and 8. Figure 3.7 shows the number of cracks on the concrete base, CRCP, before the placement of the new overlays. Figure 3.7 shows that these sections had the maximum number of moderate level transverse cracks on the CRCP.

Figures 3.4, 3.5, 3.6, and 3.7 show that at this point it seems that both the type of aggregate and the CRCP condition can affect the crack formation on the asphalt pavement, but it cannot be stated clearly whether the cause of the crack formation in asphalt pavement is the type of aggregate or the distresses on the CRCP. It seems that the cause of crack formation depends on both of them.

Table 3.2 Visual pavement condition survey results at westbound outside lane

Station Numbers	Distresses	Dimension (feet)	Photo #
1307 – 1308	1 Transverse crack, Moderate	12 feet	WBP1TC
1307 – 1308	Reflection cracking, Moderate	12 feet	WBP2ATC
1307 – 1308	Reflection cracking, Low	4.8 feet	WBP2ATC
1307 – 1308	Reflection cracking, Low	4.2 feet	WBP2ATC
1318 – 1319	Pothole, Moderate	1.6 Square feet area, 1.2 inches depth	WBP4AP
1312 – 1313	1 Transverse crack, Moderate	11 feet	WBP5ATC
1305 – 1306	1 Transverse crack, High	12 feet	WBP6ATC
1300 – 1301	1 Transverse crack, Moderate,	12 feet	WBP7ATC
1300 – 1301	1 Transverse crack, High	12 feet	WBP8ATC
On 1297	1 Transverse crack, Low	11.5 feet	WBP9ATC
On 1297	1 Transverse crack, Moderate	11.5 feet	WBP10ATC
1292 – 1293	1 Transverse crack, Moderate	6.5 feet	WBP11TC
1251 – 1250	1 Transverse crack, Moderate	6.4 feet	WBP12TC
1251 – 1250	1 Transverse crack, Low	2.8 feet	WBP13TC
1249 – 1250	Fatigue crack, Moderate	4.6 Square feet	WBP14BFC
1234 – 1235	1 Transverse crack, High	6.2 feet	WBP15BTC
1228 – 1229	1 Transverse crack, Low	2.7 feet	WBP16TC
1228 – 1229	1 Transverse crack, Moderate	12 feet	WBP17ATC
1223-1224	1 Transverse crack, Moderate	12 feet	WBP18CTC
1215-1216	1 Transverse crack, Moderate	4.5 feet	WBP19TC
1213-1214	1 Transverse crack, Low	12 feet	WBP20TC
1213-1214	1 Transverse crack, Low	12 feet	WBP21TC
1211-1212	1 Transverse crack, Moderate	3.8 feet	WBP22TC
1195 – 1196	1 Transverse crack, High	9.8 feet	WBP23TC

Table 3.3 Beginning and ending of the test sections at westbound outside lane

Section	Section Name	Station Numbers	Mixture Type	Aggregate
W1	2	1278 – 1321	Superpave	Sandstone
W2	5	1235 – 1278	CMHB–C	Sandstone
W3	8	1193 – 1235	Type C	Sandstone
W4	3	1135 – 1188	Superpave	Quartzite

Table 3.4 Visual pavement condition survey results at eastbound outside lane

Station Numbers	Distresses	Dimension	Photo #
1135 – 1136	1 Transverse crack, Low	2.2 feet	EBP1TC
1136	1 Transverse crack, Low	1.8 feet	EBP2TC
1190 – 1191	1 Transverse crack, Low	10.8 feet	EBP3TC
1222-1223	1 Transverse crack, Low	10.5 feet	EBP4TC
1223-1224	1 Transverse crack, Moderate	11.5 feet	EBP5ATC
1225-1226	1 Transverse crack, Moderate	10.7 feet	EBP6TC
1249-1250	1 Transverse crack, Moderate	4.8 feet	EBP7BTC
1258-1259	1 Transverse crack, Low	4.5 feet	EBP8TC
1259-1260	1 Transverse crack, Low	9.8 feet	EBP9TC
1288-1289	Patching, Low	36.2 Square feet	EBP10APT
1290-1291	1 Transverse crack, Low	2 feet	EBP11TC
1292-1293	1 Transverse crack, Moderate	10.8 feet	EBP12BTC
1295-1296	1 Transverse crack, Low	10.7 feet	EBP13BTC
1300-1301	1 longitudinal crack, Low	17.5 feet	EBP14ALC
1303-1304	1 Transverse crack, Moderate	3.8 feet	EBP15TC
1307-1308	1 Transverse crack, Low	2.3 feet	EBP16TC

Table 3.5 Beginning and ending of the test sections at eastbound outside lane

Section	Section Name	Station Numbers	Mixture Type	Aggregate
E1	6	1135 – 1185	CMHB–C	Quartzite
E2	9	1190 – 1218	Type C	Quartzite
E3	1	1218 – 1245	Superpave	Gravel
E4	4	1245 - 1282	CMHB–C	Gravel
E5	7	1282 - 1321	Type C	Gravel

Table 3.6 Changes in the number of transverse cracks for different test sections

Section Name	Number of Transverse cracks in December 2001	Number of Transverse cracks in January 2002				Number of Transverse cracks in November 2002			
	Total	Low	Moderate	High	Total	Low	Moderate	High	Total
2	0	2	2	0	4	1	5	2	8
5	0	2	1	0	3	1	1	0	2
8	0	5	0	0	5	3	4	2	9
3	0	0	0	0	0	0	0	0	0
6	0	0	0	0	0	2	0	0	2
9	0	0	0	0	0	1	0	0	1
1	0	0	0	0	0	1	2	0	3
4	0	0	0	0	0	2	1	0	3
7	0	1	0	0	1	3	2	0	5

Table 3.7 Existing number of cracks on CRCP

Section	Low Transverse Crack	Moderate Transverse Crack	Patching	Total Number of Cracks
2	30	33	28	119
5	12	66	27	132
8	15	115	39	208
3	8	15	10	43
6	190	0	29	248
9	219	0	37	293
1	129	0	31	191
4	141	6	39	225
7	89	1	30	150

Figure 3.1 Low-level transverse crack

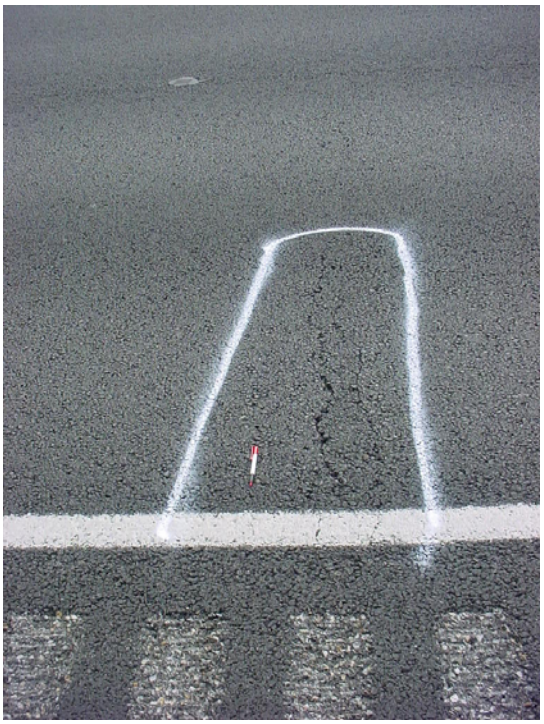

Figure 3.2 Moderate-level transverse crack

Figure 3.3 High-level transverse crack

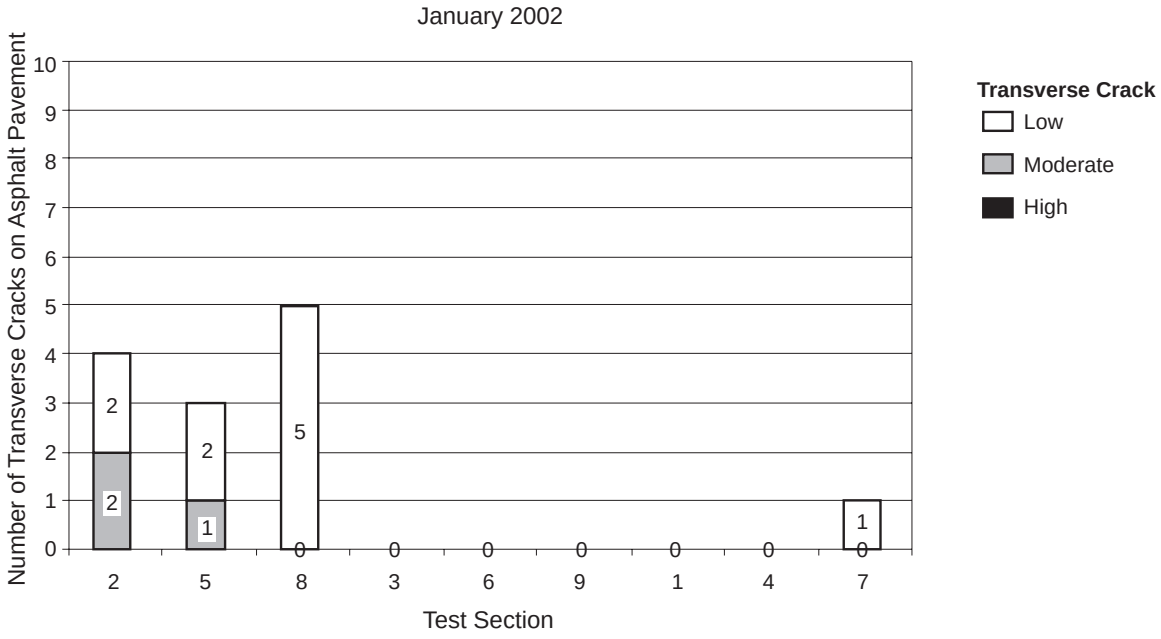

Figure 3.4 Number of transverse cracks on asphalt pavement detected on January 2002 survey

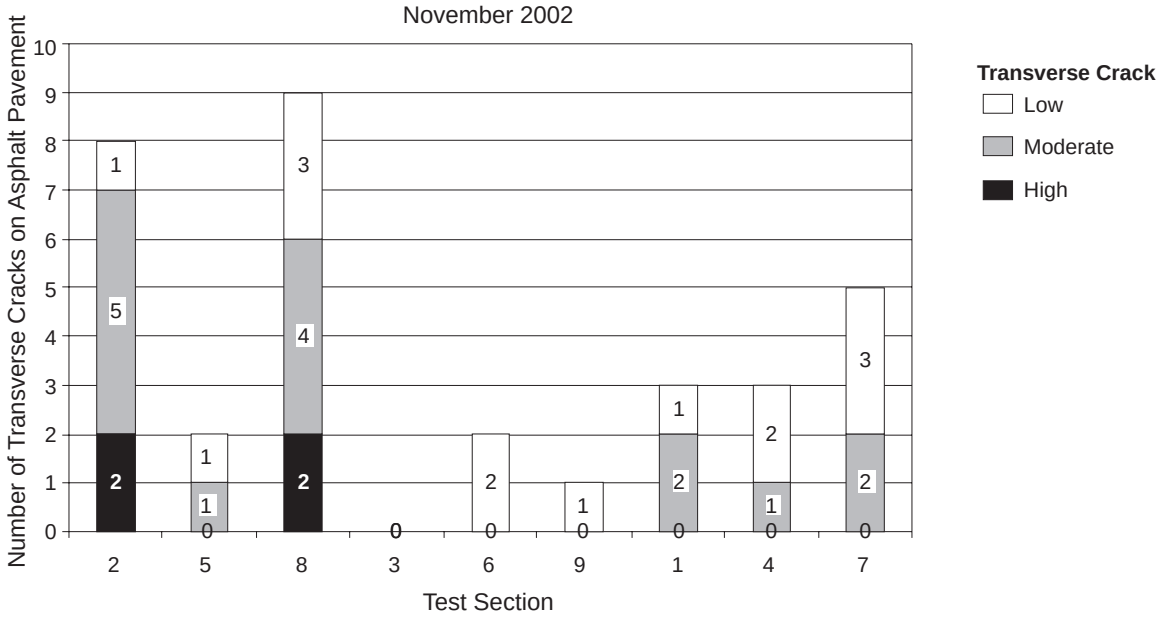

Figure 3.5 Number of transverse cracks on asphalt pavement detected on November 2002 survey

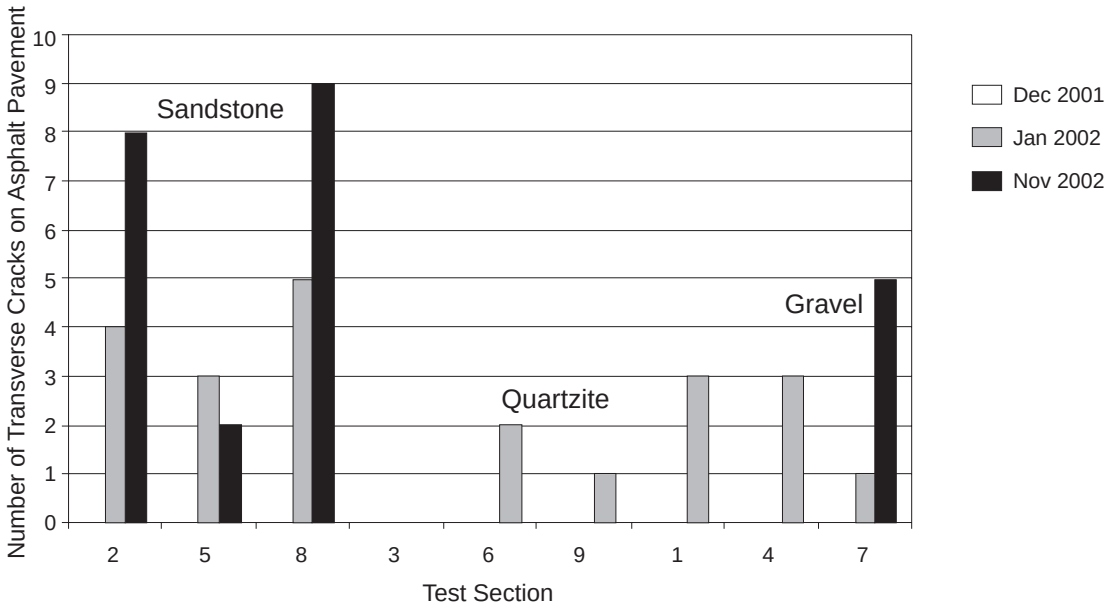

Figure 3.6 Number of transverse cracks on asphalt pavement for each section at different surveys

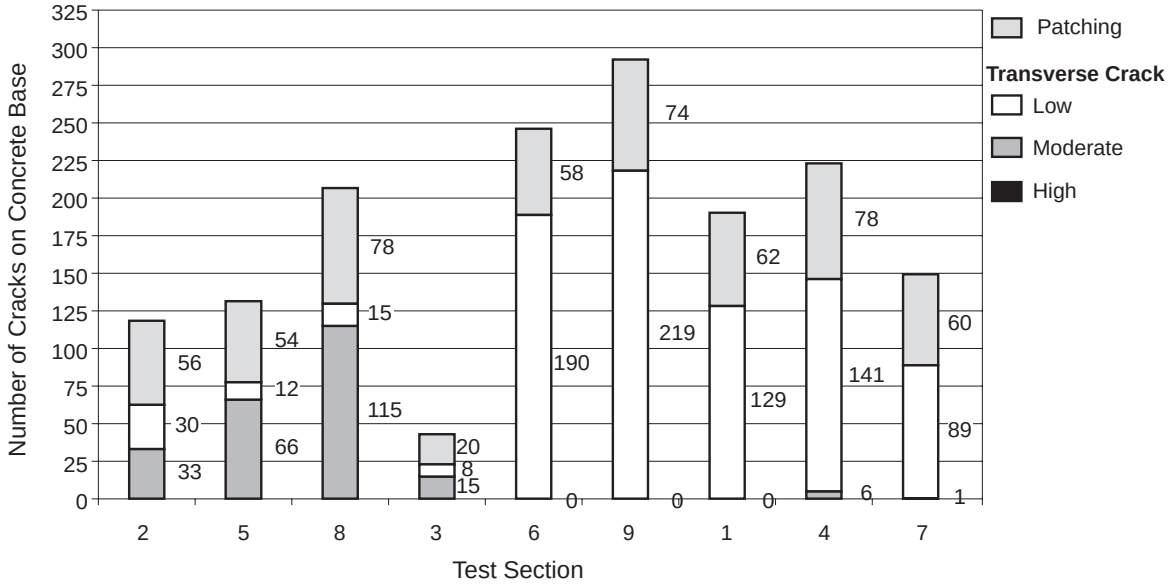

Figure 3.7 Number of cracks on the CRCP

4. PSI Measurements

After the completion of the construction of the test section, two condition surveys were conducted. The first one was conducted just after the asphalt concrete pavement was constructed, in December 2001. The second pavement condition survey was conducted on the east- and westbound test sections on IH-20 in the Atlanta District on the 13th and 14th of November 2002, respectively. Set up of the test sections is shown in Appendix D.

On both east- and westbound lanes the present serviceability index (PSI) values were calculated for the inside and outside lanes separately. PSI values were calculated by TxDOT based on the raw profile data, which is collected every 4.7 inches throughout the test sections. PSI-Nov2002 (PSI values obtained in November 2002) and PSI-Finished (PSI values obtained in December 2001) values are given in Appendix B, through Tables B.1 and B.4. The data included in Appendix B was provided by TxDOT and shows the average PSI values for every 0.1 mile. The PSI values measured at two different dates are compared for each test section separately, through Figures B.1 and B.4 in Appendix B.

The objective of this chapter is to present the PSI-Finished and PSI-Nov2002 values and to perform a statistical test for each section. The test will show us on which sections PSI values changed significantly from December 2001 to November 2002.

4.1 Statistical Analysis of Data

In order to determine whether or not PSI values changed significantly between December 2001 and November 2002, a t-test for each section was conducted. Because PSI-Finished and PSI-Nov2002 values are estimated at the same locations, the estimates are dependent; therefore it is appropriate to use a paired t-test (on the difference d).

$$d = (\text{PSI-Finished}) - (\text{PSI-Nov2002})$$

From d values, t-statistics values were calculated, where

$$\text{t-statistics} = d(ave)/ (S_D(d)/\sqrt{n})$$

d(ave) = mean of d values in each section

n = number of PSI values in each section (sample size)

S_D = Sample standard deviation of d

Dt : degree of freedom = n-1

Then t-statistics values are compared with t_α values, which are found from t-test tables. Because a 95 percent significance level was chosen,

t_α is found where $\alpha=0.05$

Tests of hypothesis were measured out according to the following:

- *Null Hypothesis*: For a given section PSI-Finished = PSI-Nov2002
- *Alternate Hypothesis*: For a given section PSI-Finished > PSI-Nov2002
- *Criteria*: Reject null hypothesis and accept alternate hypothesis if t-statistics > t_α

The t-test was used to determine whether or not the PSI-Finished and PSI-Nov2002 values were changed with a significance level of 5 percent. The value 0.05 represents the 5 percent error area under the t distribution curve. In the t-test a one tail method was used in order to establish that PSI-Nov2002 values are not smaller than the PSI-Finished values. For each test section, the t-statistics value was compared with the t_α value. If the t-statistics value is smaller than $t_{\alpha,\ \text{the}}$ t-test confirms that PSI-Finished and PSI-Nov2002 values are not different with a significance of 95 percent.

Another way of comparing the PSI-Finished and PSI-Nov2002 values with t-test is to calculate p-value for each test section. Since in the t-test the significance level was 5 percent, if the p-value is greater than 0.05, it can be said that PSI-Finished and PSI-Nov2002 values are not different at a 5 percent level.

When we compare the PSI values measured just after the construction and the ones measured on November 2002, the values seem to be very close for all sections. The averages of the PSI values and their standard deviations are shown in Table 4.1. In addition to the PSI values, the mean of the differences between them, d (ave), and their standard deviations are also given in Table 4.1. In Tables B.1 through B.4 in Appendix B, the comparison of the PSI values for east- and westbound lanes are done for PSI-Finished and PSI-November 2002 values. It is clearly seen that PSI-Finished and PSI-Nov 2002 values are very close and there are no significant decreases in PSI values. In some cases there are even some increases in the PSI-Nov2002 values in comparison with the PSI-Finished values, which are not expected and may stem from some measurement errors. In Figures B.5 and B.6 in Appendix B, the d(ave) values and their standard deviations are shown graphically.

The t-statistics, t_α and p-value are shown in Table 4.2 for each test section. Figures B.7 and B.8 in Appendix B show the comparison of t-statistics and t_α values graphically for west- and eastbound lanes. These figures show that for all sections, except Section 8 on westbound outside and inside lanes, the t-statistics values are smaller than t_α values. The t-test shows that PSI-Nov2002 values are lower than PSI-Finished values for Section 8 on westbound outside and inside lanes, while for all other sections PSI value did not change significantly from the date of the asphalt concrete pavement placement to November 2002, which is approximately a period of one year.

Similarly, Figures B.9 and B.10 in Appendix B show the p-values for different sections graphically. As we see in the comparison of t-statistics and t_α values, for all sections, p-values are higher than 0.05, except for Section 8 on westbound outside and inside lanes. This shows that except for Section 8, PSI-

November 2002 values are not significantly different than the PSI-Finished values at a 5 percent level. It can also be seen in Figures B.1 through B.4 in Appendix B that the mean of PSI-Nov 2002 values are significantly lower than the mean of PSI-Finished values for Section 8 on the westbound inside and outside lanes in comparison with the other sections.

Table 4.1 PSI values of test sections

	Section	PSI Finished Average	S_D of PSI- Finished	PSI NOV.02, Average	S_D of PSI- NOV2002	d (ave)	S_D of d(ave)
eastbound outside lane	6	4.469	0.225	4.486	0.260	-0.017	0.109
	9	4.459	0.316	4.401	0.281	0.057	0.078
	1	4.570	0.189	4.506	0.232	0.064	0.116
	4	4.670	0.108	4.711	0.118	-0.041	0.116
	7	4.470	0.234	4.493	0.294	-0.023	0.153
eastbound inside lane	6	4.604	0.117	4.629	0.135	-0.024	0.062
	9	4.464	0.234	4.406	0.254	0.059	0.101
	1	4.519	0.235	4.507	0.217	0.011	0.111
	4	4.574	0.164	4.684	0.119	-0.11	0.2
	7	4.157	0.530	4.147	0.615	0.01	0.296
westbound outside lane	2	4.386	0.214	4.405	0.299	-0.019	0.103
	5	4.408	0.139	4.393	0.167	0.015	0.139
	8	4.562	0.282	4.430	0.213	0.132	0.168
	3	4.667	0.089	4.673	0.163	-0.006	0.155
westbound inside lane	2	4.229	0.161	4.363	0.187	-0.134	0.155
	5	4.219	0.155	4.260	0.222	-0.041	0.096
	8	4.119	0.240	3.993	0.209	0.126	0.156
	3	4.520	0.177	4.546	0.165	-0.026	0.140

Table 4.2 t_α , t-statistics and p-values for each test section

	Section	d (ave)	S_D (d)	t_α	t-statistics	p-Value
eastbound outside lane	6	-0.017	0.109	1.943	-0.415	0.654
	9	0.057	0.078	1.943	1.927	0.051
	1	0.064	0.116	1.943	1.47	0.096
	4	-0.041	0.116	1.943	-0.949	0.81
	7	-0.023	0.153	1.943	-0.395	0.647
eastbound inside lane	6	-0.024	0.062	1.943	-1.043	0.831
	9	0.059	0.101	1.943	1.528	0.089
	1	0.011	0.111	1.943	0.272	0.397
	4	-0.11	0.2	1.943	-1.456	0.902
	7	0.01	0.296	1.943	0.089	0.466
westbound outside lane	2	-0.019	0.103	1.895	-0.520	0.689
	5	0.015	0.139	1.895	0.306	0.384
	8	0.132	0.168	1.860	2.360	0.023
	3	-0.006	0.155	1.833	-0.122	0.547
westbound inside lane	2	-0.134	0.155	1.895	-2.443	0.978
	5	-0.041	0.096	1.895	-1.216	0.868
	8	0.126	0.156	1.860	2.415	0.021
	3	-0.026	0.140	1.833	-0.588	0.715

4.2 Comparison of PSI Values Test Results with the Results of Visual Pavement Survey

With the exception of Section 8 on the westbound outside and inside lanes, for all sections, PSI values did not change significantly at a 5 percent level. Only for Section 8 did PSI values decrease significantly from the date of the placement of the asphalt concrete pavement to November 2002. When comparing these results to the visual pavement survey results presented in Figure B.11 in Appendix B, it is obvious that on the same section, the highest number of cracks occurred since the placement of the asphalt pavement on the CRCP. Also in Figure B.12 in Appendix B, it can be seen that the maximum number of medium transverse cracks on the CRCP before the asphalt pavement was placed were present in that same section.

Although this data is premature and the testing period is not long enough, the data collected up to November 2002 show that the maximum number of cracks occurred and PSI values decreased significantly on Section 8, which may be caused by the original CRCP conditions, the mixture type, and aggregate used in Section 8. At this time the results are very promising, but it is important that surveys continue to be conducted and analyzed until significant trends can be established.

5. FWD Measurements

5.1 Introduction

This chapter reports the results of falling weight deflectometer (FWD) tests done on the outside lanes of the various sections evaluated on IH-20 in Harrison County. The reader is referred to Appendix D for orientation of the different sections evaluated. Appendix D also outlines the different mixes used on these sections.

FWD testing is typically used to evaluate pavement structural performance. This point is emphasized given that the total thickness of asphalt surfacing overlaid on the continually reinforced concrete pavement (CRCP) in question was in the order of 100 mm (4 inches). Thin asphalt layers (less than 5 inches in thickness) overlaid on concrete pavements do not significantly contribute to the structural capacity of these pavements. The benefit of an asphalt concrete overlay is that it improves the riding quality of the pavement. It provides smoother pavements that attenuate the effects of dynamic wheel loading under heavy traffic. This may extend the structural life of the pavement, a benefit not necessarily associated with the actual performance of the asphalt concrete mixture in terms of rutting and or fatigue.

Given the above, FWD analyses were done towards identifying possible trends indicating performance contributions or respective benefits associated with the different mixes placed on the various sections of IH-20. The chapter addresses analyses towards this objective.

5.1.1 FWD Testing Completed

The results of four separate instances of FWD testing are reported. The first of these occurred towards the end of March and early April of 2001. These FWD tests were done on top of a four-inch asphalt overlay (placed over an eight-inch continuously reinforced concrete pavement) which was subsequently removed by milling. After milling of the old overlay, a second round of FWD testing was done directly on top of the milled concrete pavement towards the end of August 2001. The milled concrete pavement was overlaid with a two-inch Type B asphalt mix, which served as a base layer for the various mixes evaluated as part of the study, placed in two-inch lifts on top thereof. After construction of the various mixes, a third round of FWD testing was done on each of the newly constructed sections during January 2002. The fourth round of FWD testing was done during November 2002. Table 5.1 summarizes the FWD testing done on IH-20 as reported.

Table 5.1 Summary of FWD testing

FWD Series	Date Tested	Pavement Structure
1	April 2001	Old overlay
2	August 2001	Concrete
3	January 2002	New overlays
4	November 2002	New Overlays

Since the different FWD series were performed on the same locations, one is able to track the deflection response of the pavement structure and specific sections during the different stages of rehabilitation. An obvious question is how the deflections on the new overlay compare to those on the old and to what extent the asphalt overlays are influencing FWD deflections.

5.2 FWD Testing

5.2.1 Overview

Falling weight deflectometers are systems for performing nondestructive testing of pavement and other foundation structures. The system develops forces from the acceleration caused by the arrest of a falling weight and these forces are transmitted onto the surface of a structure causing it to deflect, much as it would due to the weight of a passing wheel load. The mass is dropped from a chosen height generating a dynamic load. The pulse load produced by the FWD simulates the effect of a moving wheel load in magnitude. The applied load is measured by a heavy-duty load cell and the load is transmitted to the pavement through a plate (300 mm diameter) resulting in a deflection of the pavement surface.

The deformation of the structure is referred to as a deflection basin. Figure 5.1 illustrates a typical FWD configuration with the deflection basin exaggerated to indicate the relative deflection beneath the FWD load. The magnitude and shape of the deflection basin is an indicator of the structural capacity of the pavement. FWD uses a series of user-positioned velocity sensors to automatically determine the amplitude and shape of this deflected basin. The deflection response, when related to the applied loading, can provide information about the strength and condition of the various elements of the pavement structure.

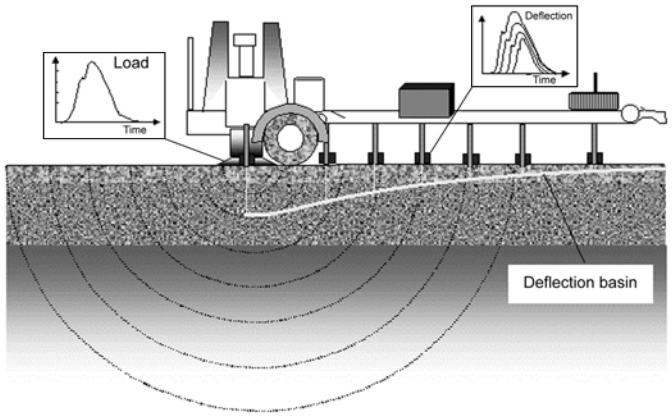

Figure 5.1 FWD configuration

5.2.2 Back-Calculation of Layer Moduli

In general, FWD deflection response may be used for the evaluation of multi-layer flexible pavement structures and back-calculation of the elastic moduli. An attempt was made to back-calculate the layer moduli of the section mixes evaluated based on the FWD deflection results collected on the various structures. The back-calculation analyses were not very successful in identifying layer moduli owing to the stiff concrete layer within the pavement structure. Part of the problem was identifying the stiffness of the cemented material beneath the concrete layer. As mentioned previously, the layer stiffness of the relatively thin asphalt layers on top of the concrete pavement would not significantly contribute to the overall stiffness of the structure. As a result, the variations of the surface layer moduli values determined based on the back-calculation analyses were too high to confidently rank the structural integrity of the various sections evaluated. For this reason an attempt was made to rank the integrity and associated performance of the various sections based on FWD deflection parameters. The following four FWD deflection parameters were evaluated statistically:

W1 = Maximum deflection beneath the FWD load (sensor 1)
W7 = Deflection at velocity sensor 7
SCI = Surface curvature index = W1 – W2
BCI = base curvature index = W4 – W5

The significance of the deflection parameters is addressed later in the chapter.

5.2.3 Normalization of FWD Deflections

FWD deflections resulting from load drops in the vicinity of 9000 lb were converted directly to standard deflections at 9000 lb. In order to compare the FWD deflections of tests done at different times of the day and year it was deemed necessary to apply a temperature correction. Air temperature measurements were

consistently collected at each FWD drop. Figures 5.2 and 5.3 show the means and standard deviations of these air temperatures for the different sections respectively. Temperatures ranged from 45 °F to 86 °F, the highest standard deviations apparent during the November 2002 FWD testing.

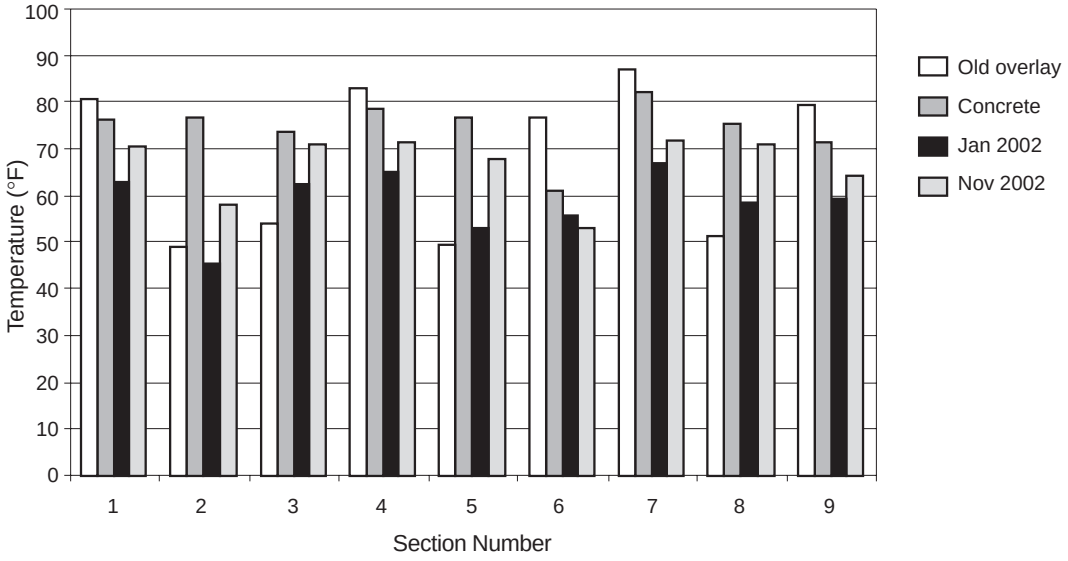

Figure 5.2 Mean air temperatures during FWD testing

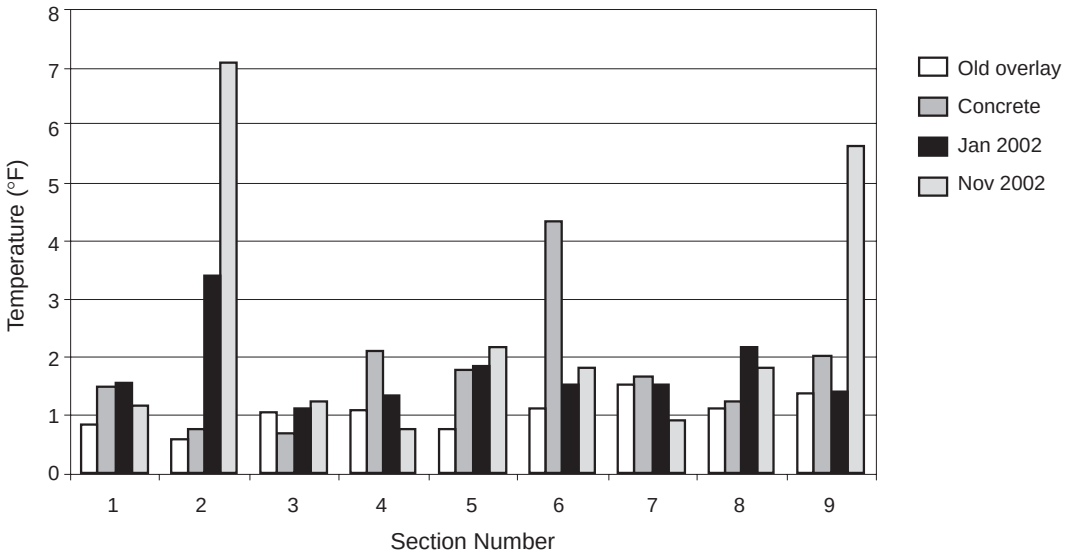

Figure 5.3 Standard deviation of air temperatures during FWD testing

Using these temperatures, the deflections measured on the asphalt sections (only) were normalized to those at a standard temperature of 20 °C (68 °F) using a correction factor based on that developed at Delft (Molenaar 1997):

$$TNF = 1 + \left(a_1 + \frac{a_2}{h_1} \right)(T_A - 20) + \left(a_3 + \frac{a_4}{h_1} \right)(T_A - 20)^2$$

where:

TNF	=	Temperature normalization factor
T_A	=	Air temperature (°C)
h_1	=	Thickness of the asphalt layer = 100 mm

TNF takes on values smaller than 1 if the measurements are taken below the reference temperature of 20 °C and larger than 1 if the measurements were taken above 20 °C. For FWD base plates having a diameter of 300 mm, the constants a_1 to a_4 in the above equation take on the following values:

$a_1 = 0.05398\ °C^{-1}$ $a_2 = -2.6113$ mm/°C
$a_3 = 0.00128439\ °C^{-1}$ a4 = -0.07493 mm/°C

The deflection measured at a specific temperature is normalized to that at 20 °C by dividing it by *TNF*.

5.3 FWD Deflection Results

FWD tests were done on the outside east- and westbound lanes of IH-20. The collected data were subdivided into subsets representing the various sections tested. Figures E.1 through E.36 in Appendix E indicate the normalized deflection parameters determined for each separate section before removal of deflection outliers.

From the figures it can be seen that the deflections along the individual sections are fairly uniform but are characterized by sporadic jumps and irregularities indicating regions of potential structural weakness. These may be due to localized cracking within the structure and are not necessarily indicative of the integrity of the section as a whole. In general, the very high W1 deflections apparent at irregular intervals along the sections on the old overlay and concrete pavement appear to have corresponding lower W1 deflections on the new overlay indicating that the overlay was influential in decreasing the deflections on the pavement.

5.3.1 Outliers

Given that one of the objectives of the study is to identify the relative performance of the specific mixes used on the different sections, it was decided to identify and eliminate deflection outliers using a statistical approach to prevent these from overly influencing the mean and standard deviation of the deflection parameters apparent on a particular section. This was done by standardizing the deflection data and defining outliers as data greater or less than 3 times the standard deviation of the sample population for a particular section. This slightly decreased the number of records used to determine statistical means and standard deviations for the deflections on a particular section as shown in Table 5.2.

Table 5.2 indicates the number of FWD deflection records collected on each of the sections for the different series of FWD tests completed. The number of outliers identified on a particular section provides an indication of the uniformity thereof, i.e., the greater the number of outliers, the greater the number of abnormalities apparent and vice versa.

Table 5.2 Number of FWD deflection records after and before eliminating outliers

Section	Overlay	Concrete	Jan 2002	Nov 2002
1	23 (24)	24 (26)	24 (24)	22 (24)
2	41 (44)	37 (40)	38 (40)	38 (40)
3	54 (56)	47 (49)	49 (50)	43 (46)
4	35 (37)	36 (40)	36 (37)	35 (37)
5	39 (41)	42 (44)	44 (45)	43 (44)
6	40 (42)	46 (50)	42 (44)	38 (40)
7	38 (40)	37 (39)	37 (39)	33 (37)
8	41 (42)	38 (41)	39 (41)	39 (41)
9	27 (29)	27 (29)	28 (29)	26 (28)

Figure 5.4 illustrates and ranks the number of outliers apparent on each of the nine sections evaluated for the different FWD series. From this figure it is clear that the greatest number of irregular deflections were apparent from the FWD tests on the concrete pavement after milling the old overlay. It is interesting to note that there was a marked decrease in the number of irregularities after the construction of the new overlay (January 2002) but that the irregularities apparent increased in November 2002. Note that there were no outliers identified for Section 1 in January 2002.

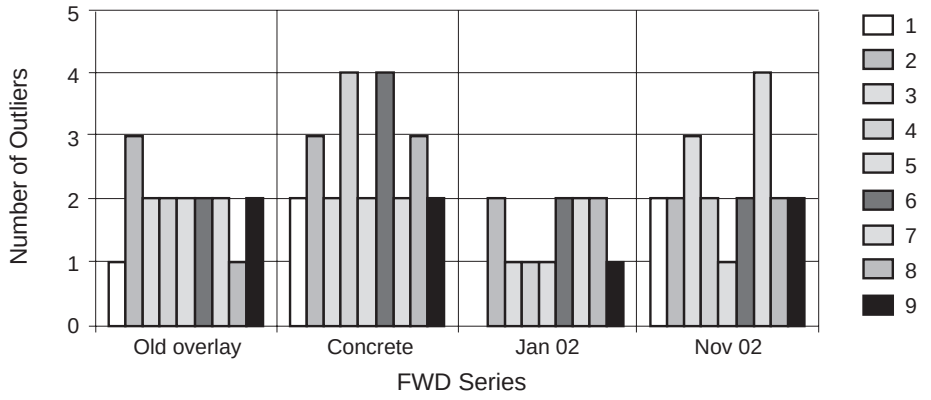

Figure 5.4 Number of outliers identified on the nine sections

Figure 5.5 indicates the difference in irregularities apparent between January 2002 and November 2002. There was an increase in the number of irregularities observed for Sections 1, 3, 4, 7, and 9. With the exception of Section 3, all of these are on the eastbound lane of IH-20.

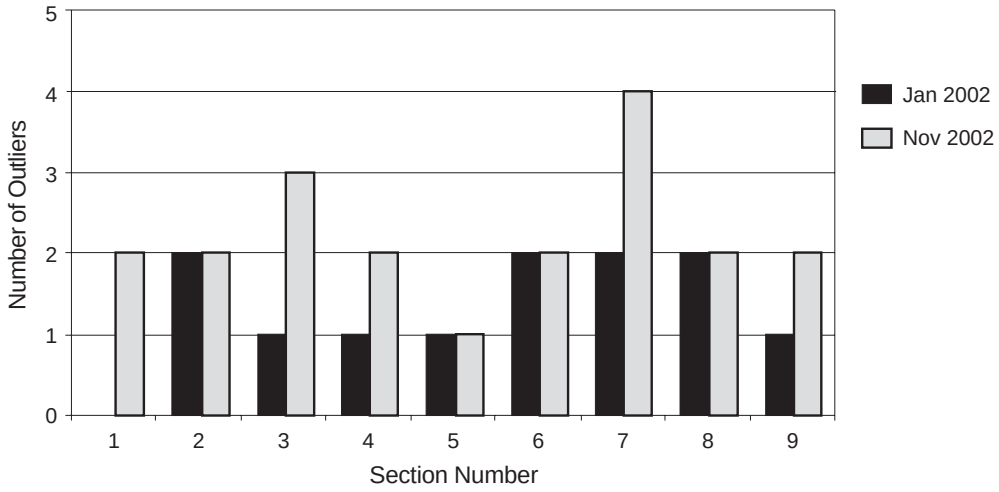

Figure 5.5 Number of outliers identified on the nine sections between January and November 2002

5.3.2 Summary Means of FWD Deflection Parameters

Tables 5.3 through 5.6 indicate the mean FWD deflection parameters (W1, W7, SCI, and BCI respectively) determined for each of the sections during each FWD testing series. The mean defection parameters for each of the sections (roadway means) are also given. These means are used later in the chapter to investigate whether the deflection on a specific section differs significantly from that on others. The results are discussed later in the chapter.

Table 5.3 Mean W1 deflections

Section	Overlay	Concrete	Jan 2002	Nov 2002
1	2.99	3.93	3.80	3.60
2	3.72	4.49	4.66	4.01
3	3.38	3.57	3.44	3.05
4	2.62	4.48	3.32	3.10
5	3.02	3.17	3.85	3.06
6	2.62	4.53	3.54	3.50
7	2.23	4.04	3.00	2.83
8	3.75	4.12	3.98	3.53
9	2.53	4.09	3.92	3.55
Mean	2.98	4.05	3.72	3.36

Table 5.4 Mean W7 deflections

Section	Overlay	Concrete	Jan 2002	Nov 2002
1	1.19	1.21	1.16	1.14
2	1.24	1.22	1.45	1.26
3	1.05	0.98	0.88	0.80
4	0.88	1.05	0.91	0.86
5	1.10	0.96	1.17	0.92
6	1.35	1.11	1.02	1.09
7	0.73	1.01	0.83	0.83
8	1.29	1.17	1.20	1.20
9	1.16	1.23	1.26	1.20
Mean	1.11	1.11	1.10	1.03

Table 5.5 Mean SCI deflections

Section	Overlay	Concrete	Jan 2002	Nov 2002
1	0.20	0.36	0.65	0.59
2	0.44	0.46	0.65	0.69
3	0.41	0.41	0.69	0.68
4	0.25	0.56	0.66	0.57
5	0.41	0.32	0.64	0.61
6	0.30	0.56	0.65	0.60
7	0.22	0.41	0.57	0.49
8	0.40	0.41	0.64	0.67
9	0.19	0.41	0.64	0.53
Mean	0.31	0.43	0.64	0.60

Table 5.6 Mean BCI deflections

Section	Overlay	Concrete	Jan 2002	Nov 2002
1	0.47	0.51	0.43	0.39
2	0.39	0.57	0.54	0.45
3	0.40	0.47	0.41	0.34
4	0.45	0.61	0.39	0.36
5	0.28	0.40	0.43	0.32
6	0.46	0.57	0.40	0.39
7	0.37	0.57	0.35	0.32
8	0.41	0.56	0.47	0.40
9	0.46	0.51	0.45	0.39
Mean	0.41	0.53	0.43	0.37

Figures 5.6 through 5.9 illustrate the mean deflection parameter data as tabulated. These results are discussed later in the chapter.

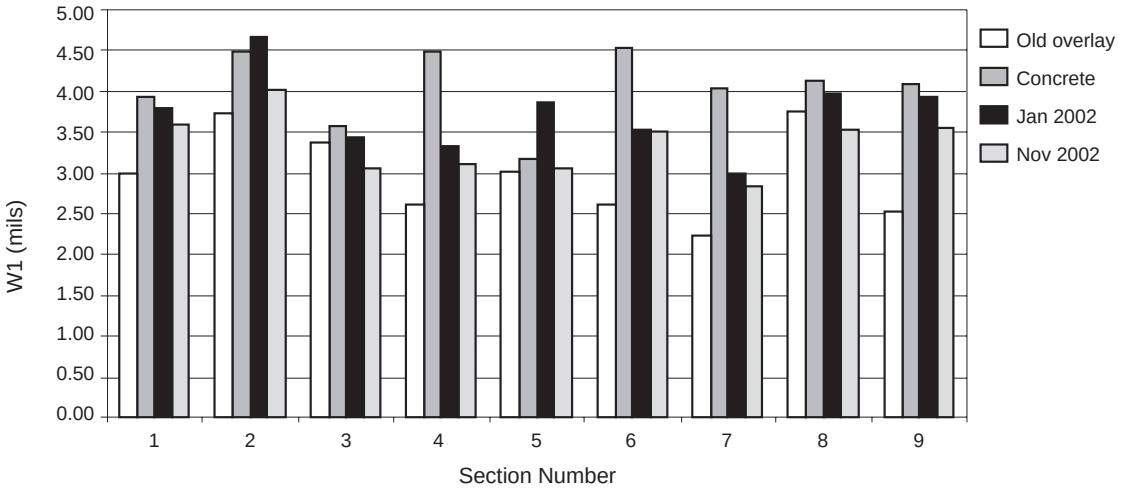

Figure 5.6 Mean W1 FWD deflections for sections evaluated

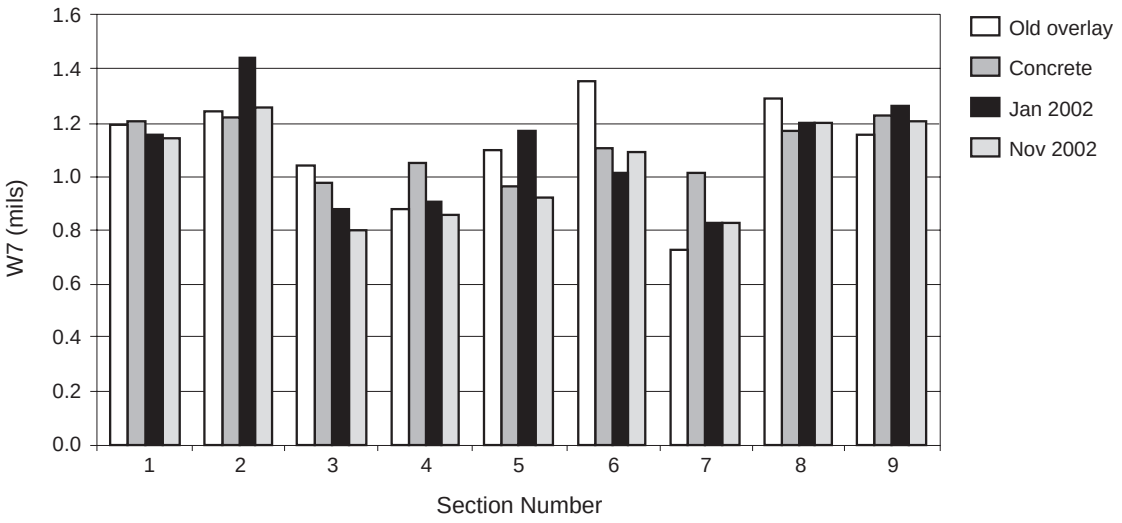

Figure 5.7 Mean W7 FWD deflections for sections evaluated

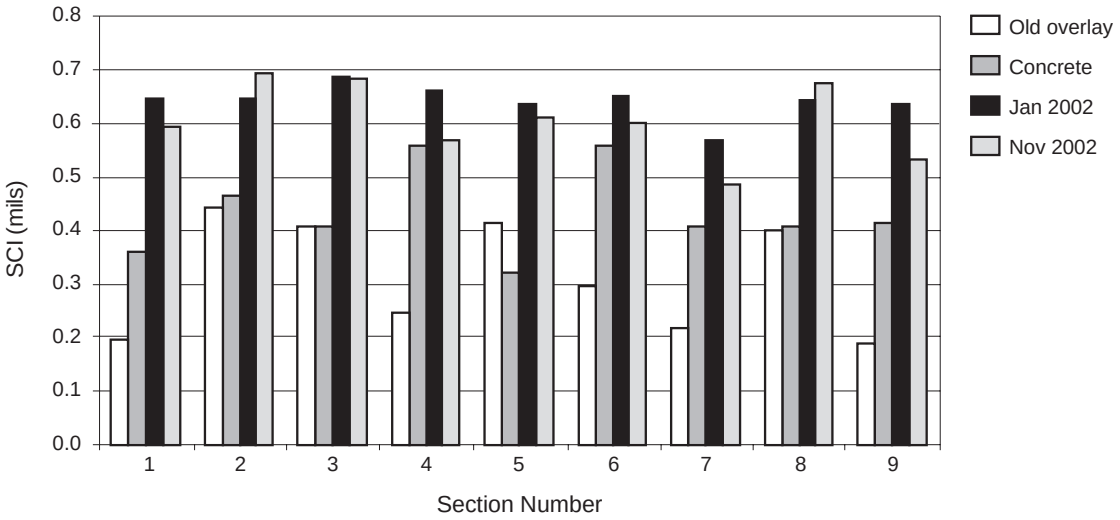

Figure 5.8 Mean SCI for sections evaluated

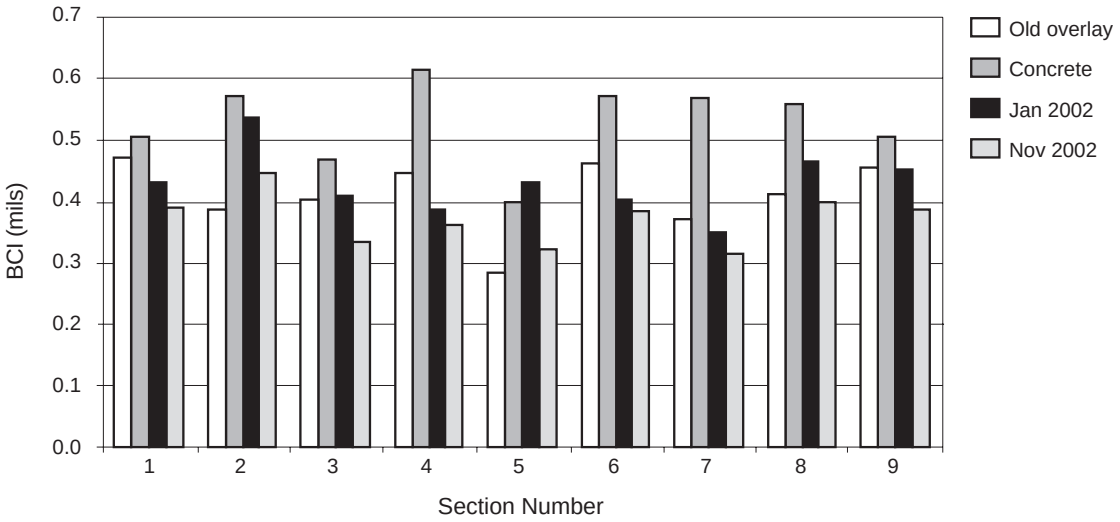

Figure 5.9 Mean BCI for sections evaluated

5.3.3 Standard Deviations

Tables 5.7 through 5.10 indicate the standard deviations of the FWD deflection parameters (W1, W7, SCI, and BCI respectively) determined for each of the sections during each FWD testing series. The results are discussed later in the chapter.

Table 5.7 Standard deviation of W1 deflections

Section	Overlay	Concrete	Jan 2002	Nov 2002
1	1.13	0.67	1.19	0.94
2	1.07	1.61	1.20	1.24
3	0.68	1.01	0.45	0.37
4	0.97	1.49	0.54	0.58
5	0.46	0.71	0.56	0.52
6	0.80	1.66	0.43	0.48
7	0.66	1.10	0.63	0.68
8	0.68	1.19	0.60	0.54
9	0.51	0.85	0.63	0.82

Table 5.8 Standard deviation of W7 deflections

Section	Overlay	Concrete	Jan 2002	Nov 2002
1	0.42	0.30	0.25	0.28
2	0.48	0.55	0.55	0.51
3	0.25	0.35	0.21	0.20
4	0.37	0.33	0.22	0.22
5	0.25	0.32	0.27	0.24
6	0.24	0.44	0.26	0.28
7	0.22	0.31	0.22	0.27
8	0.31	0.36	0.27	0.27
9	0.22	0.35	0.28	0.41

Table 5.9 Standard deviation of SCI deflections

Section	Overlay	Concrete	Jan 2002	Nov 2002
1	0.14	0.09	0.24	0.22
2	0.27	0.30	0.20	0.27
3	0.16	0.35	0.14	0.13
4	0.16	0.36	0.09	0.13
5	0.12	0.12	0.13	0.11
6	0.22	0.49	0.13	0.12
7	0.19	0.15	0.14	0.10
8	0.15	0.36	0.12	0.16
9	0.11	0.16	0.14	0.12

Table 5.10 Standard deviation of BCI deflections

Section	Overlay	Concrete	Jan 2002	Nov 2002
1	0.10	0.10	0.15	0.13
2	0.15	0.20	0.16	0.16
3	0.14	0.16	0.06	0.06
4	0.15	0.21	0.08	0.10
5	0.08	0.11	0.08	0.07
6	0.09	0.20	0.07	0.10
7	0.11	0.17	0.09	0.11
8	0.13	0.18	0.10	0.10
9	0.09	0.12	0.12	0.11

Figures 5.10 through 5.13 illustrate the standard deviations of the deflection parameter data as tabulated. From these it is clear that the highest standard deviations are associated with the FWD tests directly on the concrete pavement. The results are discussed later in the chapter.

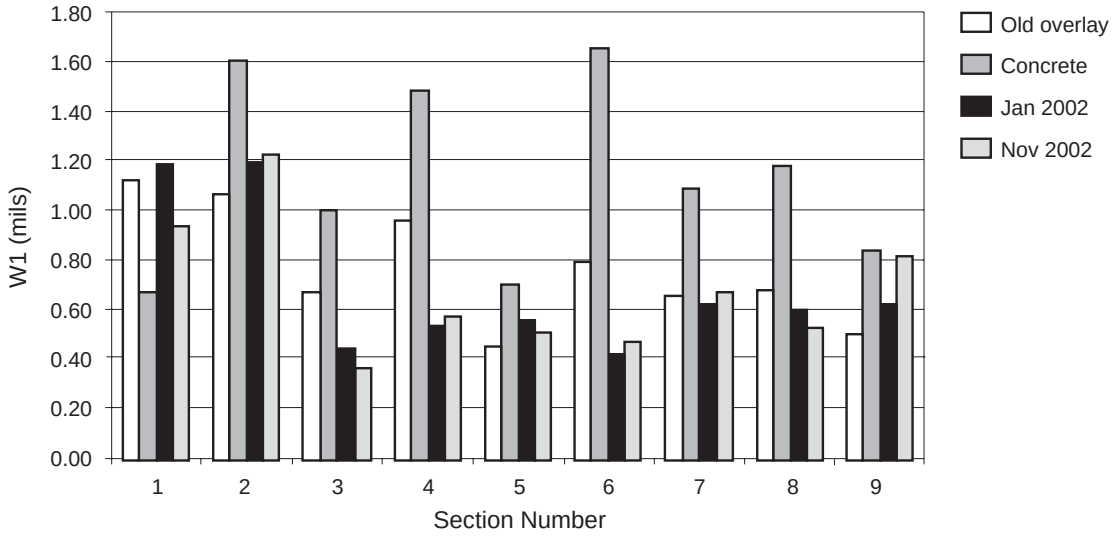

Figure 5.10 Standard deviations of W1 FWD deflections of sections as evaluated

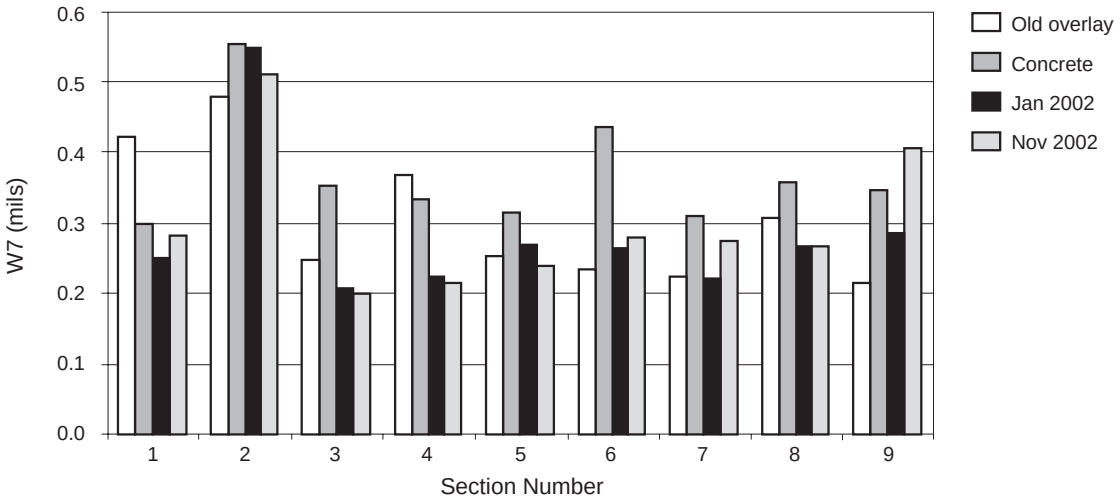

Figure 5.11 Standard deviations of W7 FWD deflections of sections as evaluated

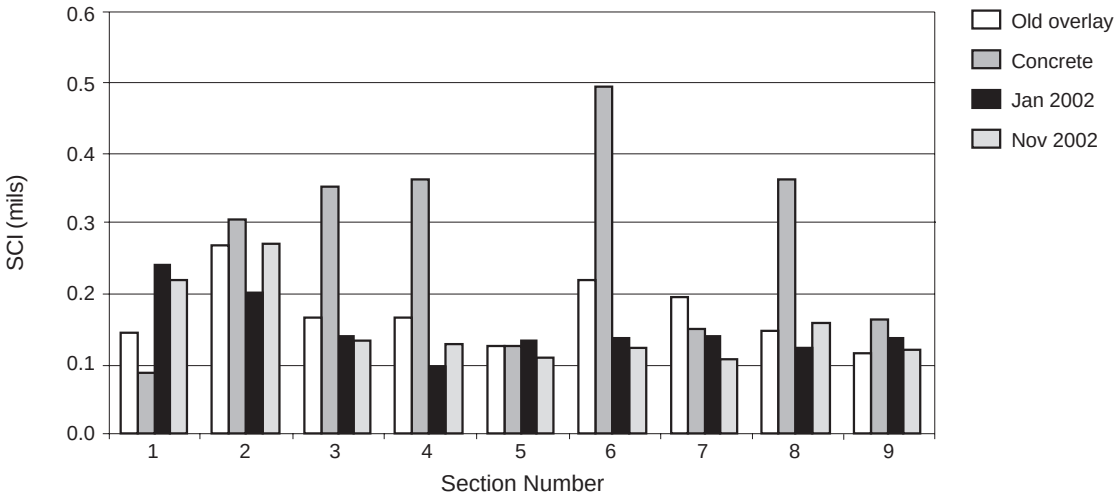

Figure 5.12 Standard deviations of SCI of sections as evaluated

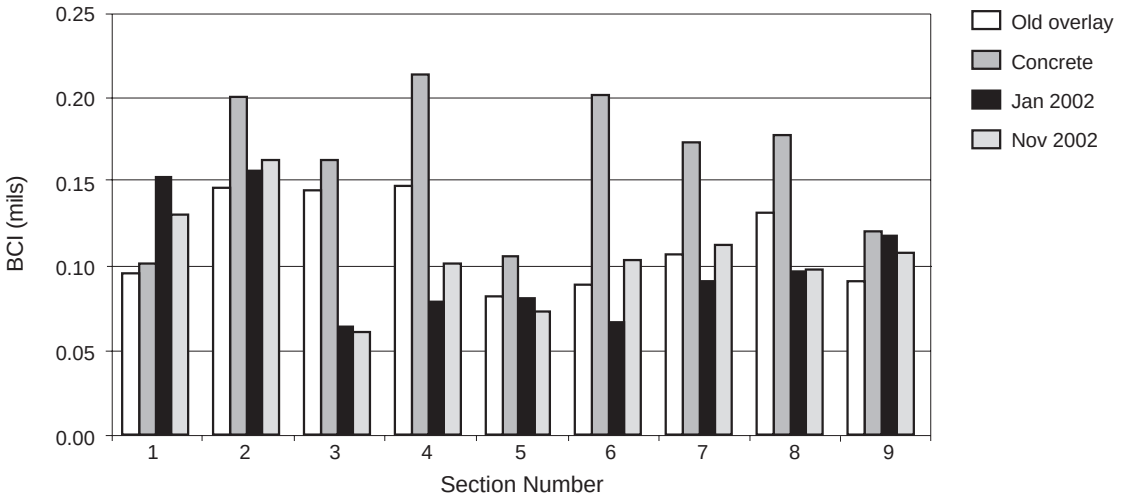

Figure 5.13 Standard deviations of BCI of sections as evaluated

5.4 Discussion of Deflection Results

The FWD results are expressed in terms of means and standard deviations of the deflection parameters W1, W7, SCI, and BCI. The reason for evaluating these deflection parameters is addressed followed by a discussion of the results towards performance ranking of the different sections.

5.4.1 Deflection Parameters

The deflection of a pavement beneath an FWD load may be used as an indicator of the structural integrity of the pavement. The greater the deflection, the weaker the pavement structure and vice versa. The maximum (W1) deflection indicates the deflection of the entire pavement structure under the load. The W1 defection collectively includes the deflection of the surfacing, base, and sub-base layers as well as the subgrade. Use is made of other deflection parameters such as W7, SCI, and BCI to differentiate between the deflections of the respective layers of the pavement structure. The W7 deflection, for example, although measured on the surface of the pavement, is commonly used as an indicator of subgrade stiffness. Subgrade deflection is influenced predominantly by the stress on the subgrade and hence the integrity or load spreading ability of the overlying pavement layers but also by seasonal variations in moisture content. The surface curvature index (SCI=W1-W2) indicates the curvature of the upper 200 mm (8 in) of the pavement. Low SCI values indicate that the W1 and W2 deflections are very similar and that the upper pavement structure is not deflecting much relative to the underlying structure under the load. The SCI value alone cannot provide information regarding the strength of the upper pavement structure. It is possible that the upper pavement structure is very weak, which would result in load punching and consequently low SCI values. Hence, in order to assess the pavement's structural integrity it is necessary to evaluate other parameters, such as the base curvature index (BCI=W4-W5). BCI is an indicator of the relative base and subbase layer deflections.

Deflection parameters allow an evaluation of the relative deflections and integrity of the respective pavement layers.

5.4.2 Paired Student's t-Test Analyses (January 2002–November 2002)

Paired sample comparisons were done to evaluate the significance of differences between the deflection parameters determined during the January 2002 and November 2002 FWD tests. The null hypothesis assumed was that there was no difference between the January and November 2002 deflections. The statistical Student's t-test was applied, the results of which are indicated in Tables 5.11 through 5.14 for the different FWD parameters respectively. Sections with significantly different deflections at the 95 percent confidence level (between the January 2002 and November 2002) are shaded in the tables. The numbers of paired sample records evaluated are also indicated.

Table 5.11 Student's t-analyses of W1 deflections

Section	1	2	3	4	5	6	7	8	9
N	22	36	43	35	43	37	32	38	26
t Stat	-0.91	6.82	8.10	3.65	15.72	1.41	1.69	6.95	5.70
t Critical two-tail	2.08	2.03	2.02	2.03	2.02	2.03	2.04	2.03	2.06
Reject Null?	No	Yes	Yes	Yes	Yes	No	No	Yes	Yes

Table 5.12 Student's t-analyses of W7 deflections

Section	1	2	3	4	5	6	7	8	9
N	22	36	43	35	43	37	32	38	26
t Stat	-0.56	4.10	8.22	3.05	10.06	-2.78	0.23	5.66	1.72
t Critical two-tail	2.08	2.03	2.02	2.03	2.02	2.03	2.04	2.03	2.06
Reject Null?	No	Yes	Yes	Yes	Yes	No	No	Yes	No

Table 5.13 Student's t-analyses of SCI deflections

Section	1	2	3	4	5	6	7	8	9
N	22	36	43	35	43	37	32	38	26
t Stat	0.52	-1.25	-0.10	6.73	1.93	2.66	4.13	-0.84	6.75
t Critical two-tail	2.08	2.03	2.02	2.03	2.02	2.03	2.04	2.03	2.06
Reject Null?	No	No	No	Yes	No	Yes	Yes	No	Yes

Table 5.14 Student's t-analyses of BCI deflections

Section	1	2	3	4	5	6	7	8	9
N	22	36	43	35	43	37	32	38	26
t Stat	0.10	7.51	9.58	2.67	15.50	1.53	3.11	4.96	5.35
t Critical two-tail	2.08	2.03	2.02	2.03	2.02	2.03	2.04	2.03	2.06
Reject Null?	No	Yes	Yes	Yes	Yes	No	Yes	Yes	Yes

As discussed previously, the deflection parameters provide an indication of the relative deflection of the layers within the pavement structure. These parameters are inter-related, i.e., a decrease in one parameter may be associated with a decrease in another deflection parameter. This is emphasized since a decrease in SCI, for example, may be related to stiffening or densification of the asphalt layer or upper pavement structure, which is to be expected for newly constructed asphalt layers after 10 months in the field. Based on the statistical analyses, the following observations are made regarding the deflections on the different sections.

Section 1

No significant differences are apparent on any of the deflection parameters evaluated. This may indicate that climatic and traffic conditions between January and November 2002 have not influenced the structural capacity of Section 1. These conditions would tend to stiffen and densify the pavement over time, resulting in a relative decrease in FWD deflections, but this is not apparent.

Section 2

The statistical analyses indicated a significant difference in the W1, W7, and BCI deflection parameters between January and November 2002. Each of these parameters decreased in magnitude between January and November 2002. No significant difference in SCI was apparent. Given the large number of factors influencing the deflections of pavement structure, it is difficult to identify the exact reason for the decrease in FWD deflection. The fact that the SCI did not decrease significantly, however, may indicate that the stiffening of the pavement structure is not directly related to the nature of the surfacing layer. The lower BCI may be an indicator of densification within the base/sub-base layers or strengthening of the subgrade. The latter may be related to moisture conditions within the subgrade. Many of the other pavement sections evaluated exhibited a similar behavior.

Section 3

As for Section 2.

Section 4

A significant decrease in each of the deflection parameters is apparent. The decrease in SCI indicates a relative stiffening or densification of the surfacing layer or upper pavement structure. This may in turn be the reason for the lower W1, W7, and BCI deflection parameters. Traffic-related densification of newly constructed asphalt layers is expected. This tends to stiffen the asphalt layer, which could be the reason for the lower deflections apparent of the section.

Section 5

As for Section 2.

Section 6

The only significant decrease in the deflection parameters on Section 6 is that of SCI. Although there were apparent decreases in the other deflection parameters between January 2002 and November 2002, these were not statistically significant. The difference between the SCI t-statistic and the t-critical values is also on the low side suggesting that although the surfacing layer appeared to densify or stiffen, the magnitude of strengthening was relatively low so as not to significantly influence the deflection of the pavement structure as a whole.

Section 7

Significant decreases in SCI and BCI are apparent on this section. The higher t-statistic determined for the SCI deflections may indicate that the corresponding decrease in BCI is consequential. It is interesting to note that neither W1 nor W7 decreased significantly. It may be concluded that the strengthening of the upper structure of Section 7 did not contribute to the overall deflection of the pavement structure as a whole.

Section 8

As for Section 2.

Section 9

Section 9 behaved differently in that all but the W7 deflections indicate a significant decrease in magnitude. As with Sections 6 and 7, the decrease in SCI could have resulted in a corresponding decrease in some but not all of the parameters evaluated. The fact that the W7 deflections did not decrease significantly over time indicates that the stiffening effect of the asphalt surfacing was not necessarily very effective in reducing the stresses on the subgrade.

5.5 Summary

No specific trends are evident from the FWD deflection data that may be used to infer the relative performance of the mixes on the different sections evaluated. It was found that construction of the new overlay resulted in a decrease in the magnitude and extent of deflections apparent on the old pavement structure but that it does not appear to significantly contribute to the structural capacity of the pavement.

6. RDD Measurements: Overview of the Rolling Dynamic Deflectometer

6.1 Introduction

Researchers at The University of Texas at Austin first developed the rolling dynamic deflectometer (RDD) in the late 1990s. A comprehensive description of the RDD is given in *Development of a Rolling Dynamic Deflectometer for Continuous Deflection Testing of Pavements* (Bay and Stokoe 1998). The RDD as described in this report is a research prototype device that was converted from a Vibroseis, a geophysical exploration tool. A schematic diagram of the RDD is shown in Figure 6.1. This device was developed under Research Project 0-1422 with the cooperation of the Texas Department of Transportation and the Federal Highway Administration.

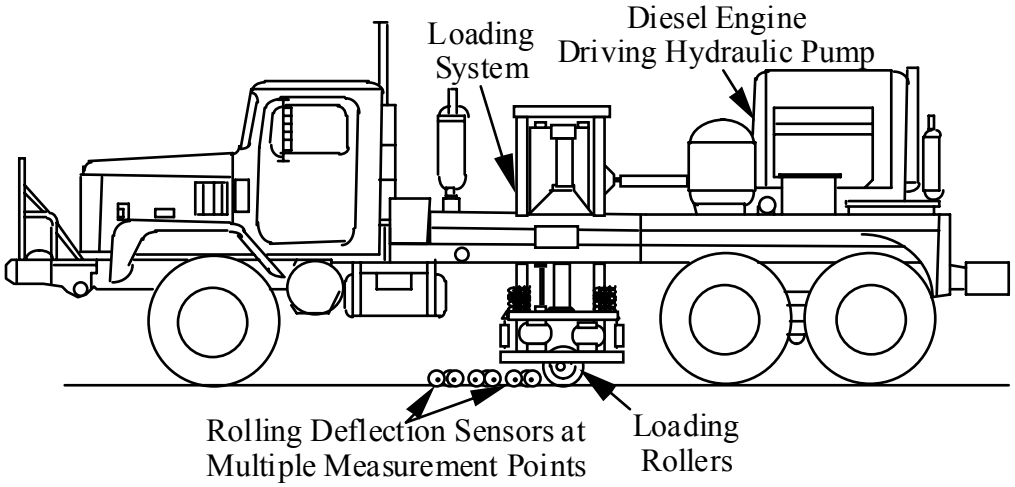

Figure 6.1 Schematic diagram of the major components of the RDD (after Bay 1997)

6.2 RDD Continuous Deflection Profiles

RDD testing was carried out along Interstate Highway 20 near Marshall, Texas at different stages of the asphalt overlay project. RDD data collection was conducted by The University of Texas at Austin under an interagency contract. Until now, RDD continuous deflection profiles were collected at four different stages. These stages are: Stage 1 – before milling off the old asphalt surface, Stage 2 – after milling off the old asphalt layer, Stage 3 – one month after the new overlay, and Stage 4 – eleven months after the new overlay. RDD profiles were obtained at these different stages of the overlay project so that a baseline could be established prior to the overlay, and the pavement response was monitored at

subsequent stages of the project. The schedule of the RDD testing is shown in Table 6.1.

Table 6.1 Schedule of the RDD testing along Interstate Highway 20

	Westbound Lane	**Eastbound Lane**
Stage 1	March 02, 2001	April 05, 2001
Stage 2	August 30, 2001	September 28, 2001
Stage 3	January 08, 2002	January 09, 2002
Stage 4	November 13, 2002	November 14, 2002

To date, the RDD testing has been focused on the westbound and eastbound outside lanes. The RDD continuous deflection profiles were collected along the outside lanes at all four stages of the overlay project. Furthermore, the continuous deflection profile along the westbound inside lane was also collected at stage 1 of the project.

During testing, the RDD applies a static hold-down force and a dynamic force to the pavement with two polyurethane-coated loading rollers. A nominal peak-to-peak dynamic force of 10 kips (44.5 kN) at 35 Hz was used at all stages. However, the nominal static hold-down force varies from 10 – 15 kips (44.5 – 66.7 kN).

The test section under investigation lies between the stations 1135+00 and 1321+00 on the eastbound and westbound lanes of Interstate Highway 20 near Marshall, Texas. The test section is divided into nine different sub-sections, and a different asphalt overlay mix design was used for each sub-section. Four of these sections are located on the westbound side, and the remaining five are located on the eastbound side. Table 6.2 is a summary of the different mix designs and the station limits for each sub-section.

The RDD continuous deflection profiles were collected at all four stages of the overlay project. For each sub-section, sensor #1 deflection readings for each stage are shown in Figures 6.2 to 6.10. By plotting the deflection profiles from different stages alongside each other, the pavement response of the entire test section can be evaluated with a sense of time. For each figure the first graph is for stage 1, the next is stage two, then stage 3 and 4.

Table 6.2 Station limits for overlay mix design on Interstate Highway 20 near Marshall, TX

WESTBOUND INTERSTATE HIGHWAY 20

STATION LIMITS		SECTION	SECTION LENGTH	MIX DESIGN
BEGIN	END			
1135+00	1188+00	3	5,300	SUPERPAVE ½", Quartzite Coarse Aggregate
1188+00	1193+00		500	WEIGHT-IN-MOTION STATION
1193+00	1235+00	8	4,200	TYPE C, Sandstone Coarse Aggregate
1235+00	1278+00	5	4,300	CMHB-C, Sandstone Coarse Aggregate
1278+00	1321+00	2	4,300	SUPERPAVE ½", Sandstone Coarse Aggregate
			18,600	

EASTBOUND INTERSTATE HIGHWAY 20

STATION LIMITS		SECTION	SECTION LENGTH	MIX DESIGN
BEGIN	END			
1135+00	1185+00	6	5,000	CMHB-C, Quartize Coarse Aggregate
1185+00	1190+00		500	WEIGHT-IN-MOTION STATION
1190+00	1218+00	9	2,800	TYPE C, Quartize Coarse Aggregate
1218+00	1245+00	1	2,700	SUPERPAVE, ½", Siliceous Gravel Coarse Aggregate
1245+00	1282+00	4	3,700	CMHB-C, Siliceous Gravel Coarse Aggregate
1282+00	1321+00	7	3,900	TYPE C, Siliceous Gravel Coarse Aggregate
			18,600	

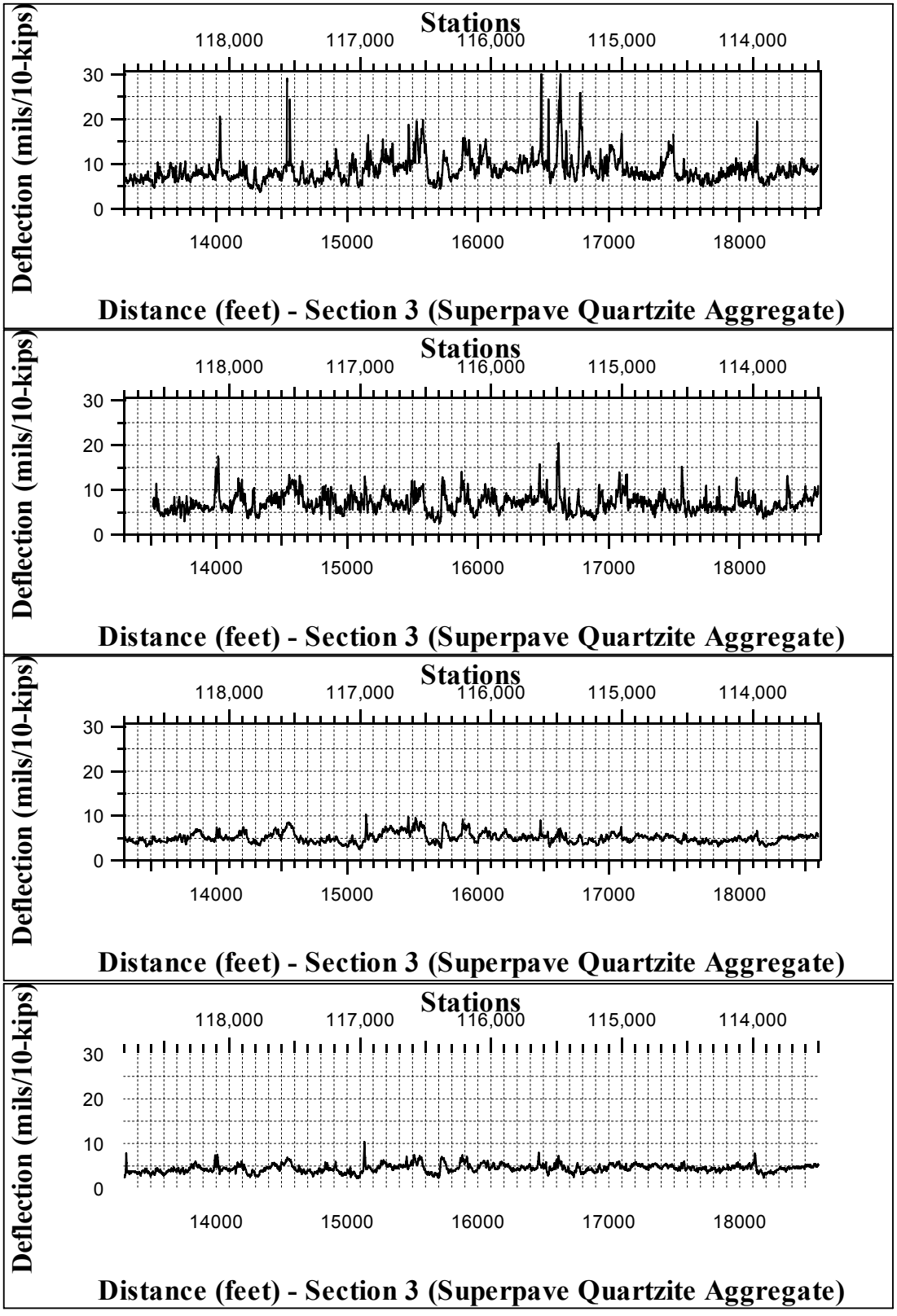

Figure 6.2 RDD deflection profile for Section 3 along Interstate Highway 20

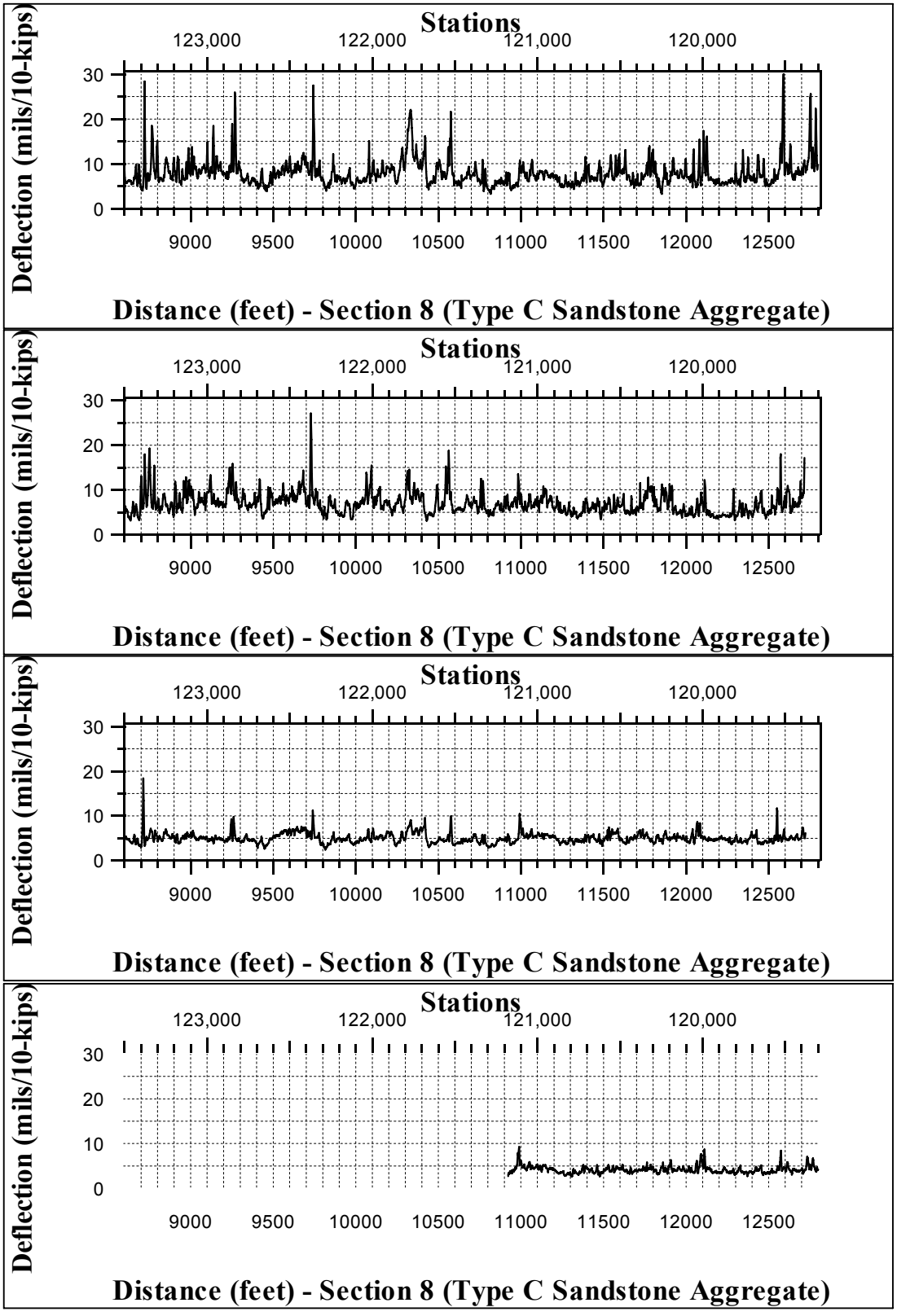

Figure 6.3 RDD deflection profile for Section 8 along Interstate Highway 20

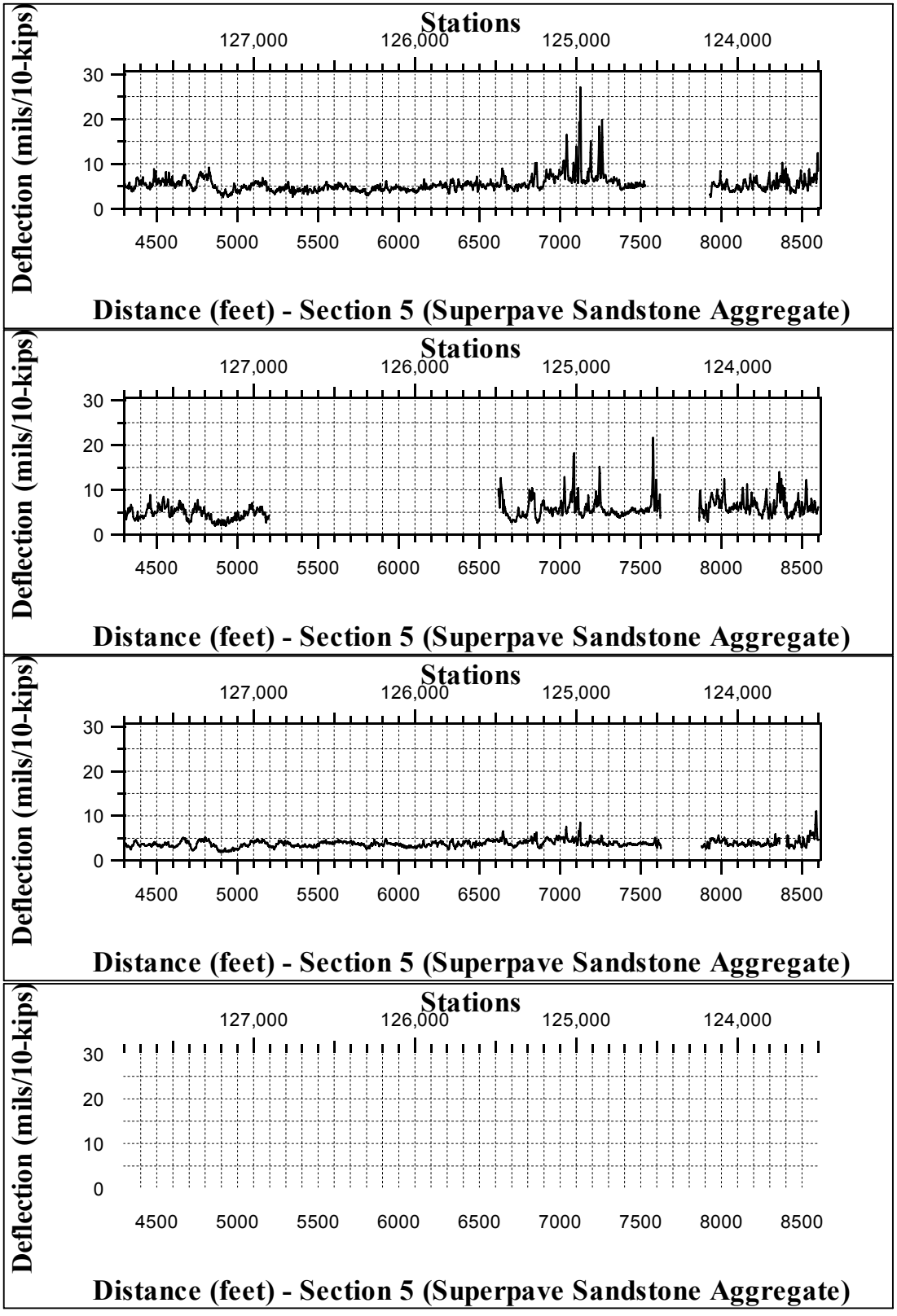

Figure 6.4 RDD deflection profile for Section 5 along Interstate Highway 20

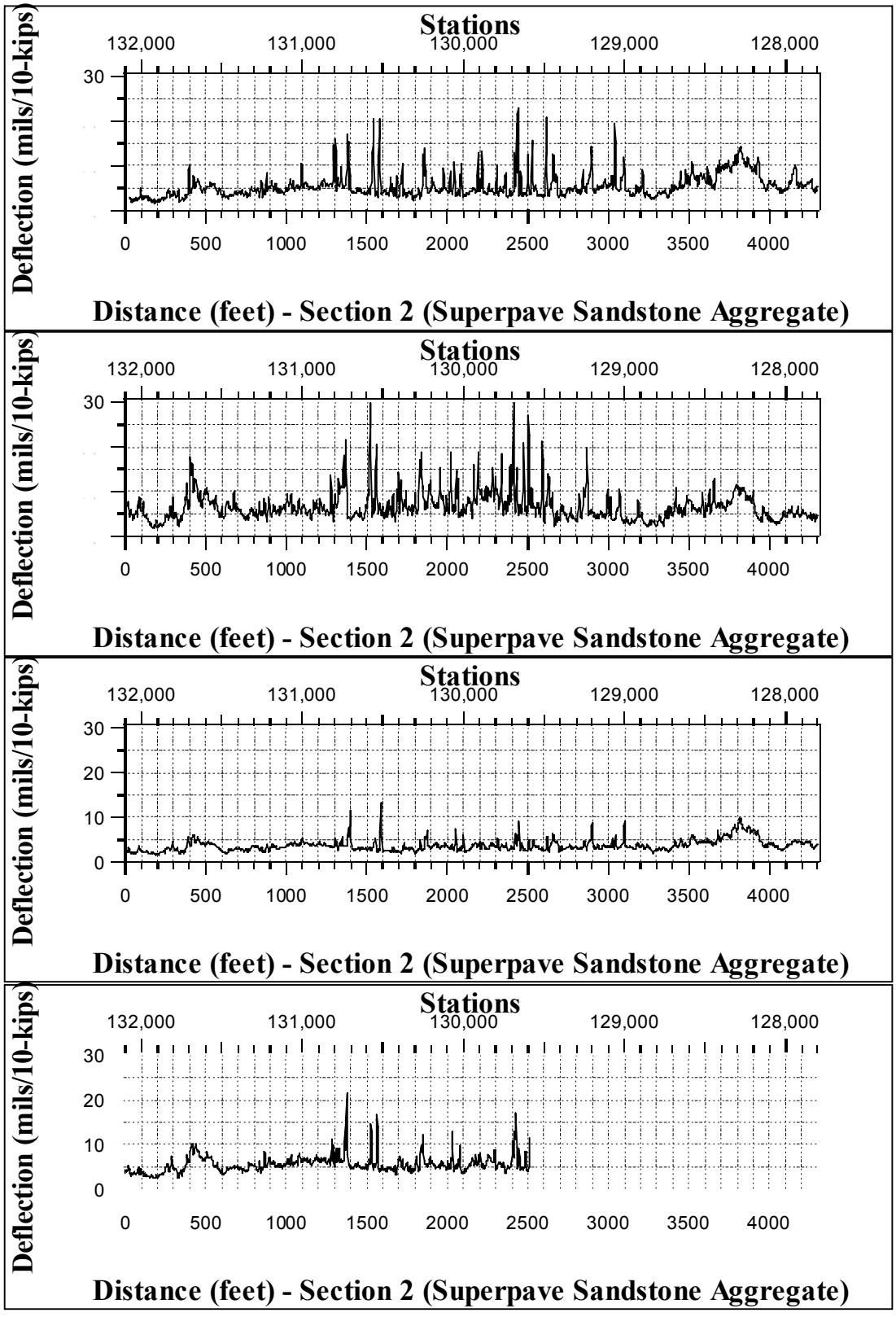

Figure 6.5 RDD deflection profile for Section 2 along Interstate Highway 20

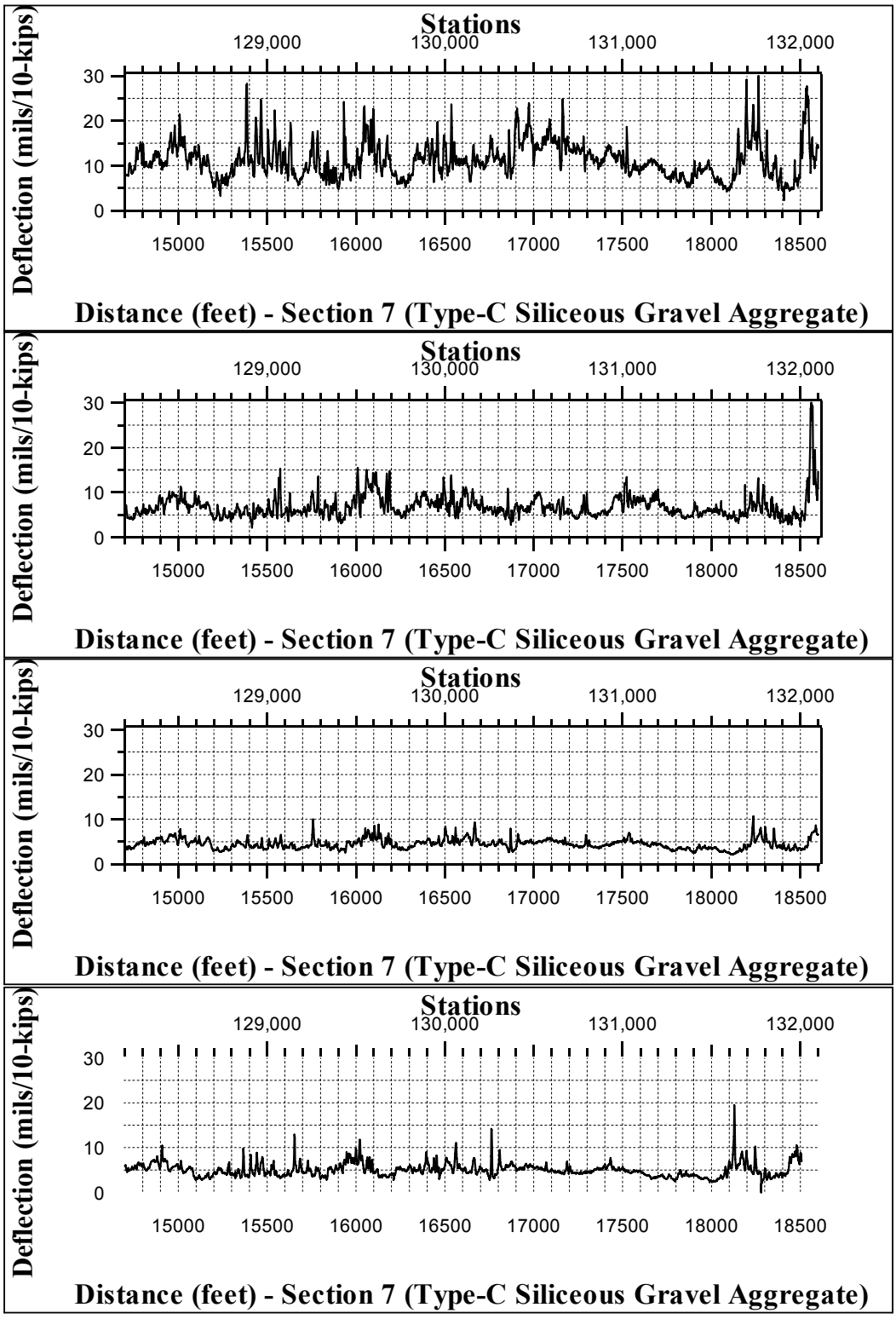

Figure 6.6 RDD deflection profile for Section 7 along Interstate Highway 20

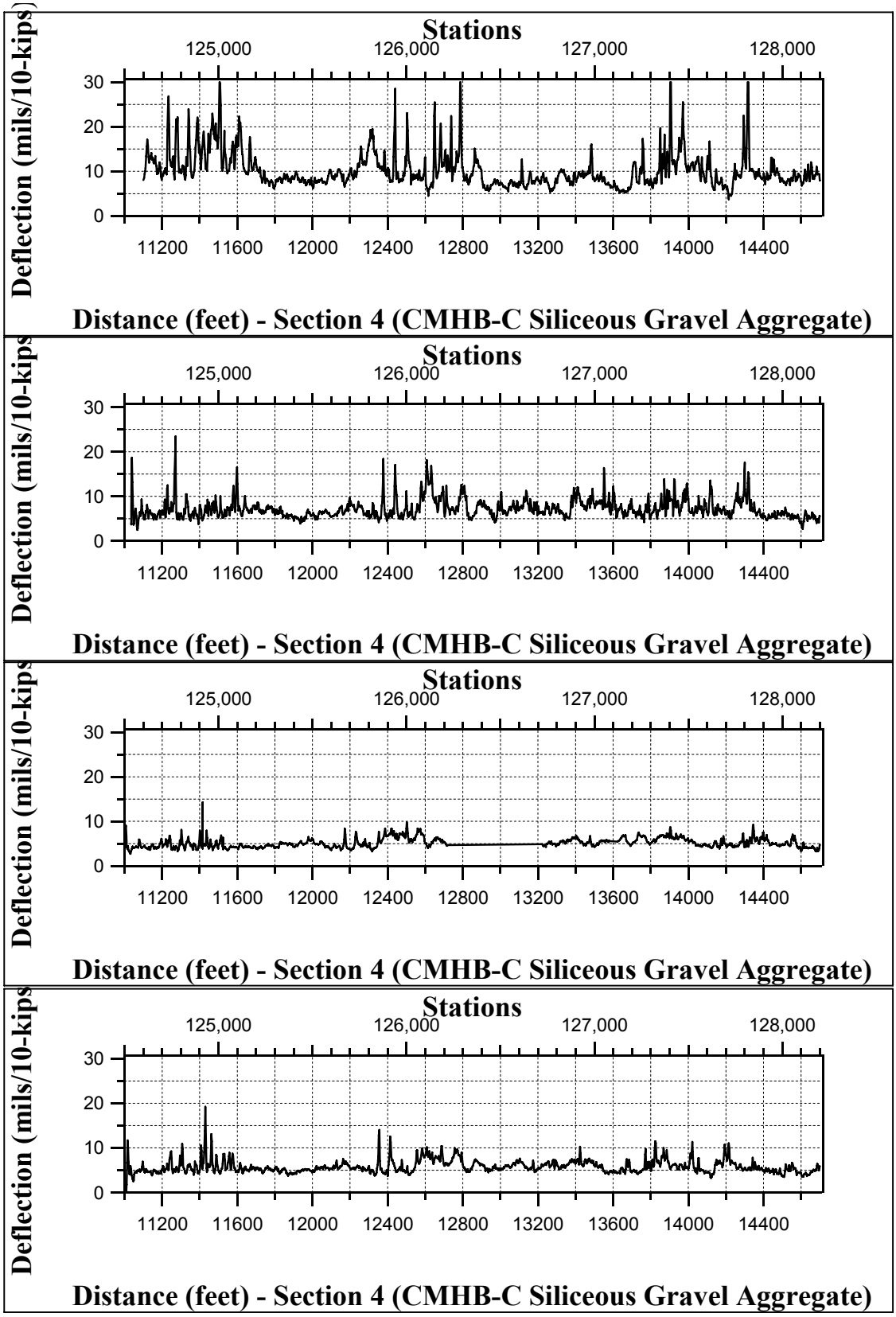

Figure 6.7 RDD deflection profile for Section 3 along Interstate Highway 20

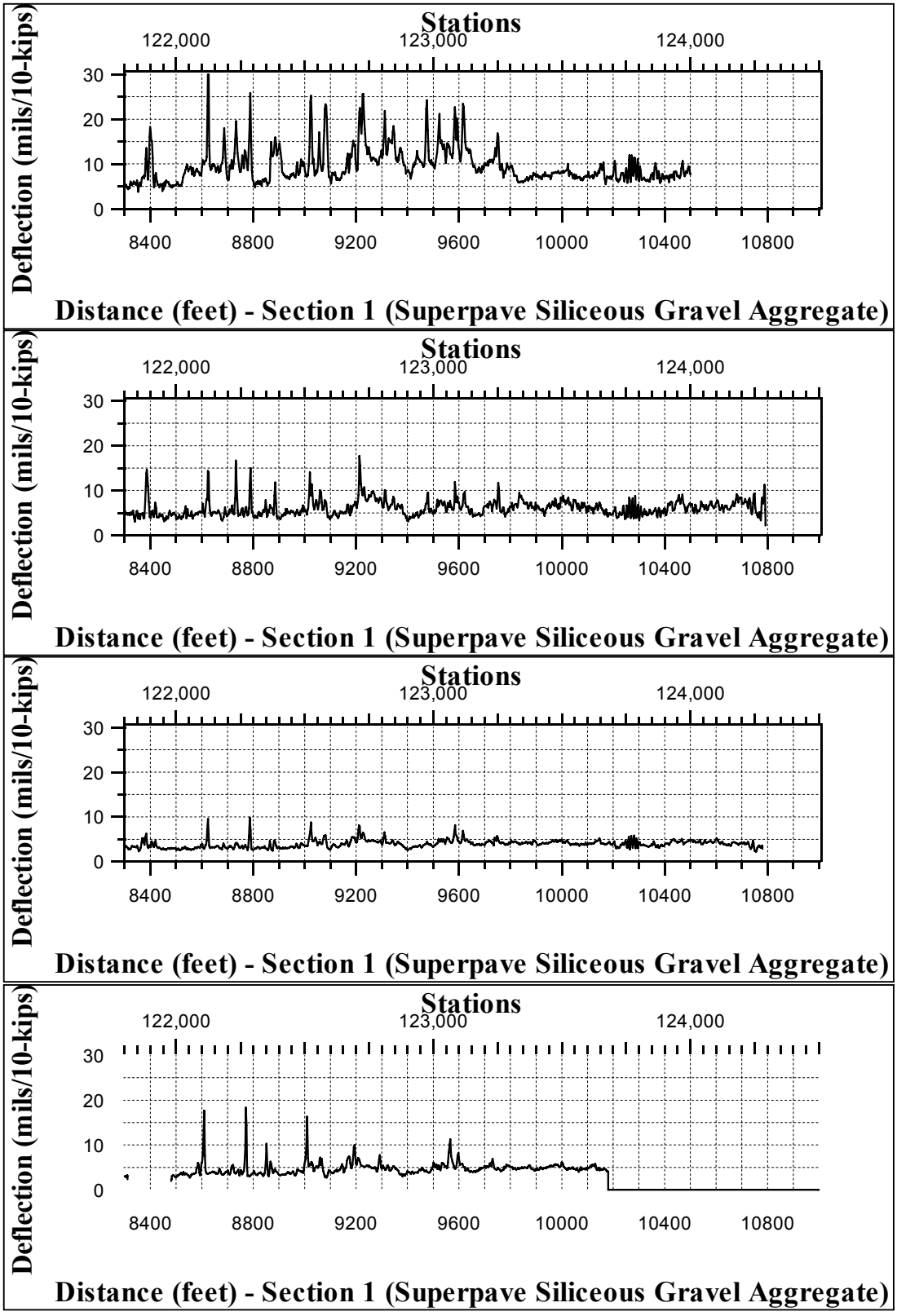

Figure 6.8 RDD deflection profile for Section 1 along Interstate Highway 20

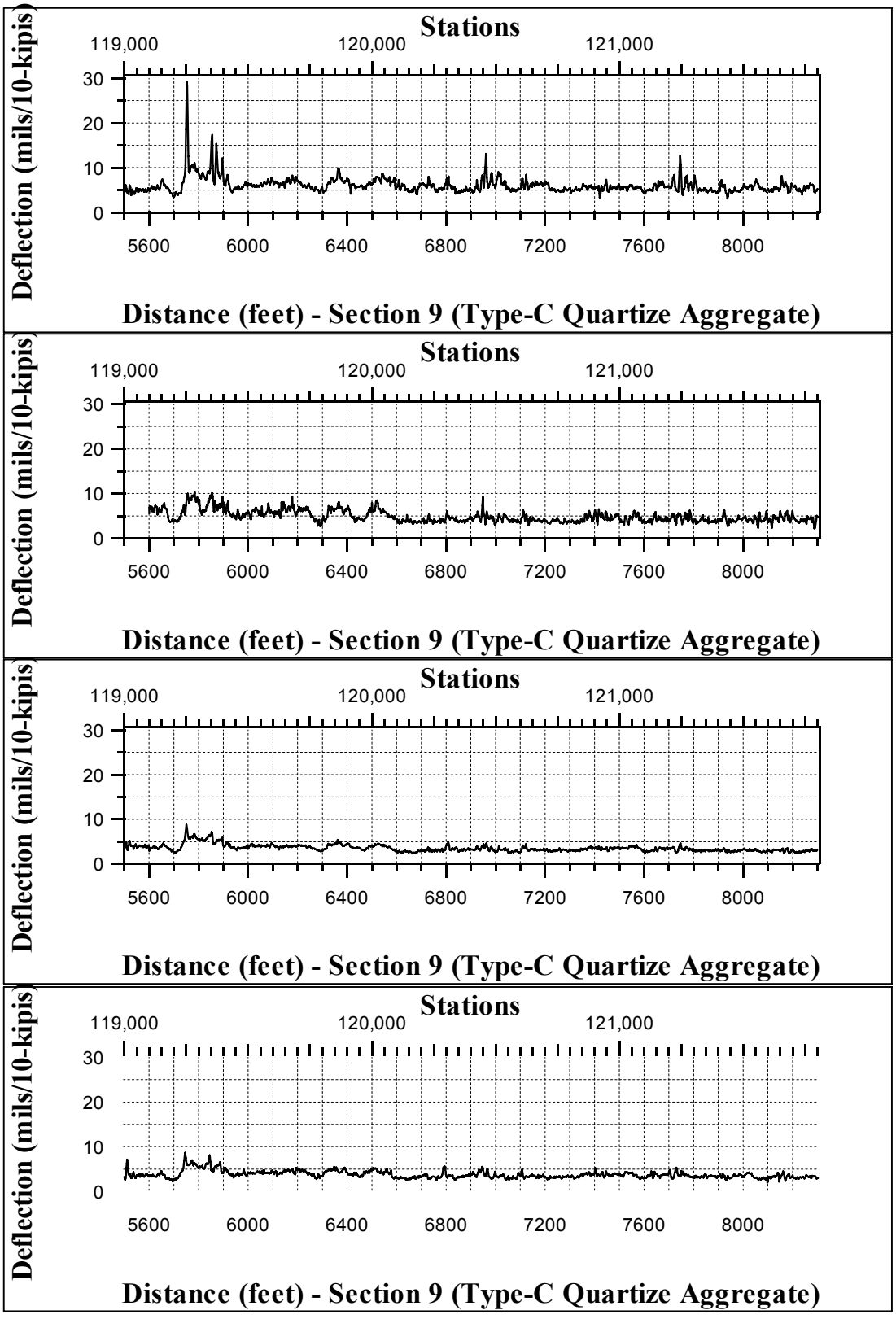

Figure 6.9 RDD deflection profile for Section 9 along Interstate Highway 20

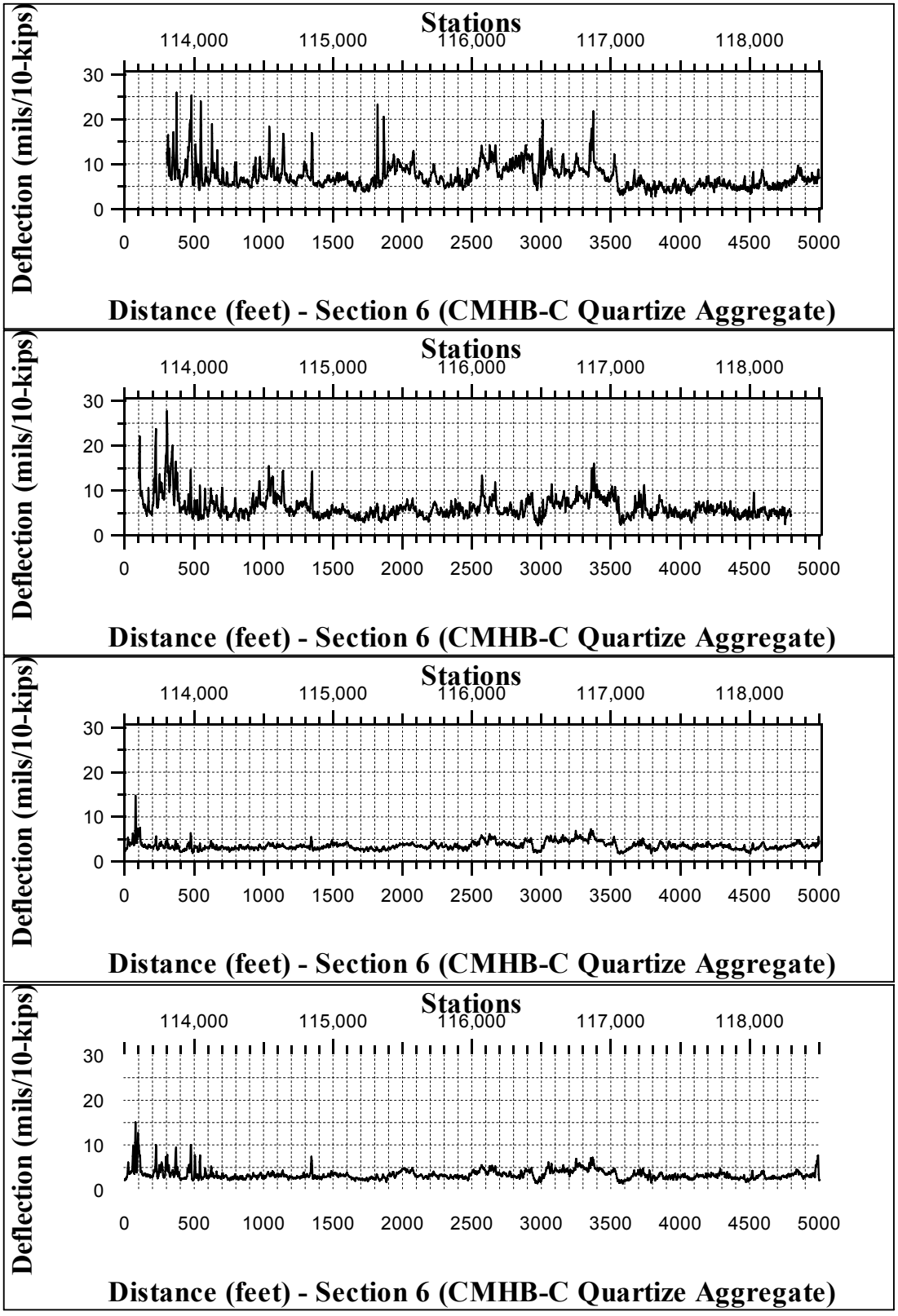

Figure 6.10 RDD deflection profile for Section 6 along Interstate Highway 20

Based on the sensor #1 deflection profiles shown in Figures 6.6 to 6.14, the summary statistics for the different mix design were calculated and shown in Table 6.3. The same information is also shown graphically in Figure 6.15.

Table 6.3 Summary statistics for the RDD deflection profile on Interstate Highway 20

	Limits (ft)		Stage 1		Stage 2		Stage 3		Stage 4	
Section	Begin	End	Mean (μ)	St.dev (δ)	Mean (μ)	St.dev (δ)	Mean (μ)	St.dev (δ)	Mean (μ)	St.dev (δ)
3	0	5300	5.39	2.38	5.82	2.73	3.64	1.26	5.62	1.98
8	5800	10000	6.53	2.72	6.59	2.42	4.40	1.18		
5	10000	14300	7.73	2.66	6.52	2.05	4.99	1.01	3.97	0.90
2	14300	18600	8.91	2.99	7.14	2.09	5.14	1.15	4.51	0.94

	Limits (ft)		Stage 1		Stage 2		Stage 3		Stage 4	
Section	Begin	End	Mean (μ)	St.dev (δ)	Mean (μ)	St.dev (δ)	Mean (μ)	St.dev (δ)	Mean (μ)	St.dev (δ)
6	0	5000	7.29	2.76	5.89	2.32	3.60	0.89	3.39	1.12
9	5500	8300	5.96	1.76	4.85	1.32	3.54	0.79	3.67	0.88
1	8300	11000	9.16	3.86	5.65	1.86	3.96	0.87	4.56	1.62
4	11000	14700	9.90	3.96	7.20	2.15	5.15	1.12	5.63	1.63
7	14700	18600	10.98	4.10	6.23	2.65	4.50	1.15	4.61	1.81

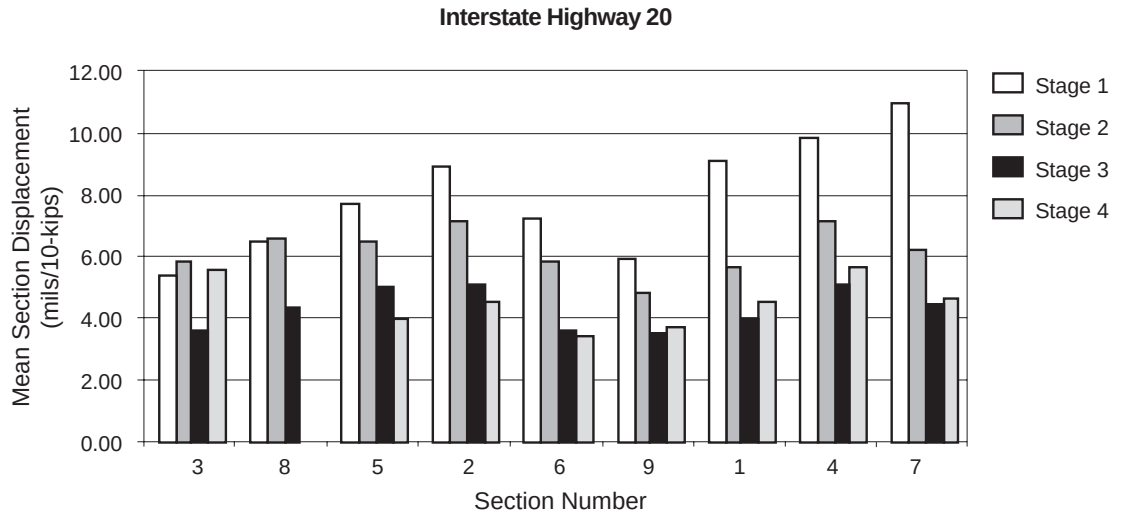

a) Mean Displacement

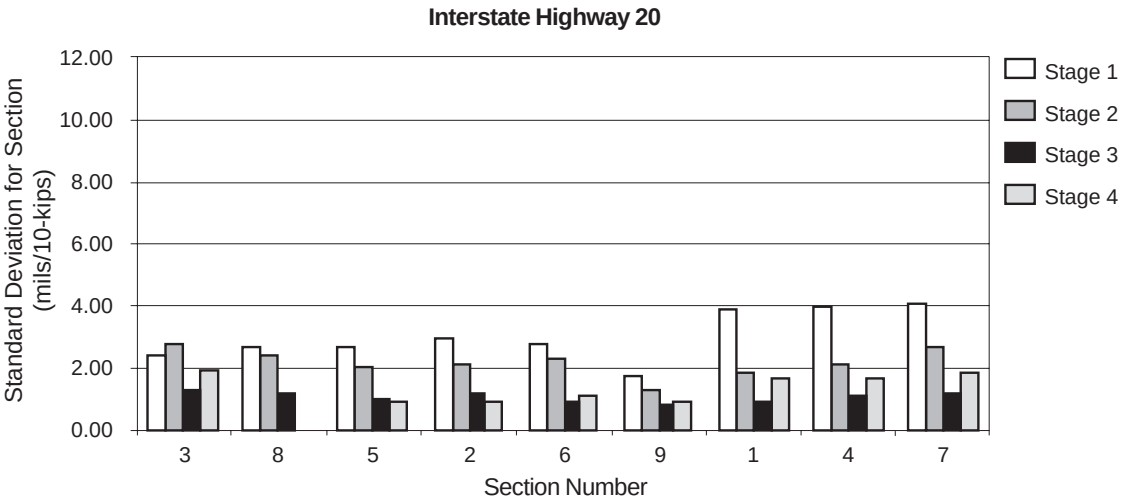

b) Standard Deviation

Figure 6.11 Summary statistics of the RDD continuous deflection profile

7. PSPA Measurements

Three series of portable seismic pavement analyzer (PSPA) measurements were done on the IH-20 sections being evaluated in Harrison County. Section details as well as the different mixes used on the sections are outlined in Appendix D. The first series of PSPA tests were done directly on top of the concrete pavement after the old overlay had been milled off. A second series of tests was done after construction of the new pavement sections in January 2002 and a third in November 2002. In addition, laboratory V-meter tests were done on cores removed from the pavement sections in March 2002. This chapter reports and discusses the results of the different PSPA tests.

The results of the first series of PSPA tests done directly on the concrete pavement are summarized in Figures 7.1 and 7.2, for tests on the east- and westbound lanes of IH-20 respectively. The figures indicate that for both the east- and westbound lanes, the measured concrete moduli values along the lanes were fairly uniform ranging between 4,000 and 6,000 ksi.

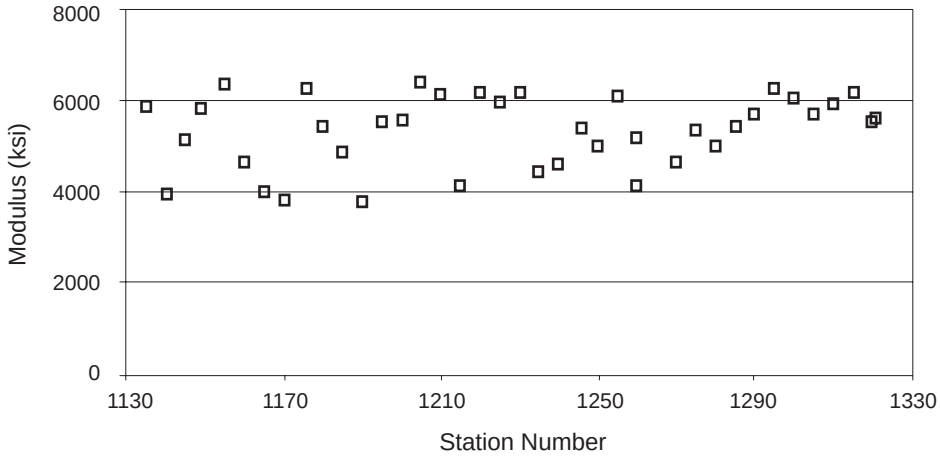

Figure 7.1 PSPA measurements on the concrete pavement, eastbound on IH-20

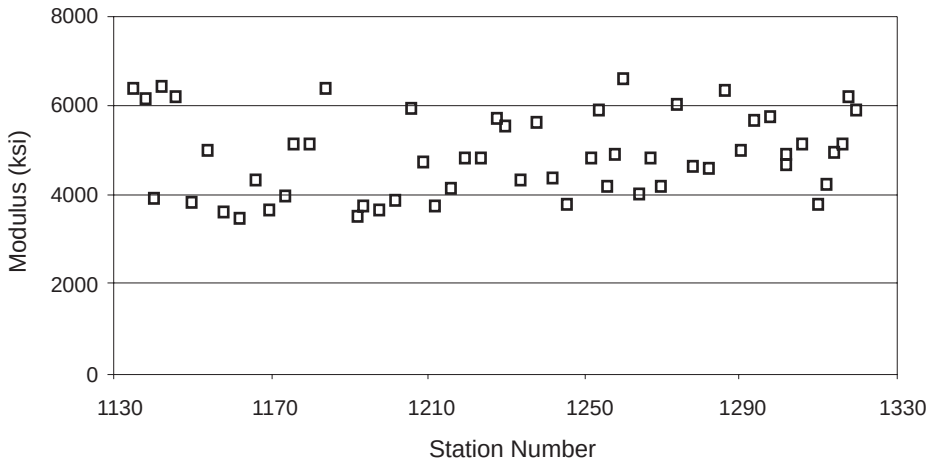

Figure 7.2 PSPA measurements on the concrete pavement, westbound on IH-20

Table 7.1 summarizes the modulus measurements done on the cores in the lab taken from the different sections, as well the measurements done in the field during January and November 2002. A V-meter was used to measure small strain modulus in the laboratory. The average (Avg), minimum (min) and maximum (max) range of the moduli values as well as the coefficients of variation (C.V.) for the PSPA tests on the different sections are shown. Modulus values shown have been adjusted to a temperature of 77 ° F and frequency of 30 Hz.

Table 7.1 Summary of PSPA measurements on sections of IH-20

Section Number	LAB (Cores) - Mar. 2002				PSPA – Jan. 2002				PSPA - Nov. 2002			
	Avg	Min	Max	C.V.	**Avg**	Min	Max	C.V.	**Avg**	Min	Max	C.V.
	Ksi	ksi	ksi	%	**ksi**	ksi	ksi	%	**ksi**	ksi	Ksi	%
1	**575**	518	630	9.2	**577**	470	659	10.8	**583**	469	733	11.1
2	**593**	563	626	5.2	**560**	487	660	5.9	**564**	412	725	11.8
3	**625**	591	669	10.7	**622**	545	832	7.7	**563**	409	792	16.0
4	**662**	618	688	4.8	**683**	515	799	12.0	**659**	471	851	14.0
5	**516**	501	539	3.2	**515**	487	660	8.6	**513**	394	634	10.8
6	**507**	432	567	11.2	**608**	395	704	13.4	**549**	397	651	12.3
7	**637**	632	645	0.9	**572**	381	698	11.5	**656**	505	743	8.9
8	**542**	508	565	4.8	**531**	437	633	8.0	**510**	421	662	13.0
9	**589**	574	606	2.7	**566**	460	618	7.2	**517**	369	622	11.4

Figure 7.3 shows the difference in the average moduli measurements done on the different sections in January and November 2002. It can be seen that on average for all the sections evaluated, the moduli values decreased slightly from January to November 2002 and that with the clear exception of Section 7, the average moduli values generally decreased for the different sections from January to November. This is contrary to expectations since the modulus of asphalt generally increases with ageing over time and densification under trafficking.

To explore this finding further, a statistical analysis of the difference between the modulus measurements in January and November 2002 was done applying a t-test with the null hypothesis being that there was no difference between the mean moduli in January and November at the 95 percent confidence level and assuming unequal variances. Results of these analyses are shown in Table 7.2. From the table it can be seen that the null hypothesis is rejected on Section 3, on the westbound lanes and Sections 6, 7, and 9 eastbound.

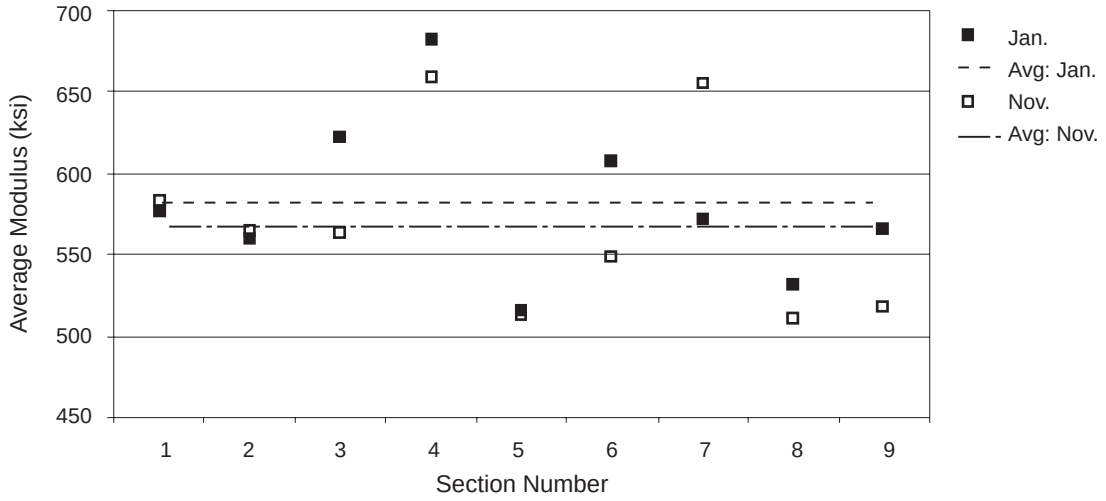

Figure 7.3 Mean January and November 2002 PSPA measurements on IH-20 sections

Table 7.2 Statistical analyses results to determine the significance difference in PSPA modulus means between January and November 2002

Section	1	2	3	4	5	6	7	8	9
df	48	69	36	69	80	89	77	48	37
t Stat	-0.776	-0.356	3.214	0.635	0.105	4.278	-6.373	1.555	2.716
t Crit	2.011	1.995	2.028	1.995	1.990	1.987	1.991	2.011	2.026
p-value	0.442	0.723	0.003	0.528	0.917	0.000	0.000	0.127	0.010
Null	Accept	Accept	Reject	Accept	Accept	Reject	Reject	Accept	Reject

Based on the results of the PSPA tests, it may be concluded that with the exception of Section 7, there was not a significant increase in asphalt modulus of the sections evaluated between January and November 2002. The increase in modulus of Section 7 may be as a result of densification of this section.

8. Conclusions

In this project, nine asphalt mixes with underlying Type B base mixture were placed on the test sections on IH-20 in Harrison County. Superpave, CMHB-C, and Type C mix designs and siliceous gravel, sandstone, and quartzite aggregates were used for the construction of the test sections. PG 76-22 asphalt binder was used for all mixtures.

The project was scheduled to continue for 5 years. During this period field performances will be monitored using nondestructive devices, and visual surveys will be carried out. The laboratory tests already have been completed and the data was presented in research reports 0-4185-1 and 0-4185-2. This report summarizes the visual pavement condition survey and the FWD, PSI, and RDD measurements collected at the test sections in the third year of the study. At the end of five years, all information from field and laboratory tests will be assembled and compared. It will be determined if the HWTD could properly predict the performance of the overlays under field conditions; and the correlations will be developed between the HWTD and the field performance data.

References

Aschenbrener, T., and G. Currier. 1993. *Influence of Testing Variables on the Results from the Hamburg Wheel Tracking Device.* CDOT-DTD-R-93-22 Colorado Department of Transportation.

Bay, James A. 1997. "Development of a Rolling Dynamic Deflectometer for Continuous Deflection Testing of Pavements." Ph.D. diss., University of Texas, Austin.

Bay, James A., and K. Stokoe II. 1998. *Development of a Rolling Dynamic Deflectometer for Continuous Deflection Testing of Pavements.* Project Summary Report 1422-3F. Austin, Tex.: University of Texas, Center for Transportation Research.

Hines, M. 1991. *The Hamburg Wheel Tracking Device*. Proceedings of the Twenty-Eighth Paving and Transportation Conference, Civil Engineering Department, University of New Mexico, Albuquerque.

Molenaar, A. A. A. 1997. *Pavement Evaluation and Overlay Design Using Falling Weight Deflectometer and Other Deflection Measurement Devices.* Delft University of Technology, Advanced Course on Pavement Evaluation, University of Stellenbosch.

Mogawer, W. S., and K. D. Stuart. 1995. *Effect of Coarse Aggregate Content on Stone Matrix Asphalt.* Transportation Research Record 1492. Washington, D.C.: TRB, National Research Council, January 1995, pp. 1–11.

Roberts, F. L., P. S. Kandhal, D. Lee, and T. W. Kennedy. 1991. *Hot Mix Asphalt Materials, Mixture Design and Construction, 2nd Edition*. National Center for Asphalt Technology. Lanham, MD: NAPA Research and Education Foundation.

Yildirim, Y., T. W. Kennedy. 2001. *Correlation of Field Performance to Hamburg Wheel Tracking Device Results.* Research Report 0-4185-1. Austin, Tex.: University of Texas, Center for Transportation Research.

Yildirim, Y., T. W. Kennedy. 2002. *Hamburg Wheel Tracking Device Results on Plant and Field Cores Produced Mixtures.* Research Report 0-4185-2. Austin, Tex.: University of Texas, Center for Transportation Research.

Appendix A:

Crack Pictures on Westbound Lane

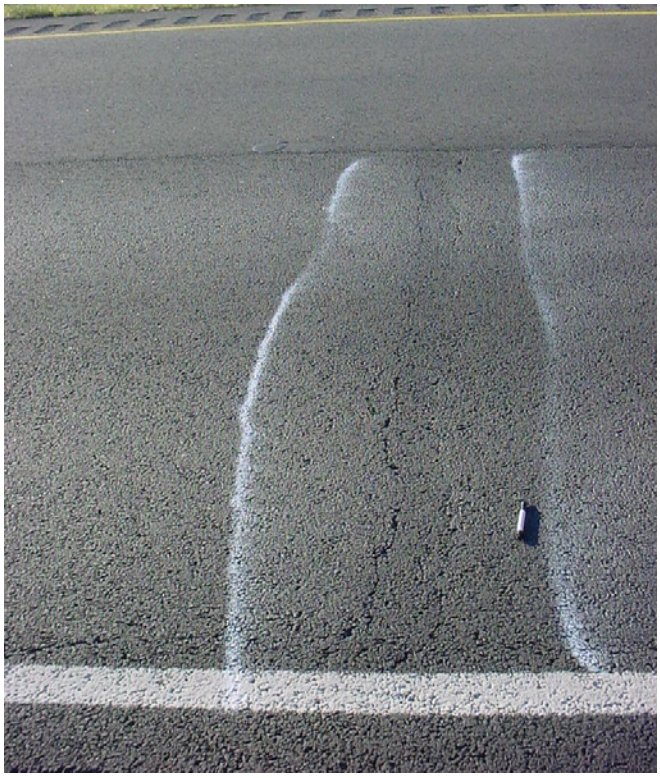

Figure A.1 WBP1TC

Figure A.2 WBP2ATC

Figure A.3 WBP3ARC

Figure A.4 WBP4AP

Figure A.5 WBP5ATC

Figure A.6 WBP6ATC

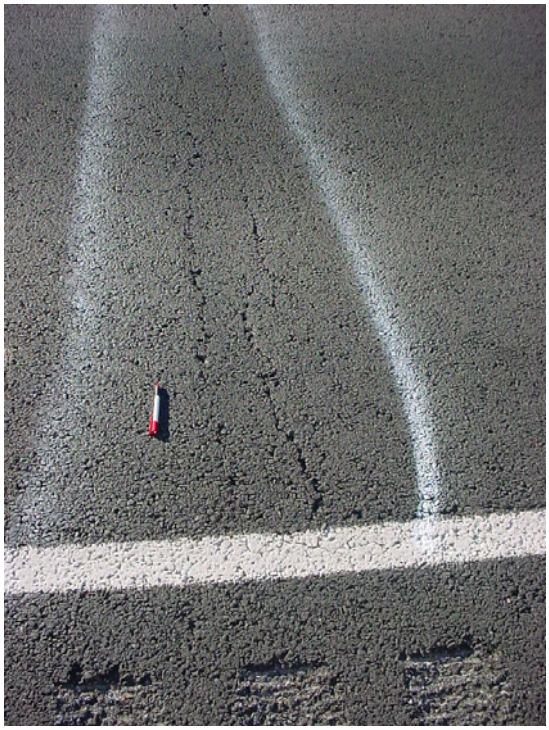

Figure A.7 WBP7ATC

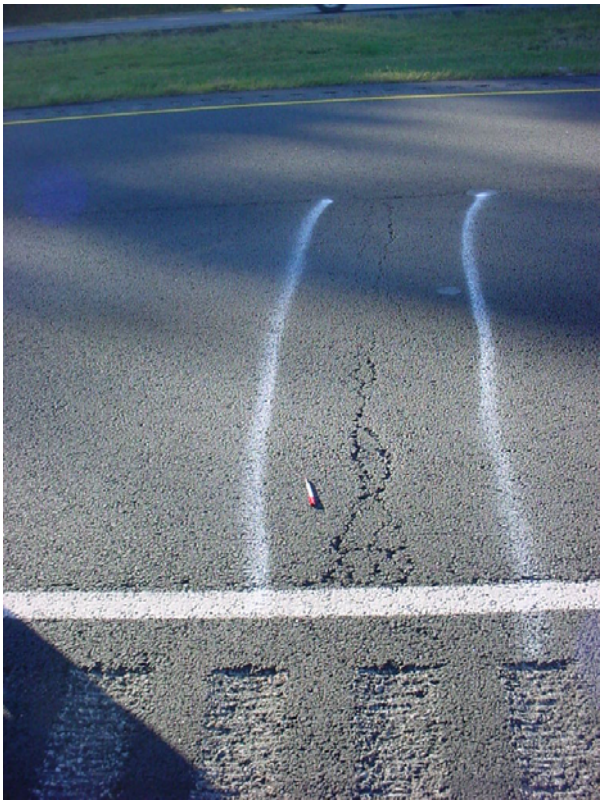

Figure A.8 WBP8ATC

Figure A.9 WBP9ATC

Figure A.10 WBP10ATC

Figure A.11 WBP11TC

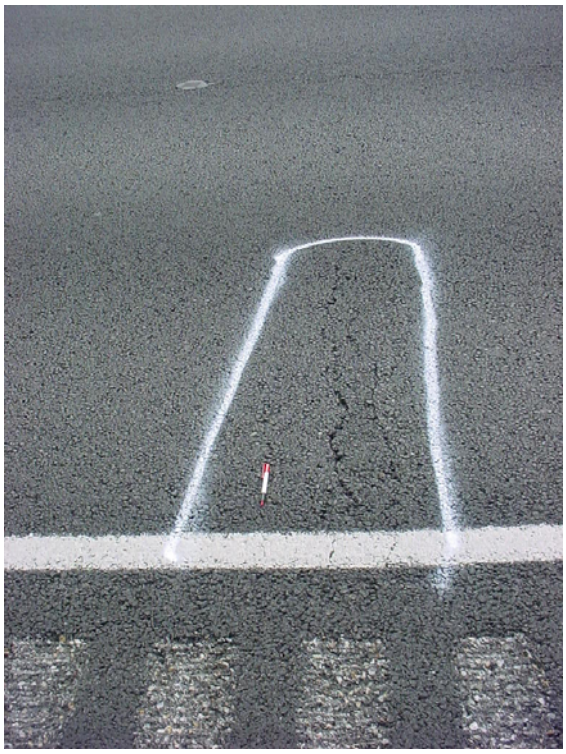

Figure A.12 WBP12TC

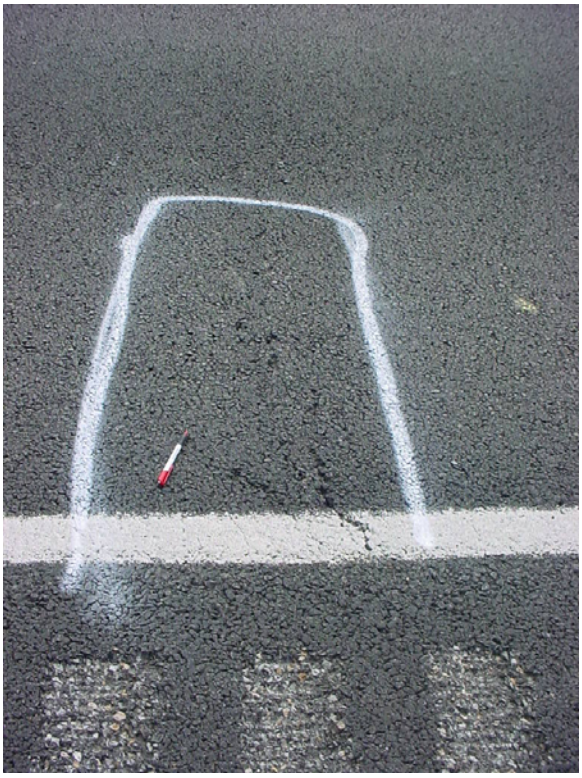

Figure A.13 WBP13TC

Figure A.14 WBP14AP

Figure A.15 WBP15BTC

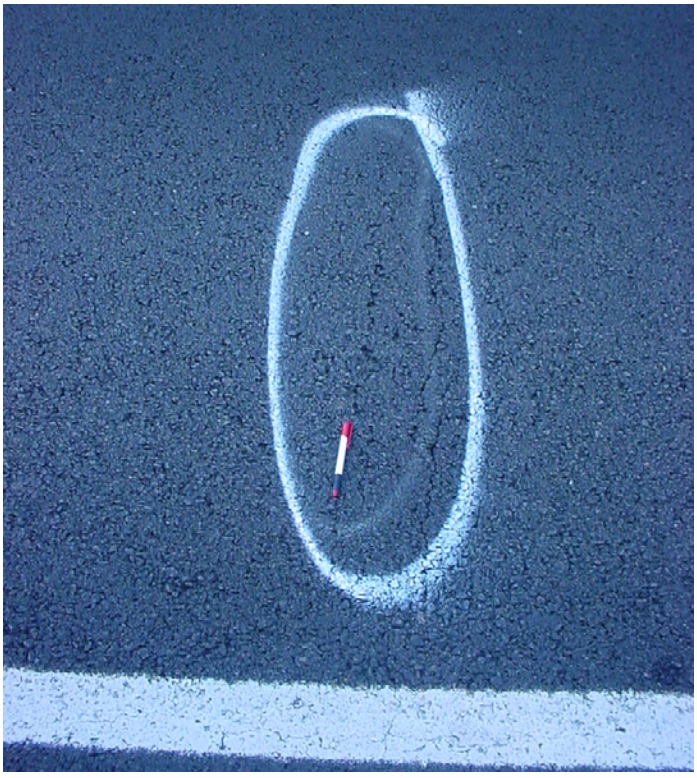

Figure A.16 WBP16TC

Figure A.17 WBP17ATC

Figure A.18 WBP18CTC

Figure A.19 WBP19TC

Figure A.20 WBP20TC

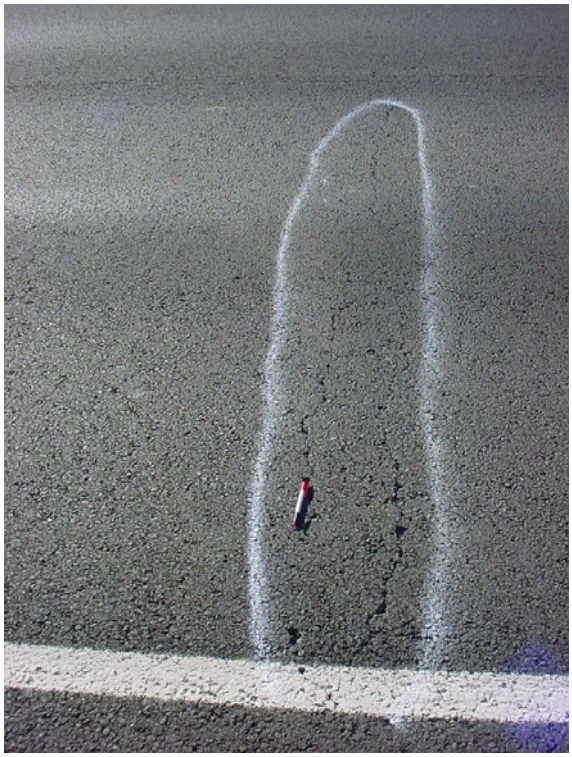

Figure A.21 WBP21TC

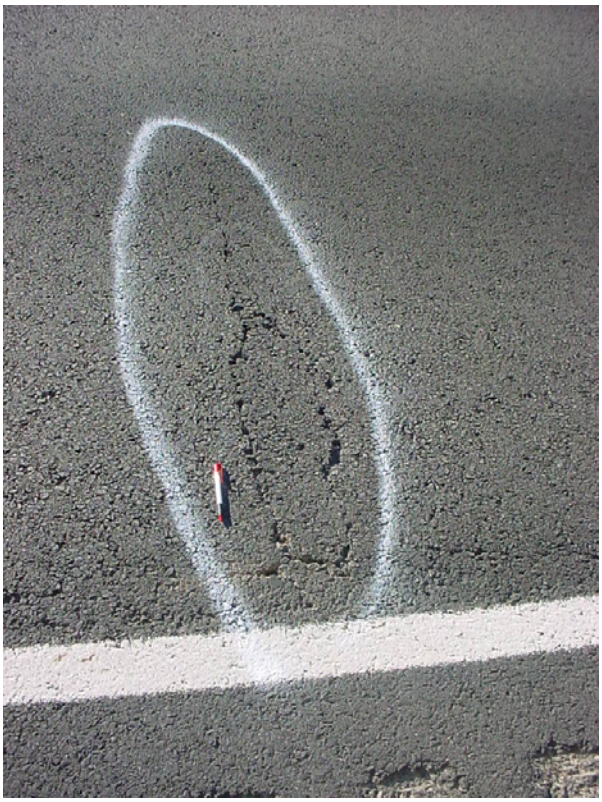

Figure A.22 WBP22TC

Figure A.23 WBP23TC

Appendix B:

PSI Values

Table B.1 PSI values on westbound IH-20 outside lane

Distance (mi)	Milepost	Station	PSI-FINISHED	PSI-NOV2002	
0.10	613.90	1326.28	4.2	4.23	
0.20	613.80	1321.00	4.11	3.94	
0.30	613.70	1315.72	4.02	3.88	SECTION 2
0.40	613.60	1310.44	4.47	4.49	
0.50	613.50	1305.16	4.17	4.05	
0.60	613.40	1299.88	4.65	4.71	
0.70	613.30	1294.60	4.46	4.55	
0.80	613.20	1289.32	4.62	4.71	
0.90	613.10	1284.04	4.34	4.49	
1.00	613.00	1278.76	4.36	4.36	
1.10	612.90	1273.48	4.57	4.26	SECTION 5
1.20	612.80	1268.20	4.59	4.7	
1.30	612.70	1262.92	4.36	4.49	
1.40	612.60	1257.64	4.5	4.53	
1.50	612.50	1252.36	4.3	4.34	
1.60	612.40	1247.08	4.44	4.35	
1.70	612.30	1241.80	4.29	4.26	
1.80	612.20	1236.52	4.21	4.21	
1.90	612.10	1231.30	4.7	4.51	SECTION 8
2.00	612.00	1226.02	4.67	4.73	
2.10	611.90	1220.74	4.58	4.41	
2.20	611.80	1215.46	4.45	4.4	
2.30	611.70	1210.18	4.66	4.29	
2.40	611.60	1204.90	4.68	4.58	
2.50	611.50	1199.62	4.76	4.4	
2.60	611.40	1194.34	4.71	4.57	
2.70	611.30	1189.06	3.85	3.98	
2.80	611.20	1183.78	4.55	4.25	SECTION 3
2.90	611.10	1178.50	4.72	4.71	
3.00	611.00	1173.22	4.53	4.82	
3.10	610.90	1167.94	4.77	4.72	
3.20	610.80	1162.66	4.65	4.79	
3.30	610.70	1157.38	4.7	4.72	
3.40	610.60	1152.10	4.64	4.66	
3.50	610.50	1146.82	4.59	4.64	
3.60	610.40	1141.54	4.75	4.62	
3.70	610.30	1136.26	4.77	4.8	
3.80	610.20	1130.98	4.25	4.57	
3.90	610.10	1125.70	4.85	4.7	
4.00	610.00	1120.42	4.86	4.69	

Table B.2 PSI values on westbound IH-20 inside lane

Distance (mi)	Milepost	Station	PSI-FINISHED	PSI-NOV2002	
0.10	613.90	1326.28	4.75	4.35	
0.20	613.80	1321.00	4.4	4.12	
0.30	613.70	1315.72	3.91	4.28	SECTION 2
0.40	613.60	1310.44	4.22	4.21	
0.50	613.50	1305.16	4.21	4.31	
0.60	613.40	1299.88	4.25	4.33	
0.70	613.30	1294.60	4.46	4.6	
0.80	613.20	1289.32	4.38	4.61	
0.90	613.10	1284.04	4.21	4.48	
1.00	613.00	1278.76	4.19	4.08	
1.10	612.90	1273.48	4.51	4.66	SECTION 5
1.20	612.80	1268.20	4.27	4.33	
1.30	612.70	1262.92	4.18	4.34	
1.40	612.60	1257.64	4.22	4.25	
1.50	612.50	1252.36	4.28	4.21	
1.60	612.40	1247.08	4.2	4.22	
1.70	612.30	1241.80	4.13	4.22	
1.80	612.20	1236.52	3.96	3.85	
1.90	612.10	1231.30	4.19	4	SECTION 8
2.00	612.00	1226.02	4.17	4.16	
2.10	611.90	1220.74	4	3.91	
2.20	611.80	1215.46	4.12	3.88	
2.30	611.70	1210.18	4.37	3.98	
2.40	611.60	1204.90	3.66	3.62	
2.50	611.50	1199.62	4.15	3.93	
2.60	611.40	1194.34	4.48	4.38	
2.70	611.30	1189.06	3.93	4.08	
2.80	611.20	1183.78	4.37	4.31	SECTION 3
2.90	611.10	1178.50	4.35	4.48	
3.00	611.00	1173.22	4.73	4.82	
3.10	610.90	1167.94	4.67	4.55	
3.20	610.80	1162.66	4.25	4.56	
3.30	610.70	1157.38	4.53	4.63	
3.40	610.60	1152.10	4.6	4.64	
3.50	610.50	1146.82	4.34	4.26	
3.60	610.40	1141.54	4.71	4.55	
3.70	610.30	1136.26	4.65	4.66	
3.80	610.20	1130.98	4.53	4.72	
3.90	610.10	1125.70	4.87	4.81	
4.00	610.00	1120.42	4.88	4.79	

Table B.3 PSI values on eastbound IH-20 outside lane

Distance (mi)	Milepost	Station	PSI-FINISHED	PSI-NOV2002	
0.10	610.10	1125.64	4.7	4.44	
0.20	610.20	1130.92	4.81	4.68	
0.30	610.30	1136.20	4.23	4.09	
0.40	610.40	1141.48	4.1	4.08	SECTION 6
0.50	610.50	1146.76	4.45	4.69	
0.60	610.60	1152.04	4.55	4.58	
0.70	610.70	1157.32	4.82	4.79	
0.80	610.80	1162.60	4.6	4.65	
0.90	610.90	1167.88	4.43	4.35	
1.00	611.00	1173.16	4.33	4.26	
1.10	611.10	1178.44	4.48	4.54	SECTION 9
1.20	611.20	1183.72	4.62	4.58	
1.30	611.30	1189.00	3.81	3.84	
1.40	611.40	1194.28	4.4	4.3	
1.50	611.50	1199.56	4.81	4.71	
1.60	611.60	1204.84	4.61	4.45	
1.70	611.70	1210.12	4.48	4.39	
1.80	611.80	1215.40	4.73	4.5	SECTION 1
1.90	611.90	1220.63	4.34	4.15	
2.00	612.00	1225.91	4.46	4.36	
2.10	612.10	1231.19	4.68	4.77	
2.20	612.20	1236.47	4.8	4.78	
2.30	612.30	1241.75	4.64	4.61	
2.40	612.40	1247.03	4.34	4.37	
2.50	612.50	1252.31	4.77	4.72	SECTION 4
2.60	612.60	1257.59	4.74	4.87	
2.70	612.70	1262.87	4.57	4.49	
2.80	612.80	1268.15	4.73	4.72	
2.90	612.90	1273.43	4.66	4.8	
3.00	613.00	1278.71	4.74	4.69	
3.10	613.10	1283.99	4.48	4.69	
3.20	613.20	1289.27	4.39	4.39	SECTION 7
3.30	613.30	1294.55	4.3	4.05	
3.40	613.40	1299.83	4.15	4.3	
3.50	613.50	1305.11	4.36	4.37	
3.60	613.60	1310.39	4.71	4.69	
3.70	613.70	1315.67	4.8	4.83	
3.80	613.80	1320.95	4.58	4.82	
3.90	613.90	1326.23	4.5	4.37	

Table B.4 PSI values on eastbound IH-20 inside lane

Distance (mi)	Milepost	Station	PSI-FINISHED	PSI-NOV2002	
0.10	610.10	1125.64	4.76	4.72	
0.20	610.20	1130.92	4.77	4.68	
0.30	610.30	1136.20	4.42	4.34	
0.40	610.40	1141.48	4.43	4.49	SECTION 6
0.50	610.50	1146.76	4.49	4.42	
0.60	610.60	1152.04	4.57	4.64	
0.70	610.70	1157.32	4.76	4.81	
0.80	610.80	1162.60	4.65	4.62	
0.90	610.90	1167.88	4.71	4.7	
1.00	611.00	1173.16	4.62	4.72	
1.10	611.10	1178.44	4.65	4.68	SECTION 9
1.20	611.20	1183.72	4.54	4.43	
1.30	611.30	1189.00	4.06	4.04	
1.40	611.40	1194.28	4.25	4.06	
1.50	611.50	1199.56	4.45	4.53	
1.60	611.60	1204.84	4.72	4.55	
1.70	611.70	1210.12	4.58	4.55	
1.80	611.80	1215.40	4.65	4.54	SECTION 1
1.90	611.90	1220.63	4.12	4.23	
2.00	612.00	1225.91	4.61	4.46	
2.10	612.10	1231.19	4.67	4.81	
2.20	612.20	1236.47	4.57	4.48	
2.30	612.30	1241.75	4.75	4.75	
2.40	612.40	1247.03	4.26	4.28	
2.50	612.50	1252.31	4.68	4.52	SECTION 4
2.60	612.60	1257.59	4.76	4.85	
2.70	612.70	1262.87	4.32	4.62	
2.80	612.80	1268.15	4.66	4.72	
2.90	612.90	1273.43	4.65	4.57	
3.00	613.00	1278.71	4.57	4.72	
3.10	613.10	1283.99	4.38	4.79	
3.20	613.20	1289.27	3.42	3.44	SECTION 7
3.30	613.30	1294.55	3.48	3.25	
3.40	613.40	1299.83	4.32	3.93	
3.50	613.50	1305.11	4.17	4.41	
3.60	613.60	1310.39	4.69	4.51	
3.70	613.70	1315.67	4.76	4.75	
3.80	613.80	1320.95	4.26	4.74	
3.90	613.90	1326.23	4.28	4.56	

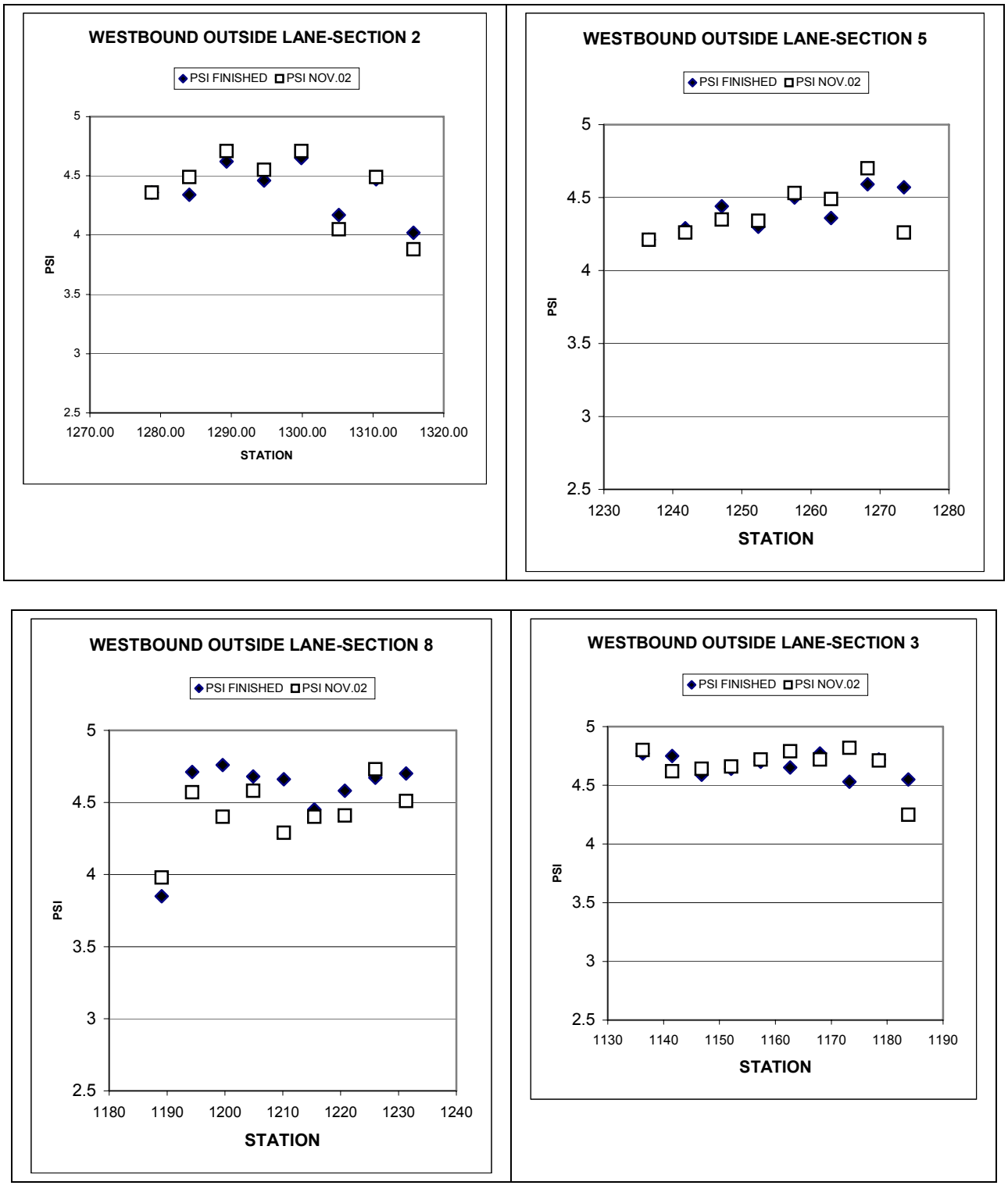

Figure B.1 PSI values on westbound outside lane measured on November 2002 and just after construction

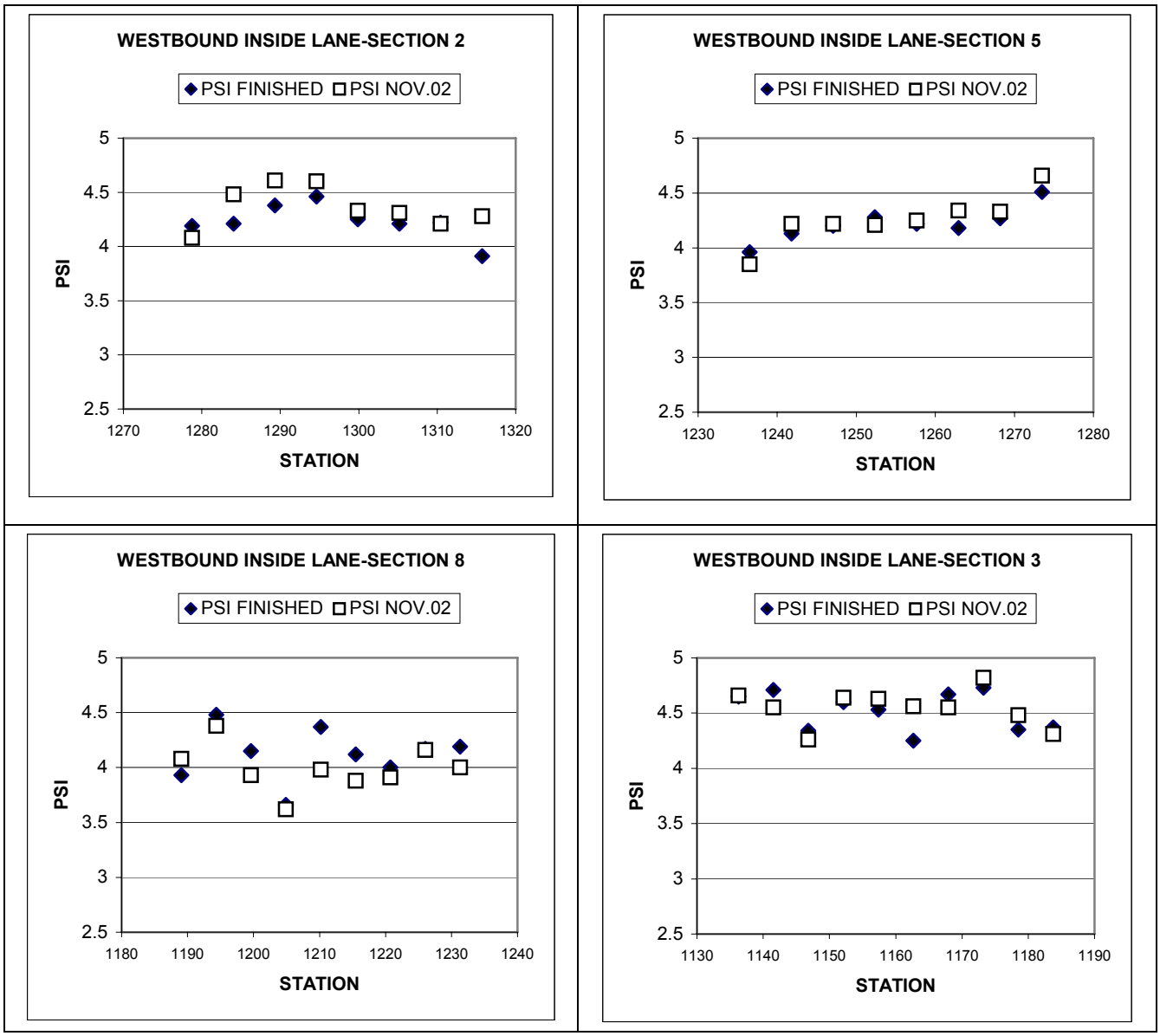

Figure B.2 PSI values on westbound inside lane measured on November 2002 and just after construction

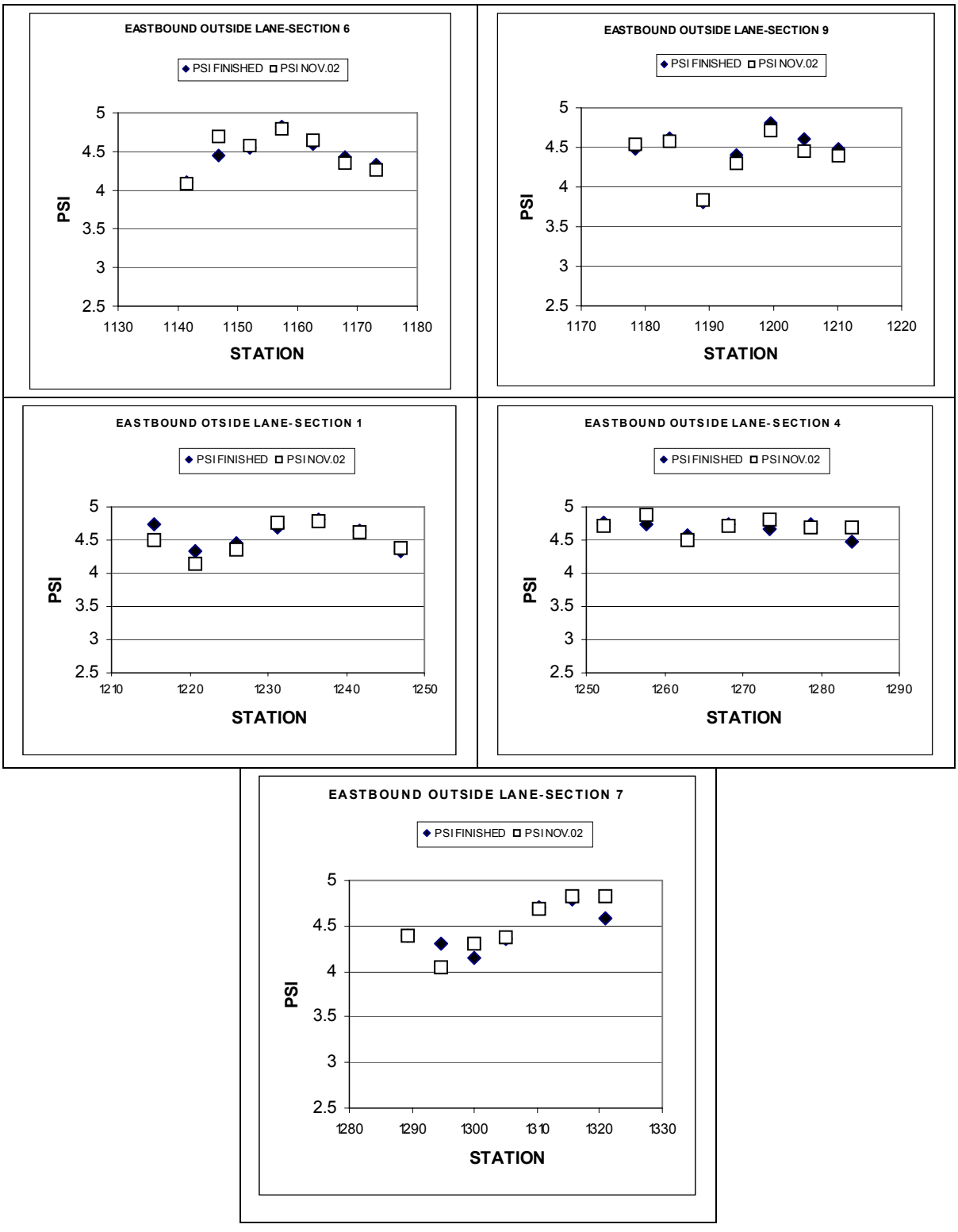

Figure B.3 PSI values on eastbound outside lane measured on November 2002 and just after construction

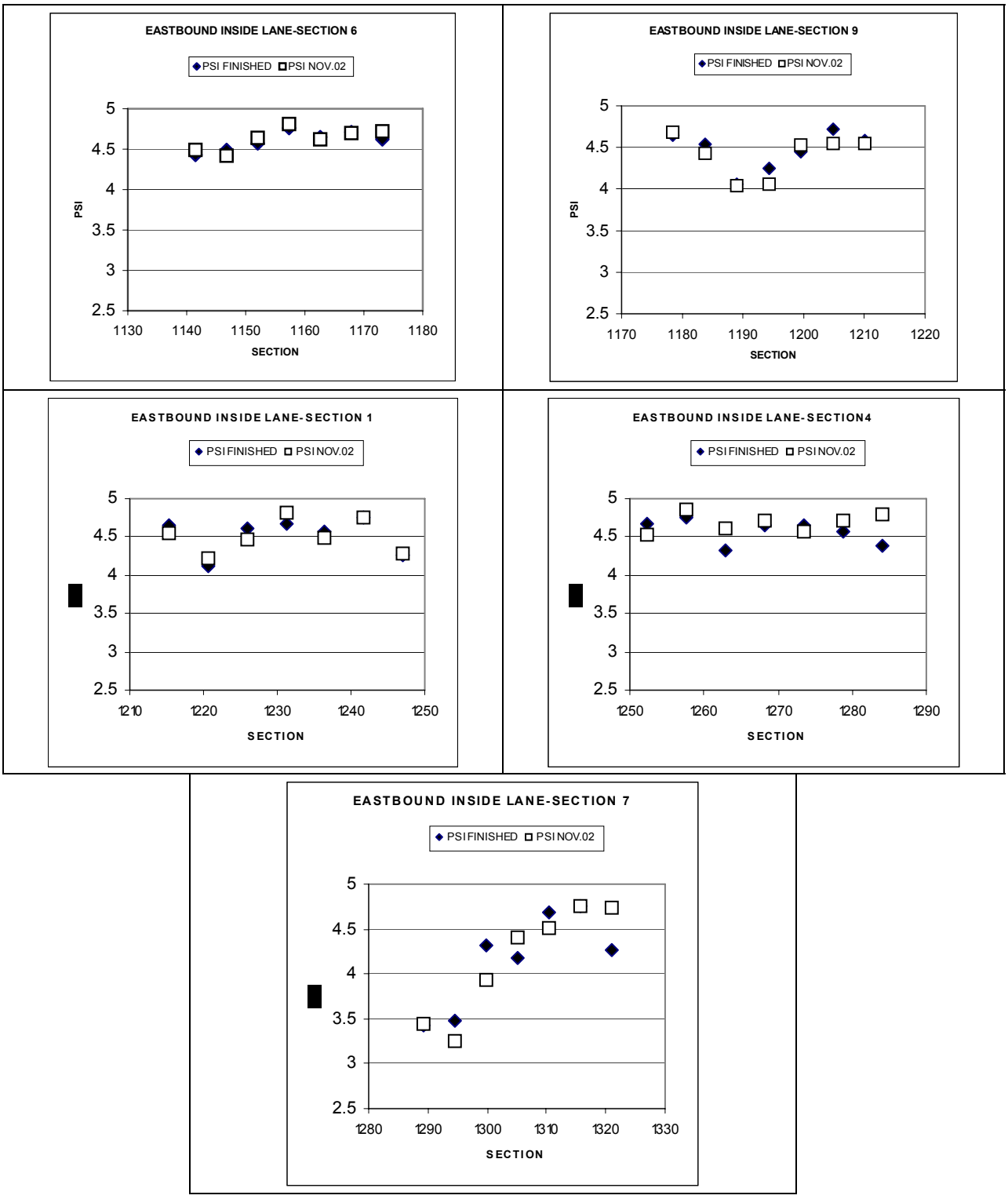

Figure B.4 PSI values on eastbound inside lane measured on November 2002 and just after construction

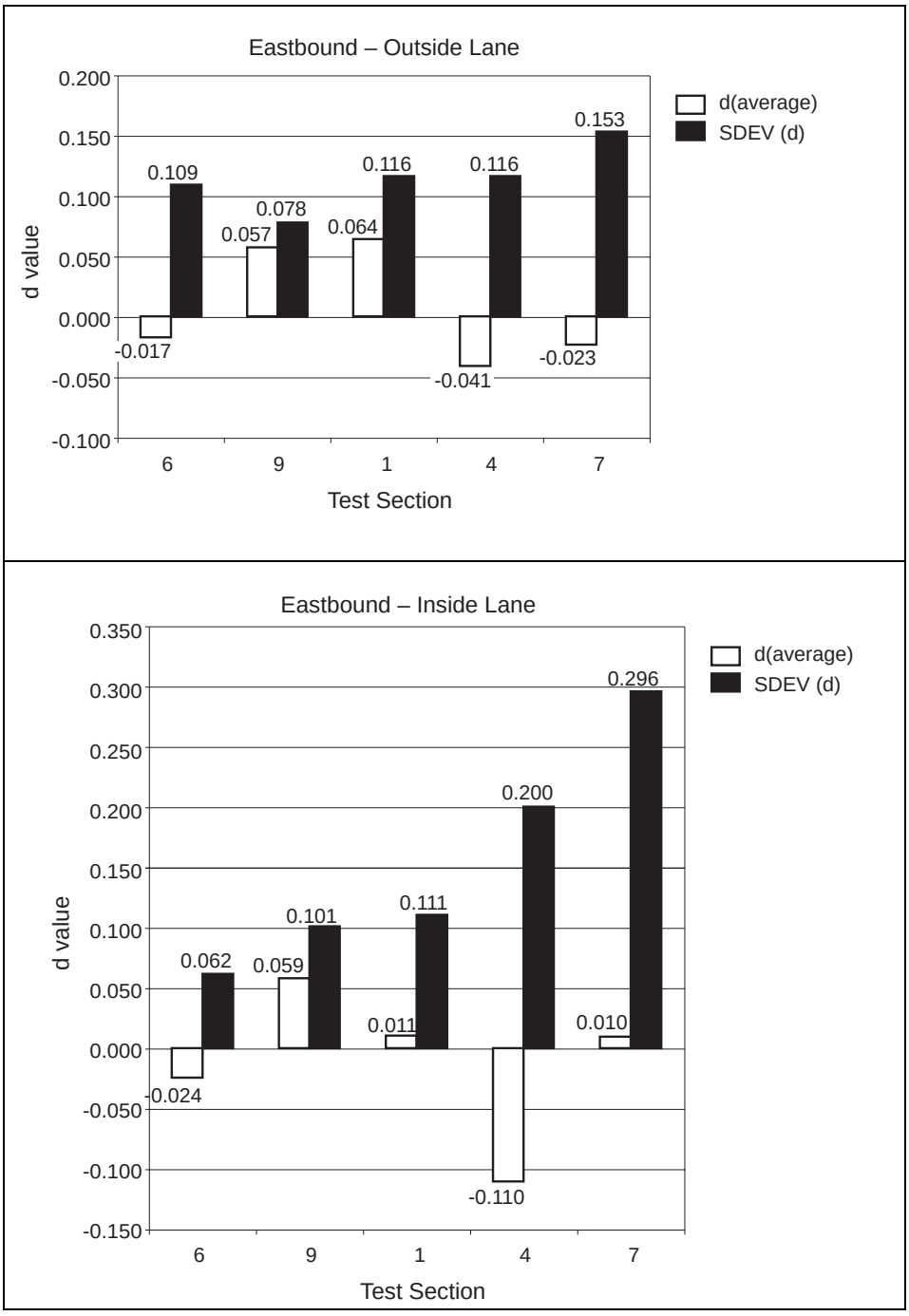

Figure B.5 d(average) values and their standard deviations for eastbound inside and outside lanes

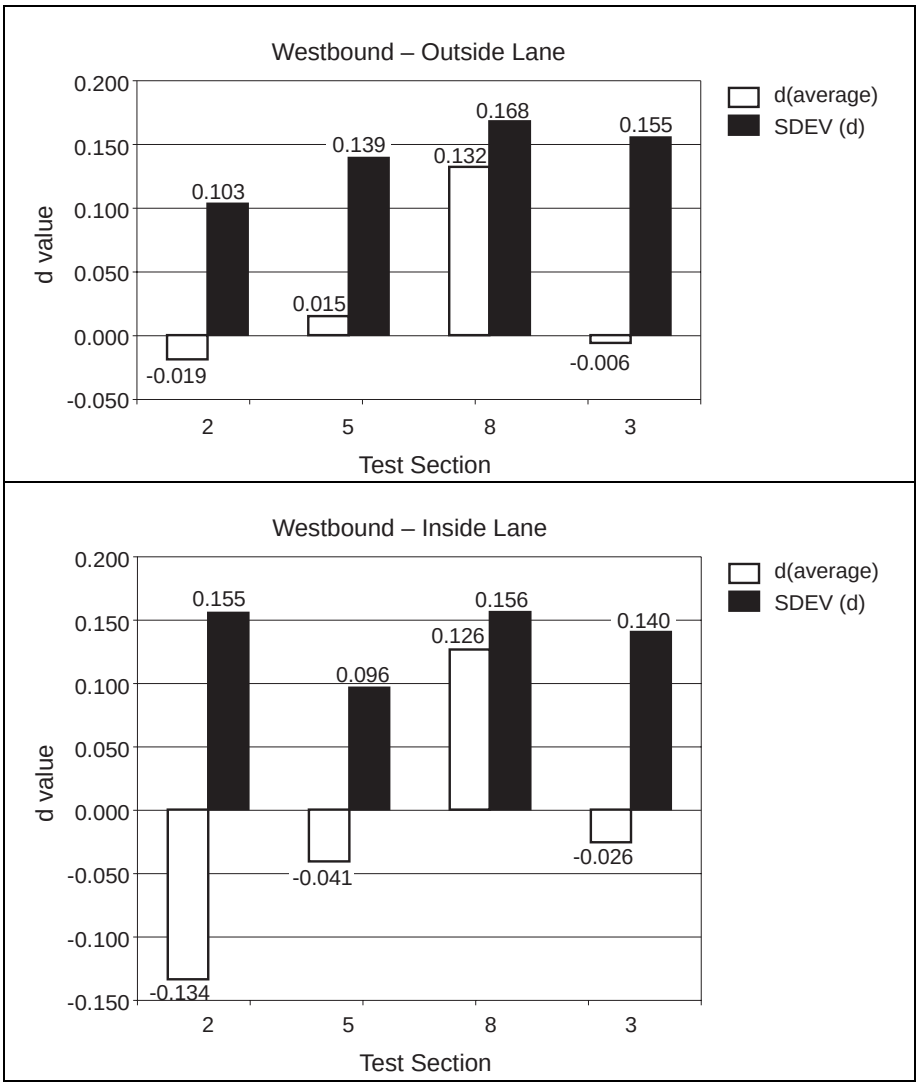

Figure B.6 d(average) values and their standard deviations for westbound inside and outside lanes

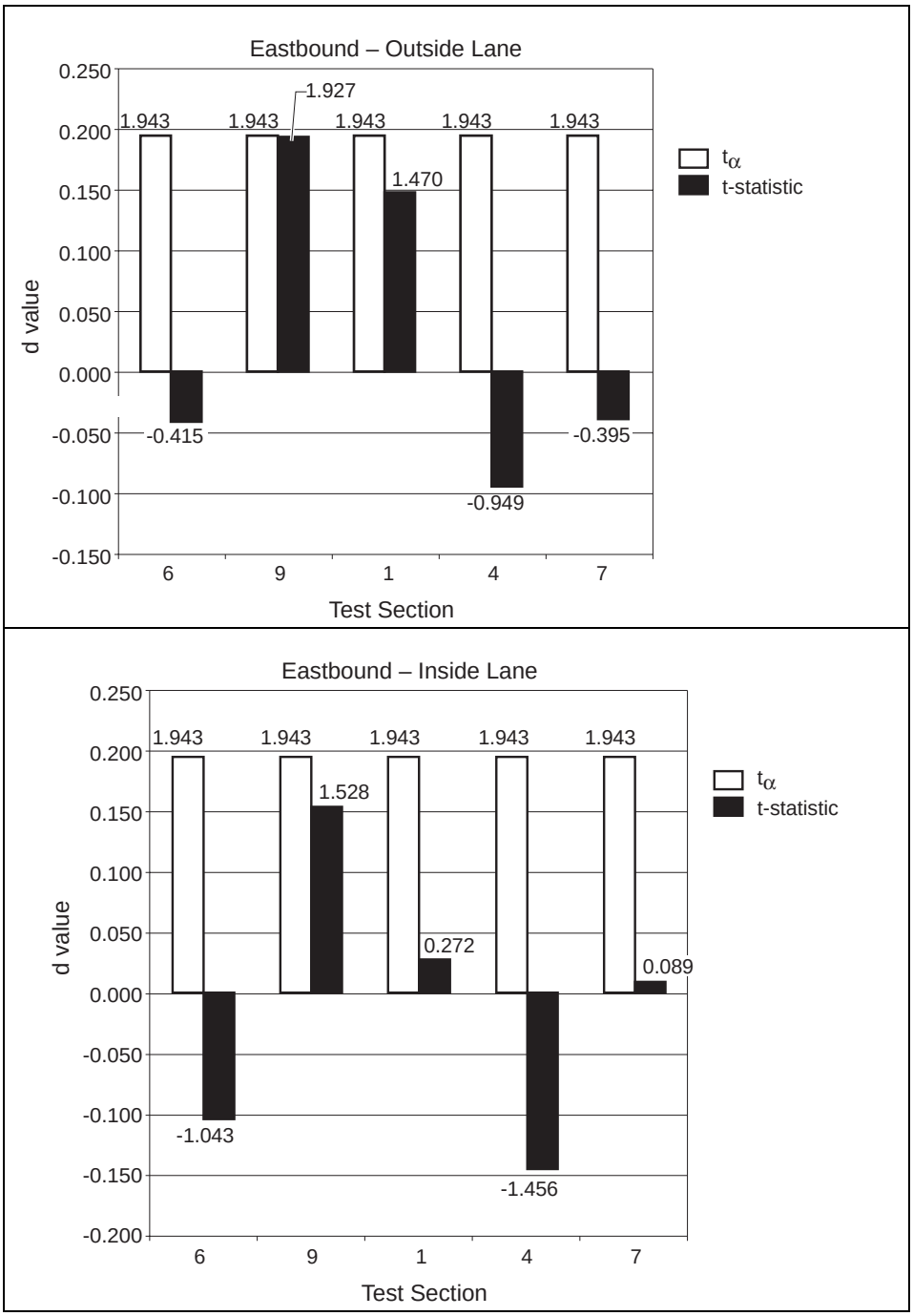

Figure B.7 Comparison of t-statistics and t_α values for sections on eastbound outside and inside lanes

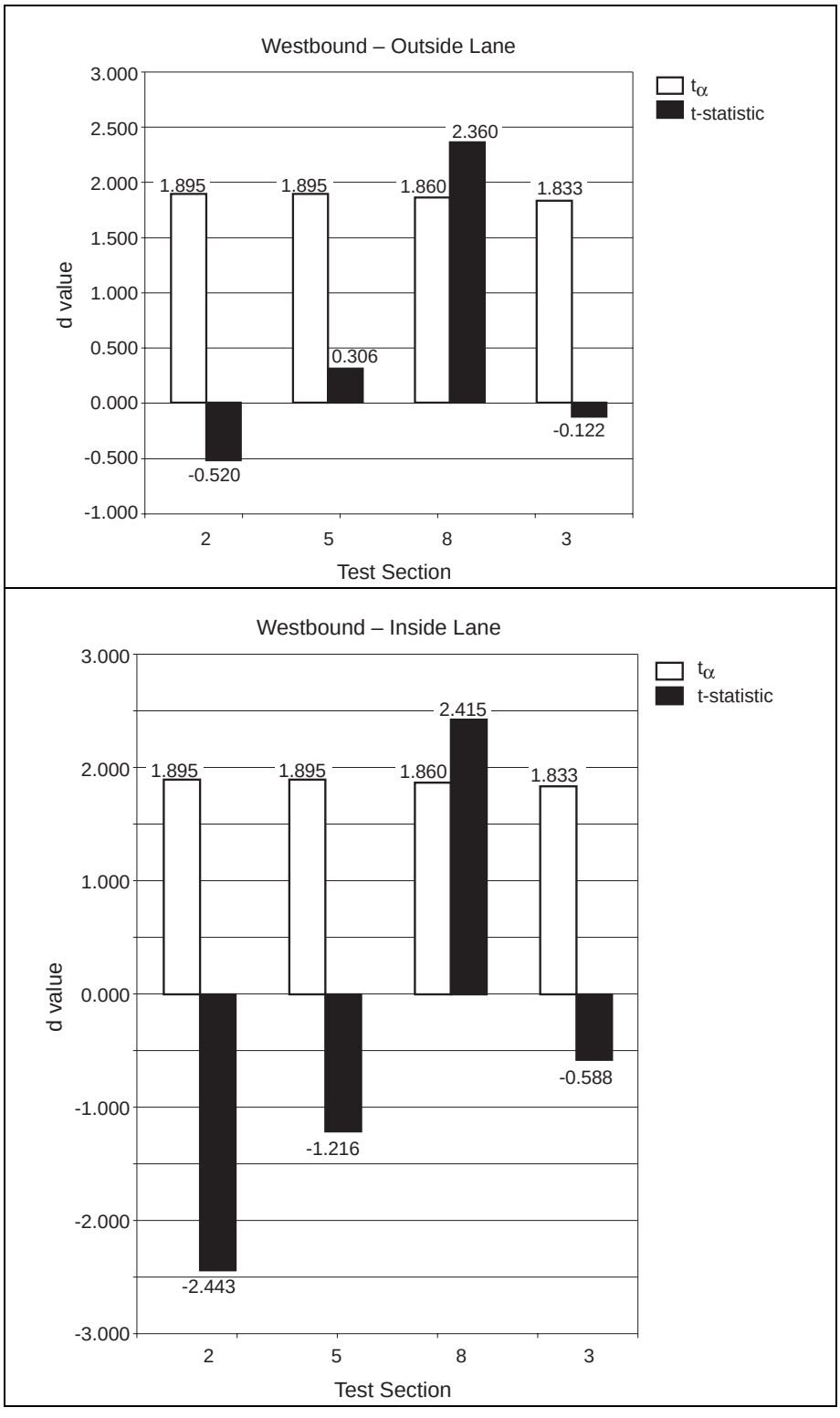

Figure B.8 Comparison of t-statistics and t_α values for sections on westbound outside and inside lanes

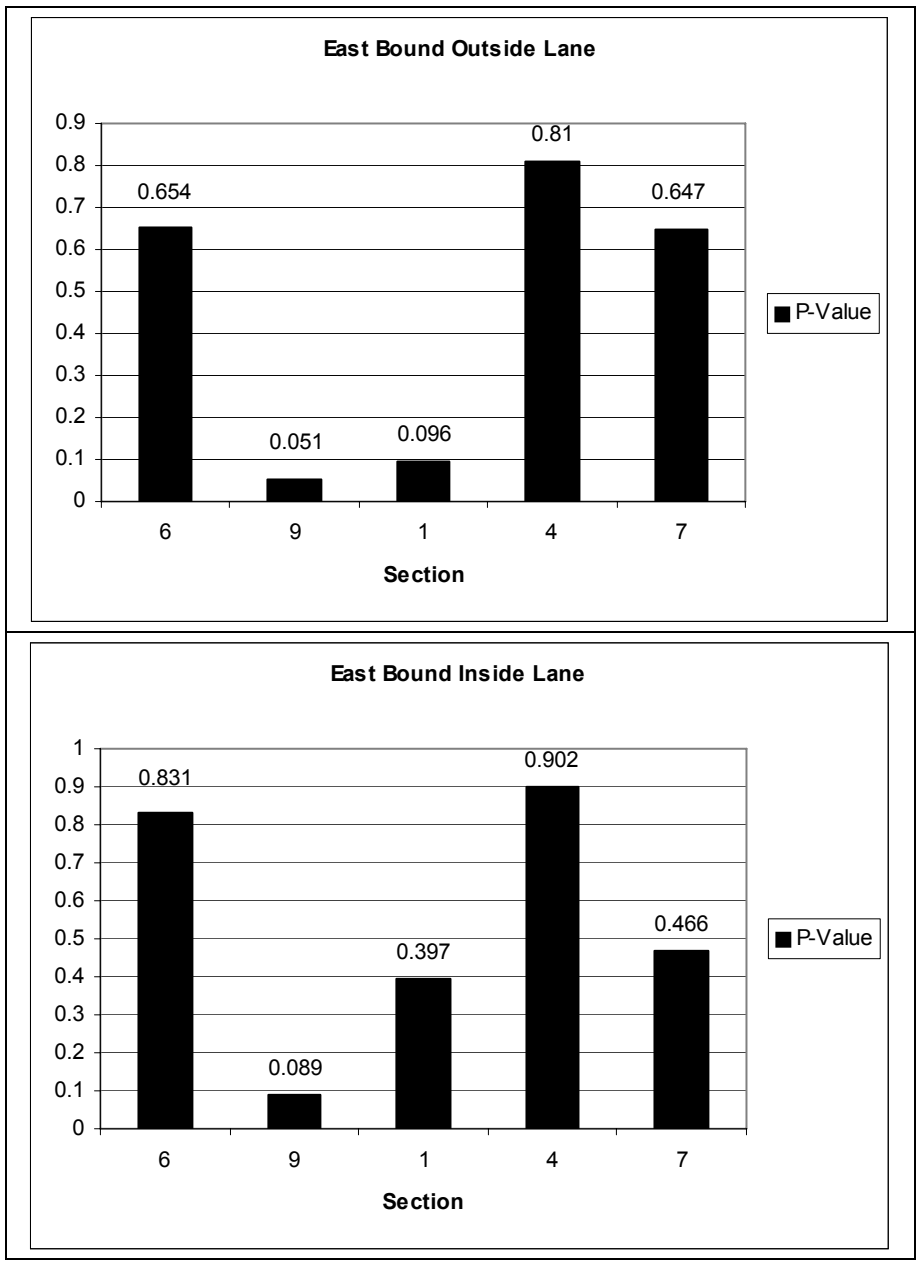

Figure B.9 p-values for sections on eastbound outside and inside lanes

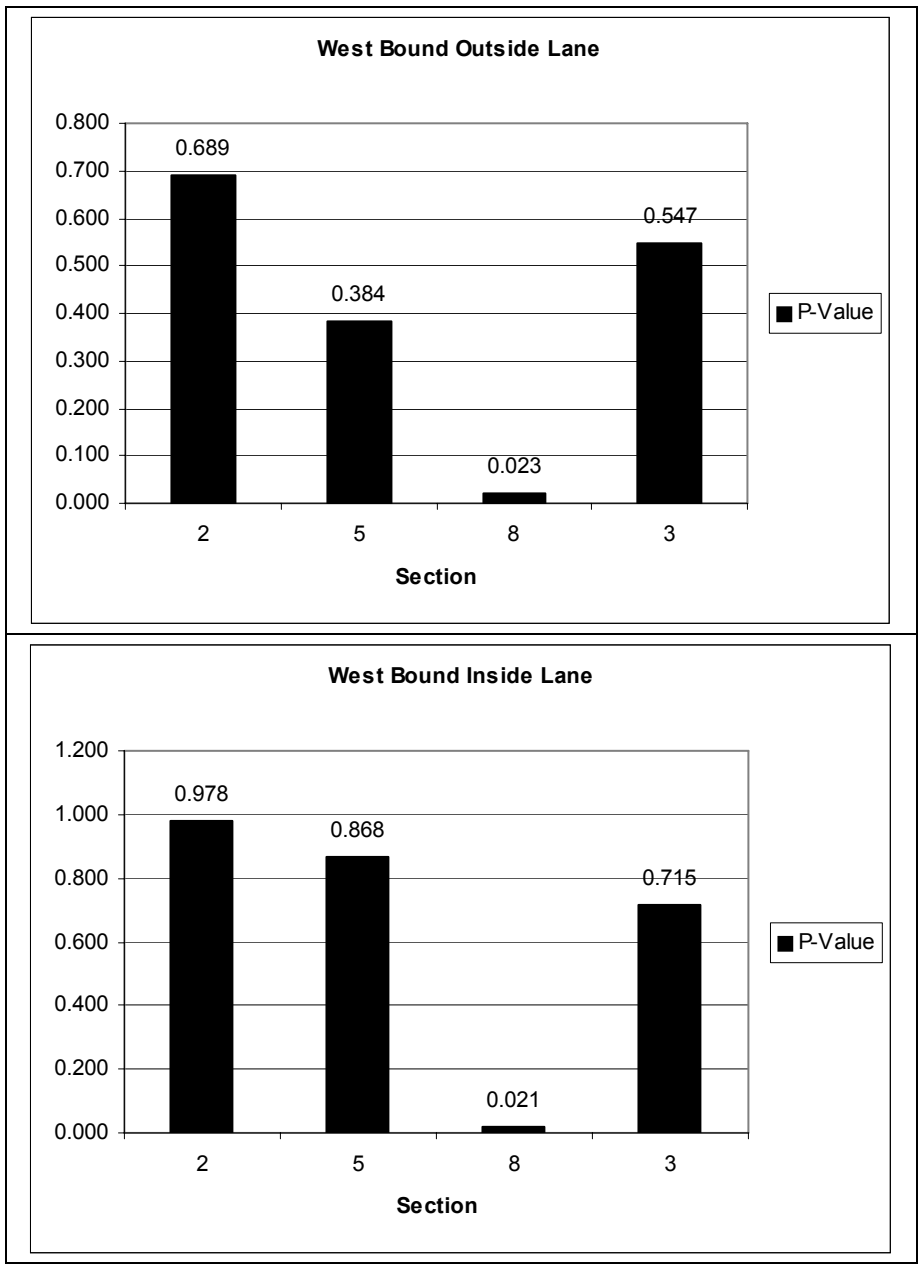

Figure B.10 p-values for sections on westbound outside and inside lanes

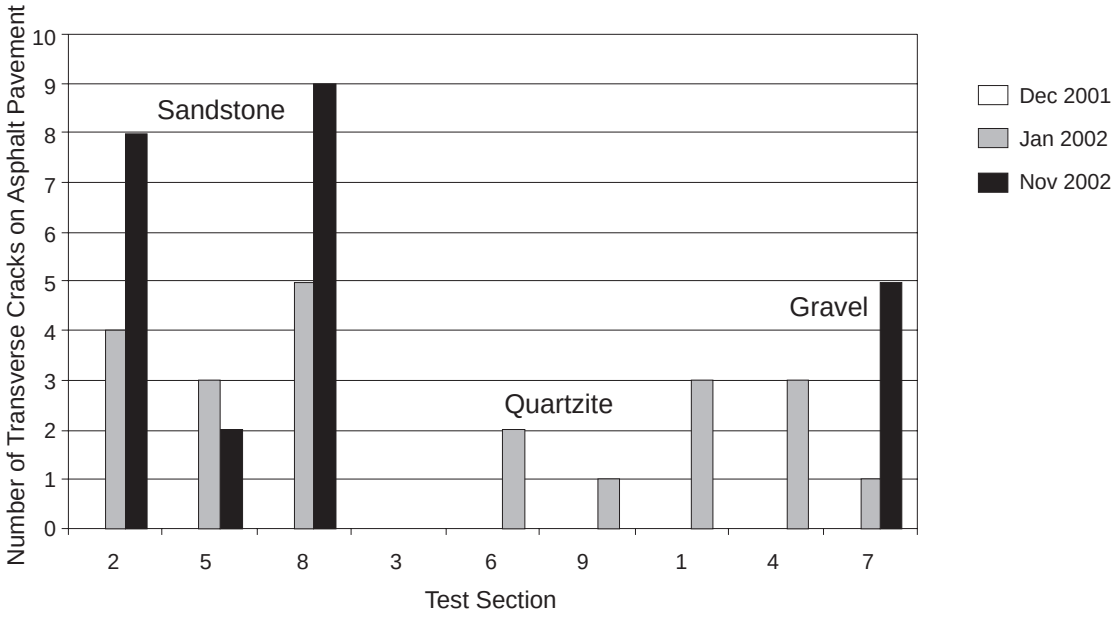

Figure B.11 Number of transverse cracks on asphalt pavement for each section at different surveys

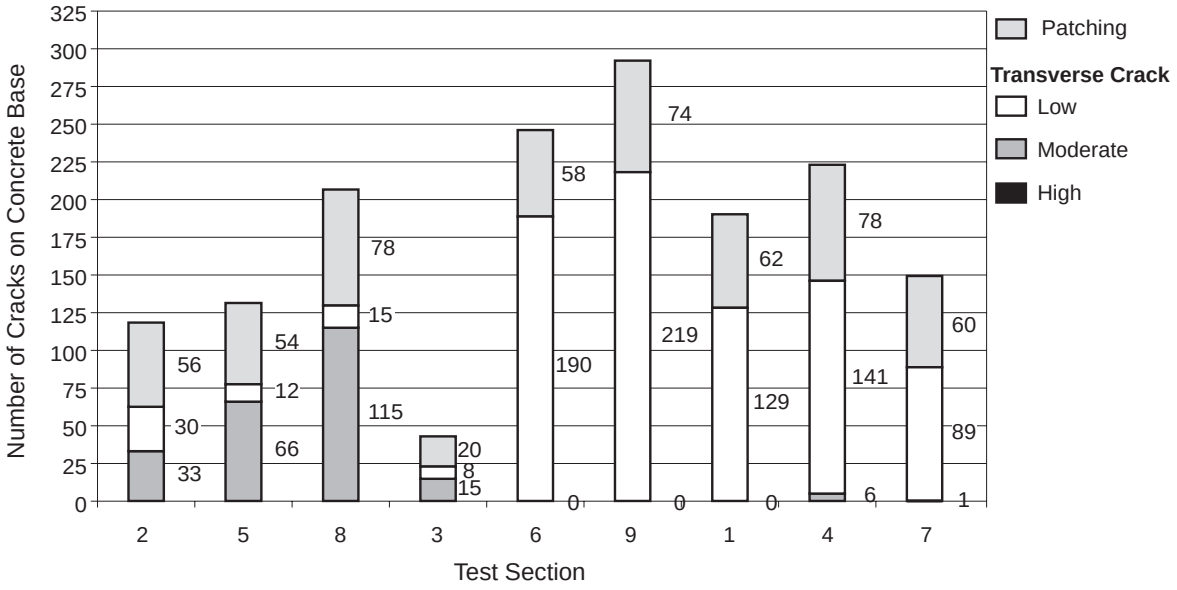

Figure B.12 Number of cracks on the CRCP

Appendix C:

Aggregate and Mix Design Properties of the Specimens

Table C.1 Sources of the materials used in this research project

ID Marks	Mix Design	Aggregate Type	Aggregate Location
A 0111 (H 01-07)	12.5 mm Superpave	Siliceous Gravel	Prescott
A 0112 (H 01-08)	12.5 mm Superpave	Sandstone	Sawyer
A 0113 (H 01-09)	12.5 mm Superpave	Quartzite	Jones
A 0114 (H 01-15)	CMHB-C	Siliceous Gravel	Prescott
A 0115 (H 01-16)	CMHB-C	Quartzite	Jones
A 0116 (H 01-17)	CMHB-C	Sandstone	Sawyer
A 0117 (H 01-18)	Type C	Siliceous Gravel	Prescott
A 0118 (H 01-19)	Type C	Quartzite	Jones
A 0119 (H 01-20)	Type C	Sandstone	Sawyer
A 0120 (H 01-21)	Type B	Limestone	Perch Hill

Table C.2 Aggregate gradations for superpave mixes

Sieve Size	Cumulative Pass A0111(H01-07) Siliceous Gravel	Cumulative Pass A0112(H01-08) Sandstone	Cumulative Pass A0113(H01-09) Quartzite
19	100	100	100
12.5	92	92.1	93.7
9.5	84.8	79.4	81.7
4.75	52.4	49	45.5
2.36	30.9	29.2	31.4
1.18	20.4	22.4	21
0.6	13.9	18.9	17.7
0.3	8.8	14.9	11.8
0.15	4.5	10.2	8.2
0.075	3.2	6.5	5.6
Pan			

Table C.3 Summary of design mixture properties for superpave mixes

ID Marks	% Air Voids	% VMA	%VFA	$\%G_{mm}@N_{ini}$	$\%G_{mm}@N_{ini}$	DP
A 0111 (H 01-07)	3.7	15.3	73.9	86.9	86.9	0.6
A 0112 (H 01-08)	3.8	15.1	73.1	86.0	86.0	1.3
A 0113 (H 01-09)	3.8	15.6	73.1	86.5	86.5	1.1
Specifications	4.0±1.0	14.0 min	65-75	Max. 89.0	Max. 89.0	0.6-1.2

Table C.4 Aggregate gradations for CMHB-C mixes

Sieve Size	Cumulative Pass A0114(H01-15) Siliceous Gravel	Cumulative Pass A0115(H01-16) Quartzite	Cumulative Pass A0116(H01-17) Sandstone
7/8”	100	100	100
5/8”	99.7	99.6	100
3/8”	64.5	65.6	65.4
#4	34.3	34.2	38
#10	21.8	24	24
#40	16.2	14.5	16.4
#80	9.8	9.1	10.9
#200	6.4	5.9	6.4
pan			

Table C.5 Summary of design mixture properties for CMHB-C mixes

ID Marks	% Asphalt	% Air Voids	% VMA
A 0114 (H 01-15)	4.7	3.5	14.1
A 0115 (H 01-16)	4.8	3.5	14.6
A 0116 (H 01-17)	4.8	3.5	14.1

Table C.6 Aggregate gradations for Type C mixes

Sieve Size	Cumulative Pass A0117(H01-18) Siliceous Gravel	Cumulative Pass A0118(H01-19) Quartzite	Cumulative Pass A0119(H01-20) Sandstone
7/8”	100	100	100
5/8”	100	99.8	99.8
3/8”	75.8	79.1	80.7
#4	49.2	51.4	46.2
#10	31.5	34	30.9
#40	18.2	17.9	15.6
#80	11.7	10	9.6
#200	5.8	5.3	5.8

Table C.7 Summary of stability, TSR, and HWTD tests results

ID Marks	Mix Design	Stability	TSR	HWTD (mm)
A 0111 (H 01-07)	12.5 mm Superpave	43	0.97	3.1
A 0112 (H 01-08)	12.5 mm Superpave	51	0.93	1.8
A 0113 (H 01-09)	12.5 mm Superpave	41	0.94	2.2
A 0114 (H 01-15)	CMHB-C	42	0.99	2.5
A 0115 (H 01-16)	CMHB-C	-	0.99	2.7
A 0116 (H 01-17)	CMHB-C	-	1.05	1.4
A 0117 (H 01-18)	Type C	48	0.96	2.5
A 0118 (H 01-19)	Type C	50	1.06	2.2
A 0119 (H 01-20)	Type C	43	0.90	1.6
A 0120 (H 01-21)	Type B	46	0.92	2.9

Appendix D:

Orientation of the Test Sections

MIX DESIGN SUMMARY (SURFACE)

WESTBOUND

Table D.1 Summary of test section, westbound

STATIONS	SECTION	MIX DESIGN	SY	TONS
1135 to 1188	3	SUPERPAVE ½", Quartzite Coarse Aggregate (MARTIN MARIETTA JONES MILL)	24482	2693
1193 to 1235	8	TY C, Sandstone Coarse Aggregate (MERIDIAN SAWYER)	18037	1984
1235 to 1278	5	CMHB-C, Sandstone Coarse Aggregate (MERIDIAN SAWYER)	18037	1984
1278 to 1321	2	SUPERPAVE ½", Sandstone Coarse Aggregate (MERIDIAN SAWYER)	18040	1984
		SUBTOTAL	78596	8645

EASTBOUND

Table D.2 Summary of test section, eastbound

STATION LIMITS	SECTION	MIX DESIGN	SY	TONS
1135 to 1185	6	CMHB-C, Quartize Coarse Aggregate (MARTIN MARIETTA JONES MILL)	15530	1708
1190 to 1218	9	TY C, Quartize Coarse Aggregate (MARTIN MARIETTA JONES MILL)	15197	1672
1218 to 1245	1	SUPERPAVE ½", Siliceous Gravel Coarse Aggregate (HANSON EAGLE MILLS, PRESCOTT, OR LITTLE RIVER)	15956	1755
1245 to 1282	4	CMHB-C, Siliceous Gravel Coarse Aggregate (HANSON EAGLE MILLS, PRESCOTT, OR LITTLE RIVER)	15956	1755
1282 to 1321	7	TY C, Siliceous Gravel Coarse Aggregate (HANSON EAGLE MILLS, PRESCOTT, OR LITTLE RIVER)	15958	1755
		SUBTOTAL	78597	8645
		TOTAL	157193	17290

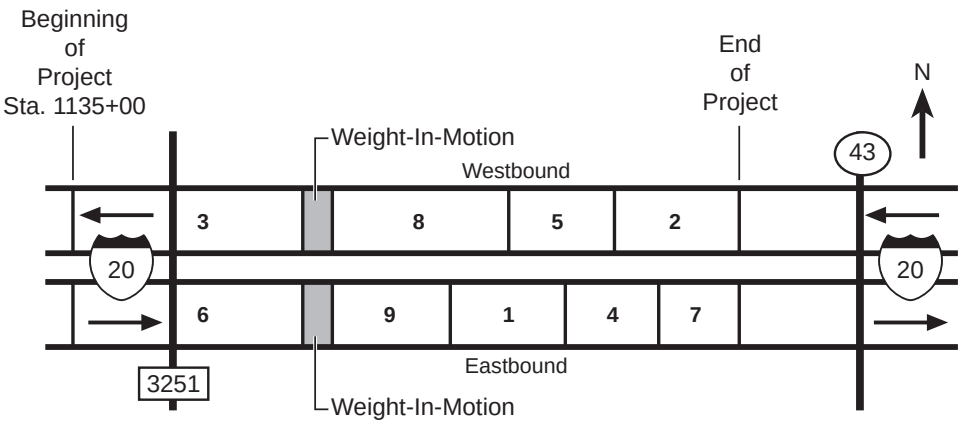

Figure D.1 Layout of the test sections

Appendix E:

FWD Measurements

Section 1

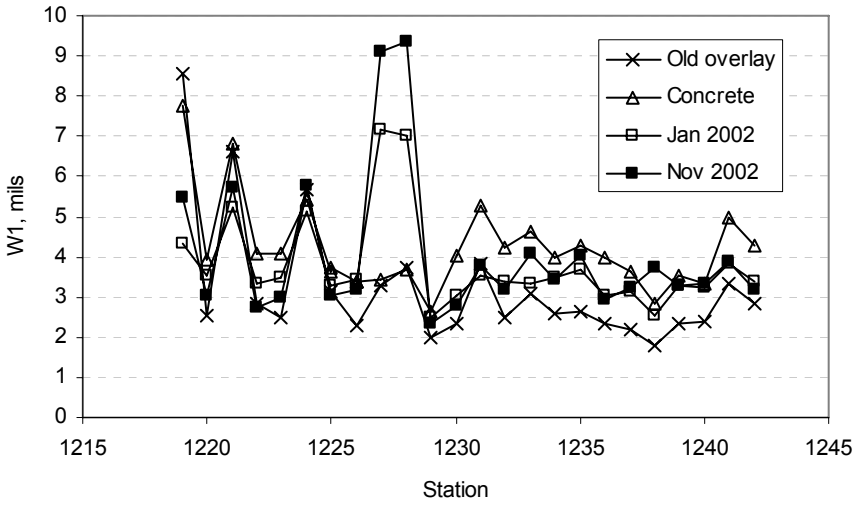

Figure E.1 Section 1 normalized W1 deflections

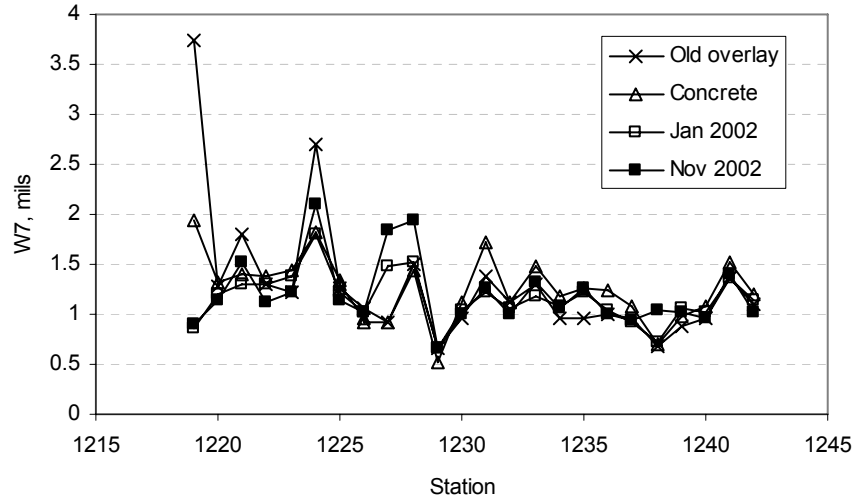

Figure E.2 Section 1 normalized W7 deflections

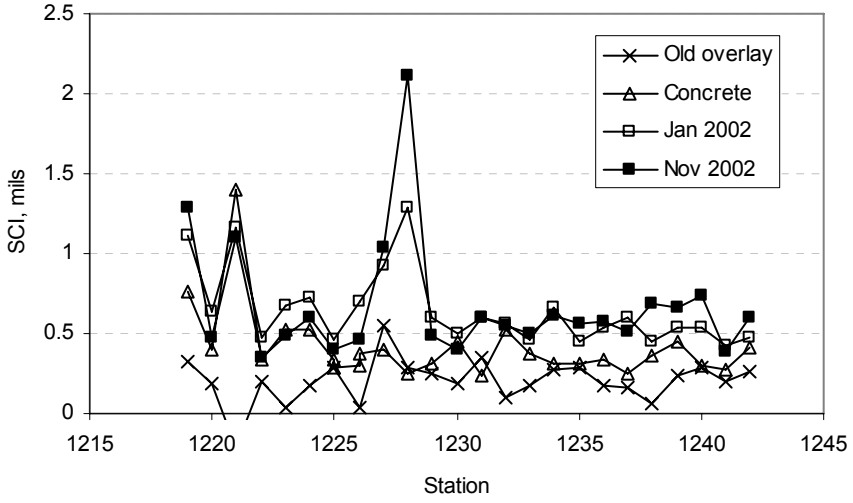

Figure E.3 Section 1 normalized SCI

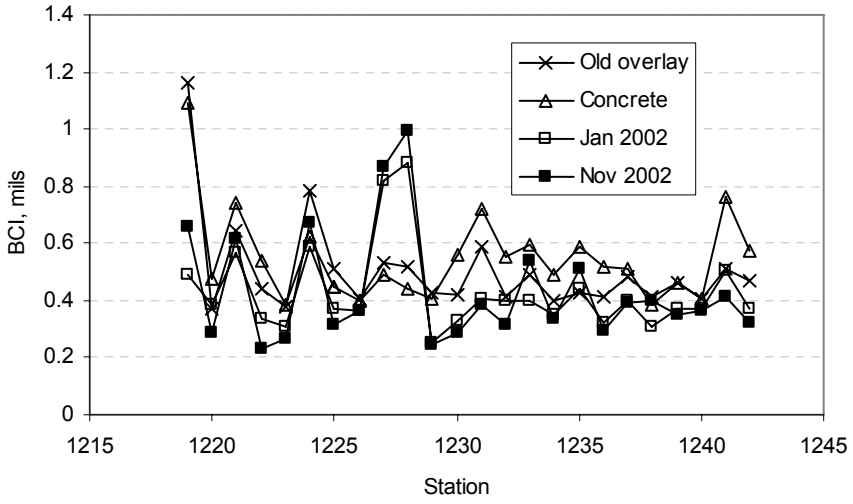

Figure E.4 Section 1 normalized BCI

Section 2

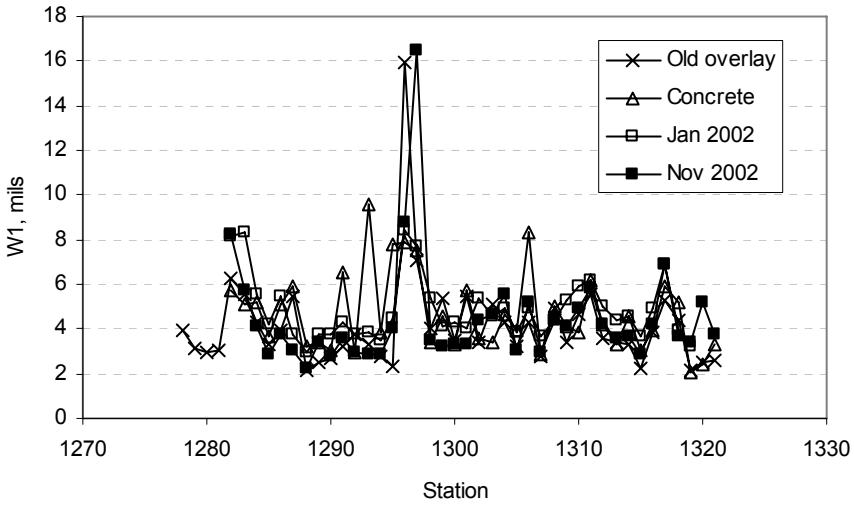

Figure E.5 Section 2 normalized W1 deflections

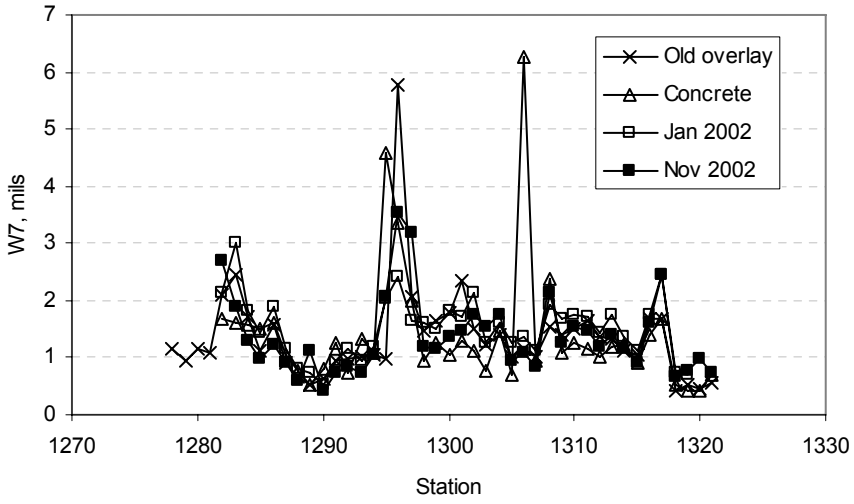

Figure E.6 Section 2 normalized W7 deflections

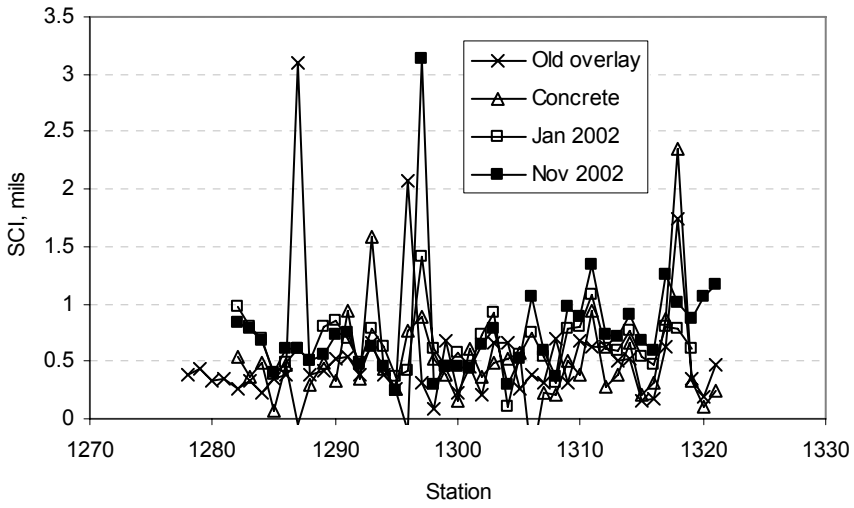

Figure E.7 Section 2 normalized SCI

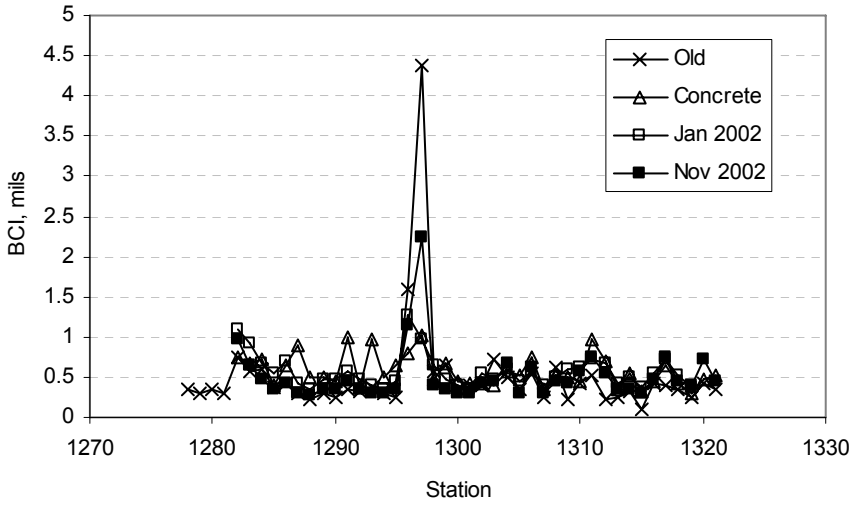

Figure E.8 Section 2 normalized BCI

Section 3

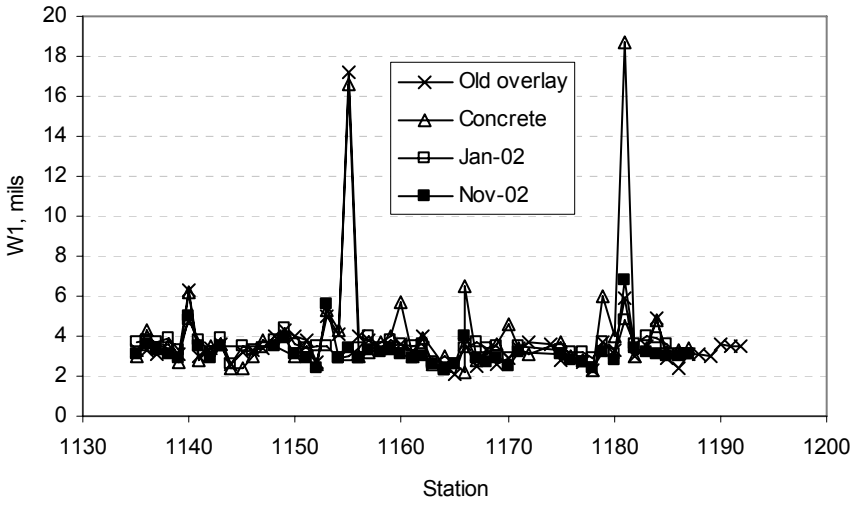

Figure E.9 Section 3 normalized W1 deflections

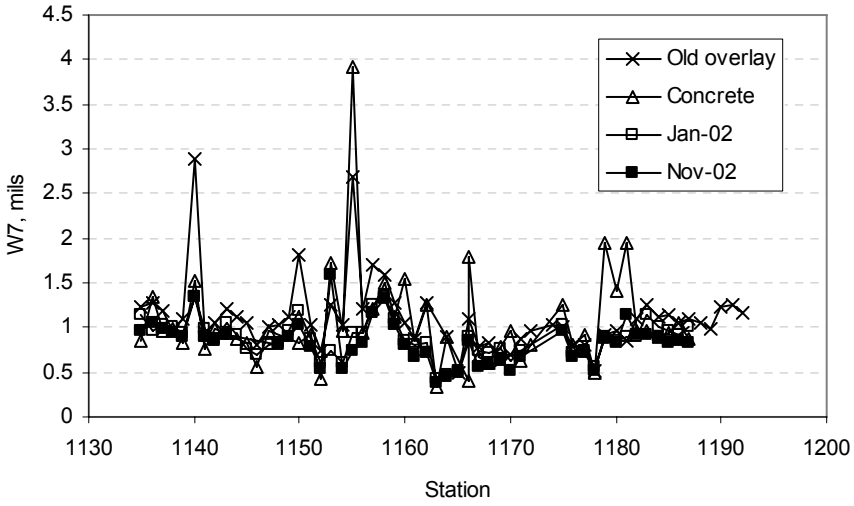

Figure E.10 Section 3 normalized W7 deflections

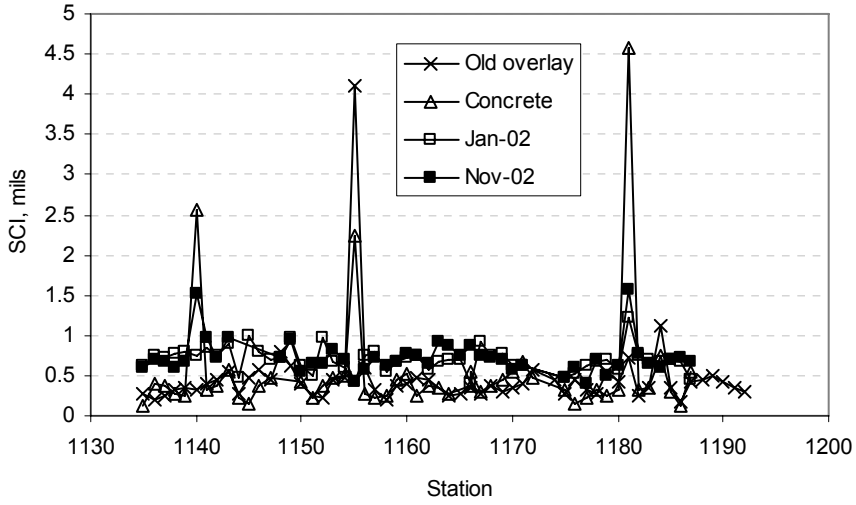

Figure E.11 Section 3 normalized SCI

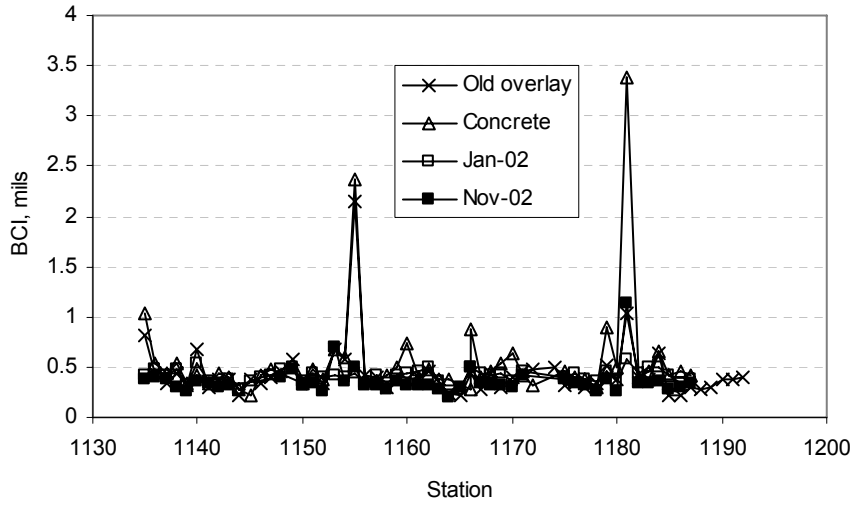

Figure E.12 Section 3 normalized BCI

Section 4

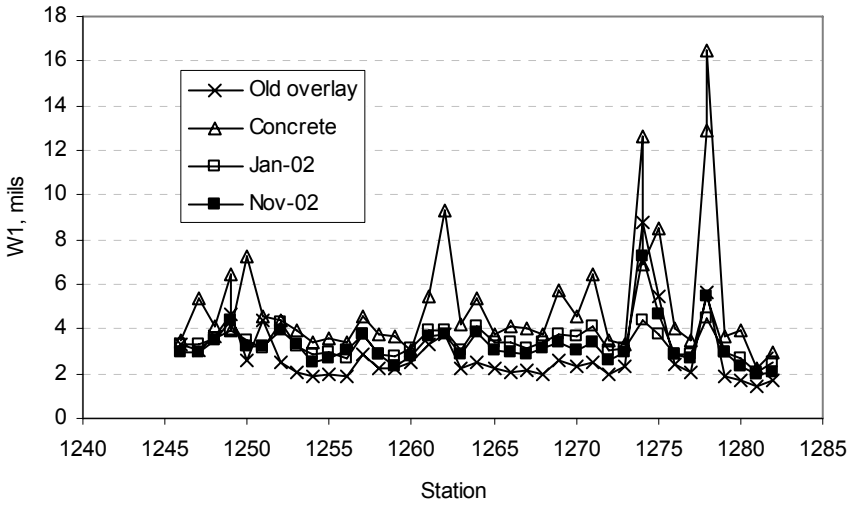

Figure E.13 Section 4 normalized W1 deflections

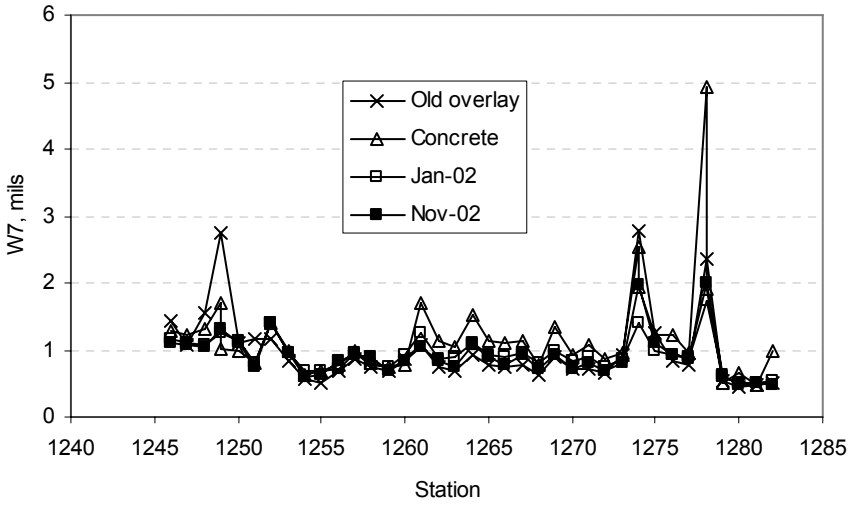

Figure E.14 Section 4 normalized W7 deflections

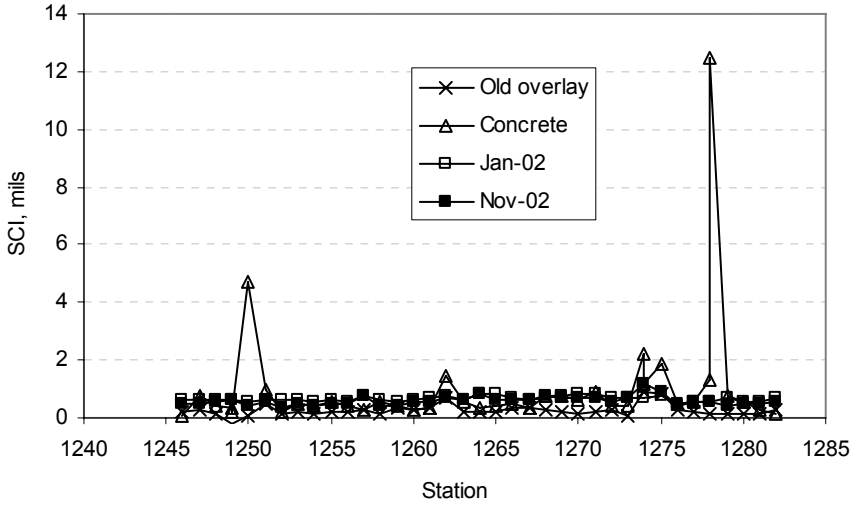

Figure E.15 Section 4 normalized SCI

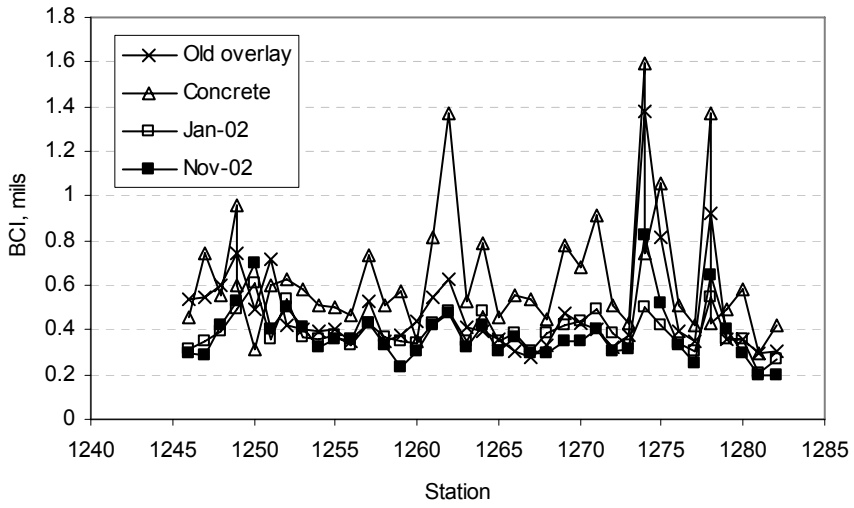

Figure E.16 Section 4 normalized BCI

Section 5

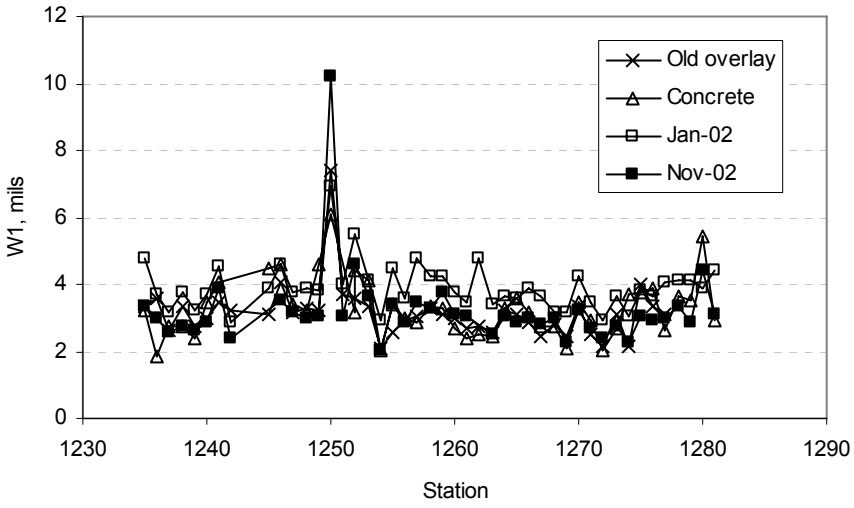

Figure E.17 Section 5 normalized W1 deflections

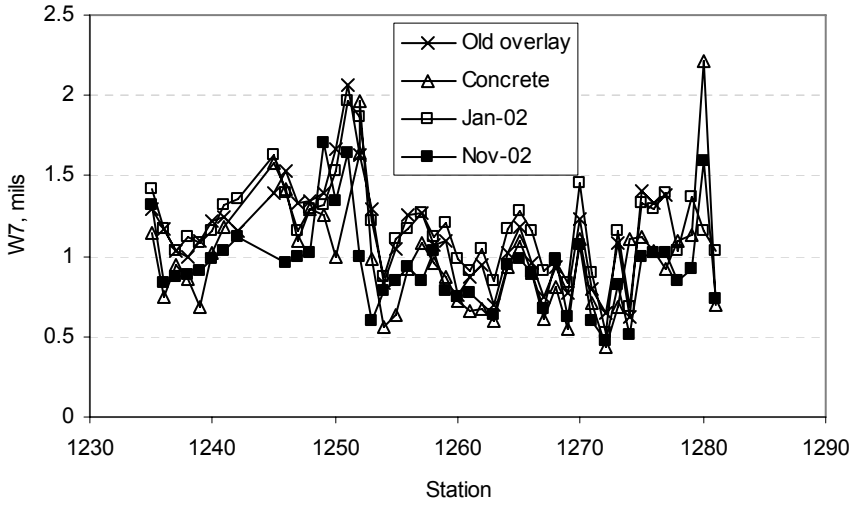

Figure E.18 Section 5 normalized W7 deflections

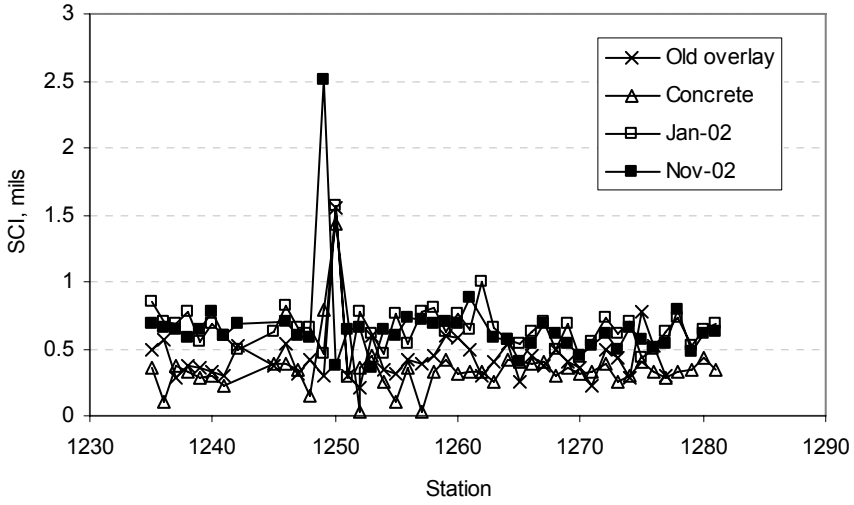

Figure E.19 Section 5 normalized SCI

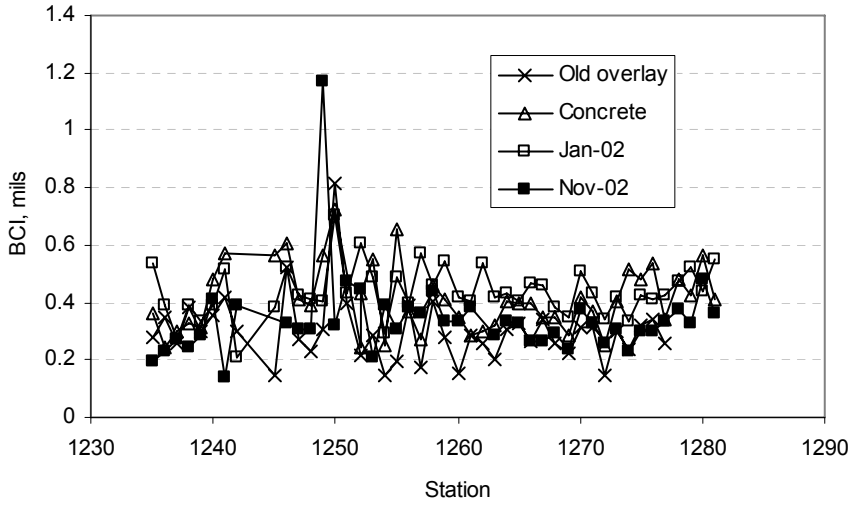

Figure E.20 Section 5 normalized BCI

Section 6

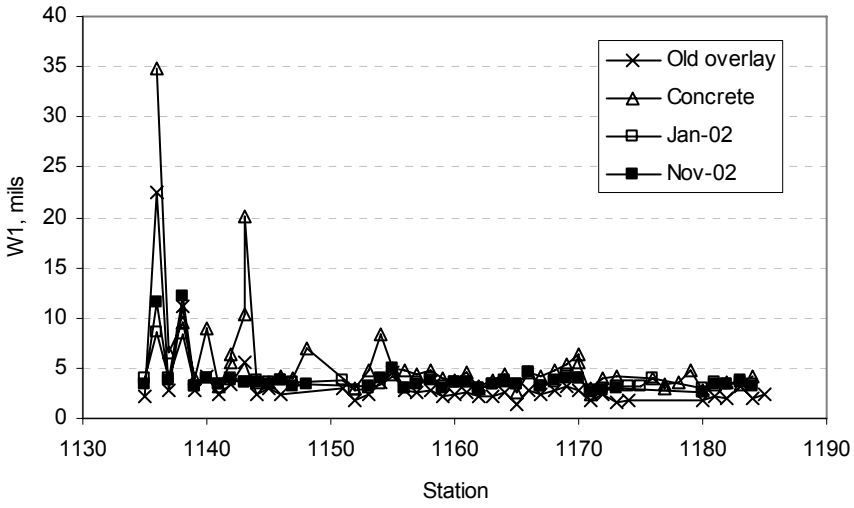

Figure E.21 Section 6 normalized W1 deflections

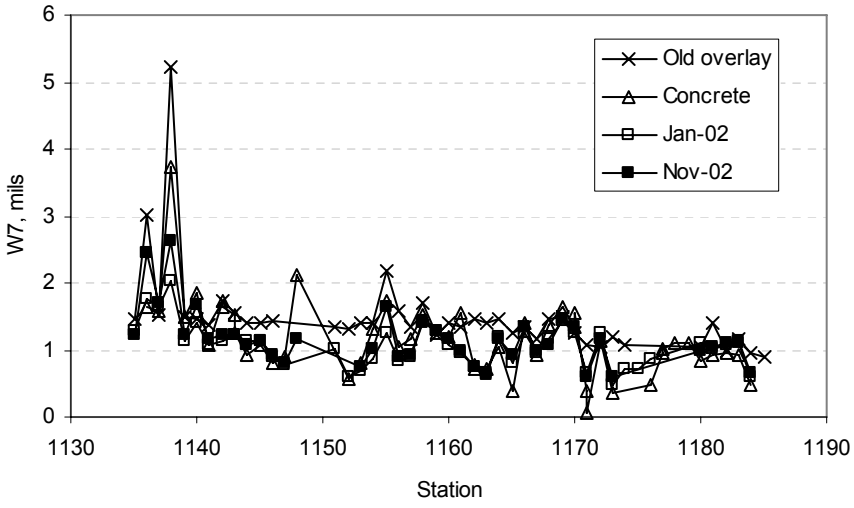

Figure E.22 Section 6 normalized W7 deflections

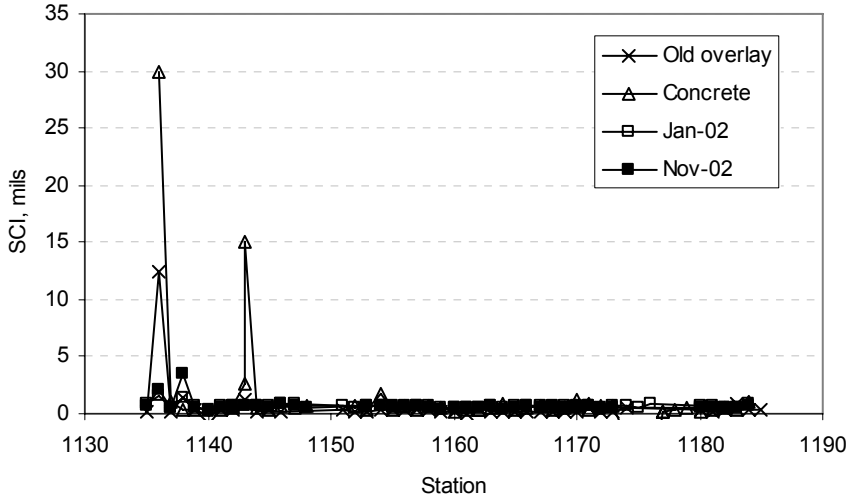

Figure E.23 Section 6 normalized SCI

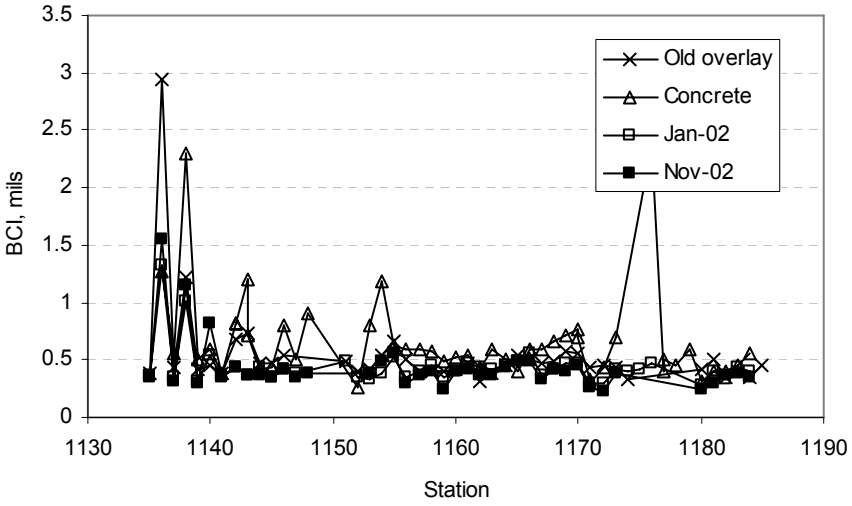

Figure E.24 Section 6 normalized BCI

Section 7

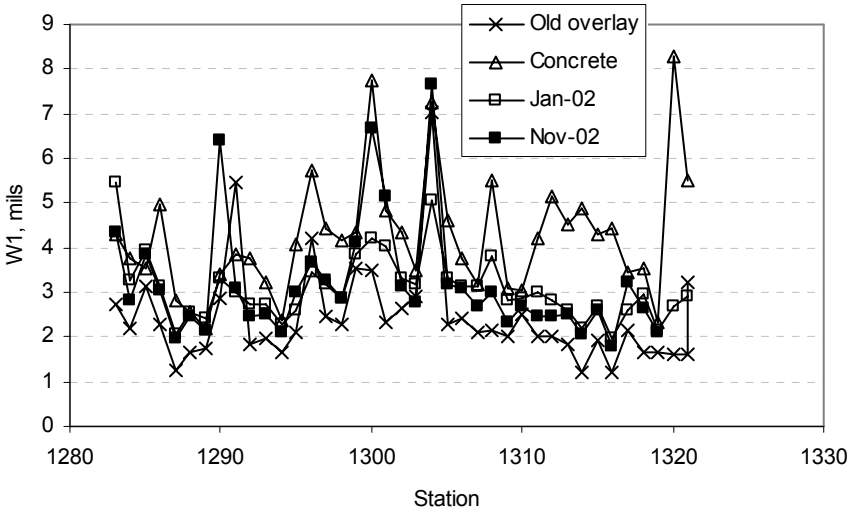

Figure E.25 Section 7 normalized W1 deflections

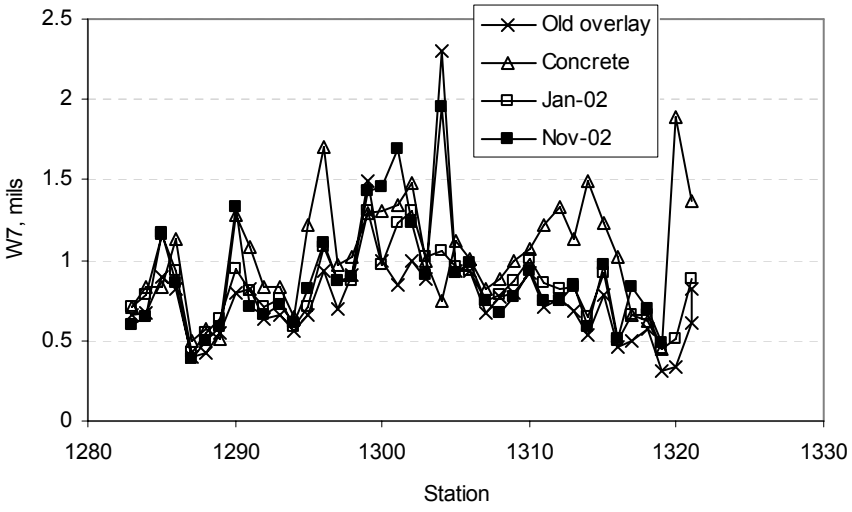

Figure E.26 Section 7 normalized W7 deflections

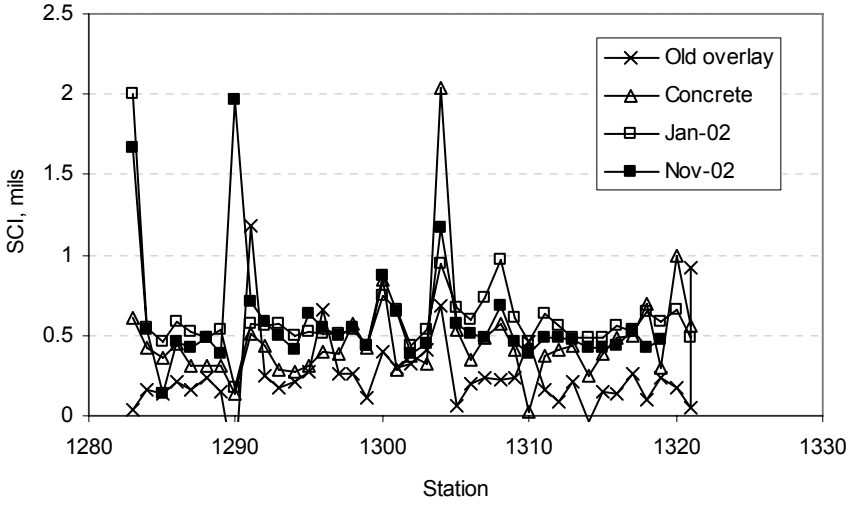

Figure E.27 Section 7 normalized SCI

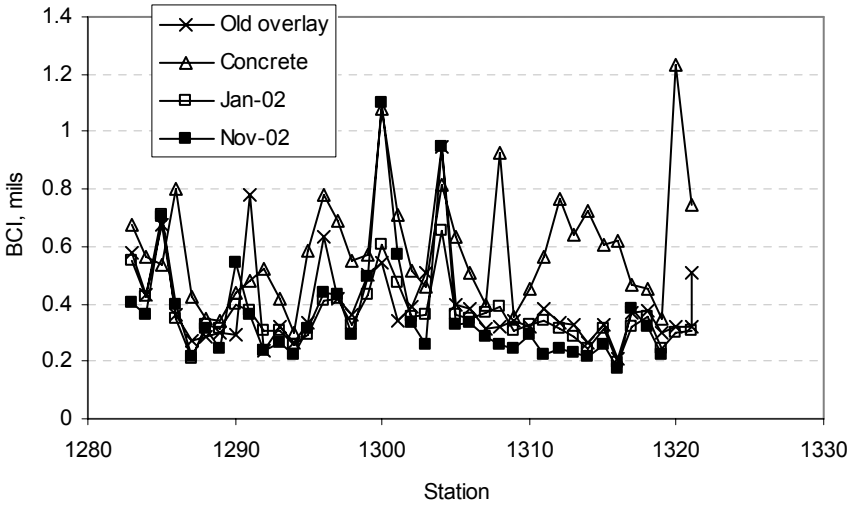

Figure E.28 Section 7 normalized BCI

Section 8

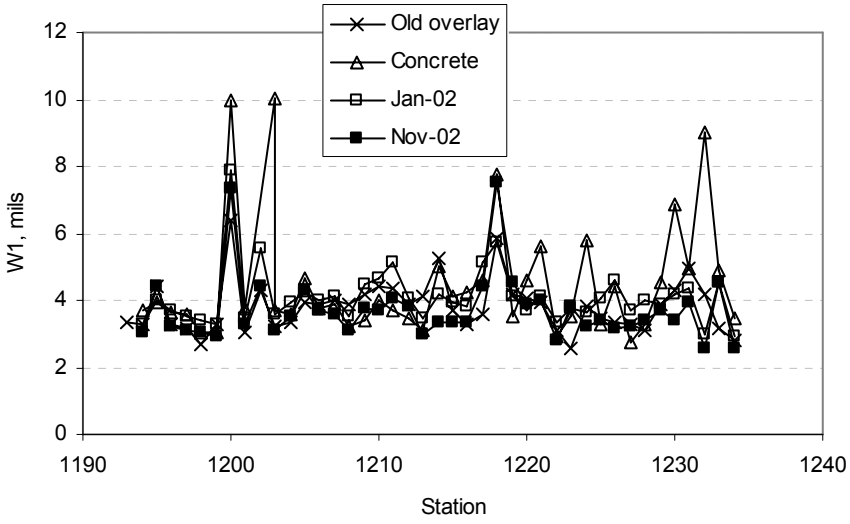

Figure E.29 Section 8 normalized W1 deflections

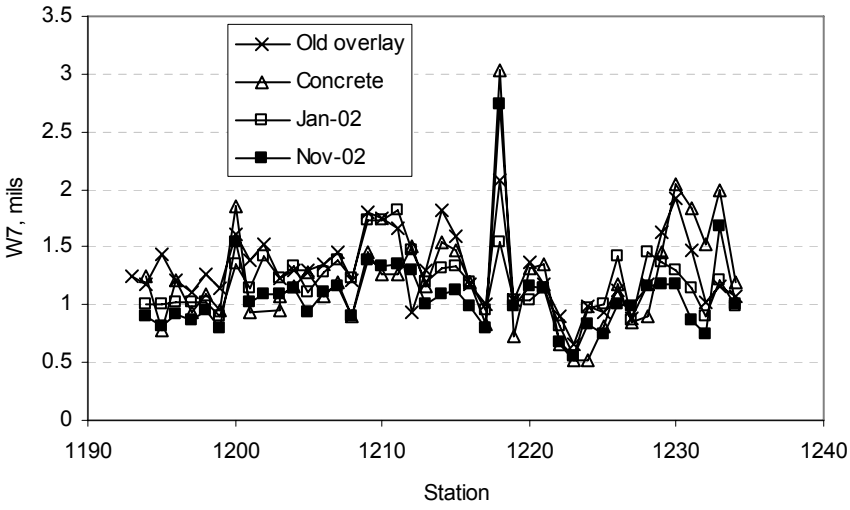

Figure E.30 Section 8 normalized W7 deflections

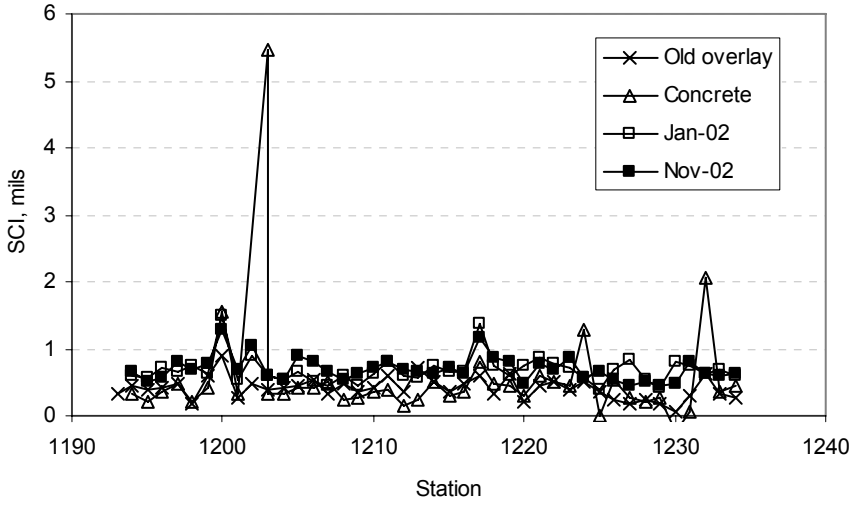

Figure E.31 Section 8 normalized SCI

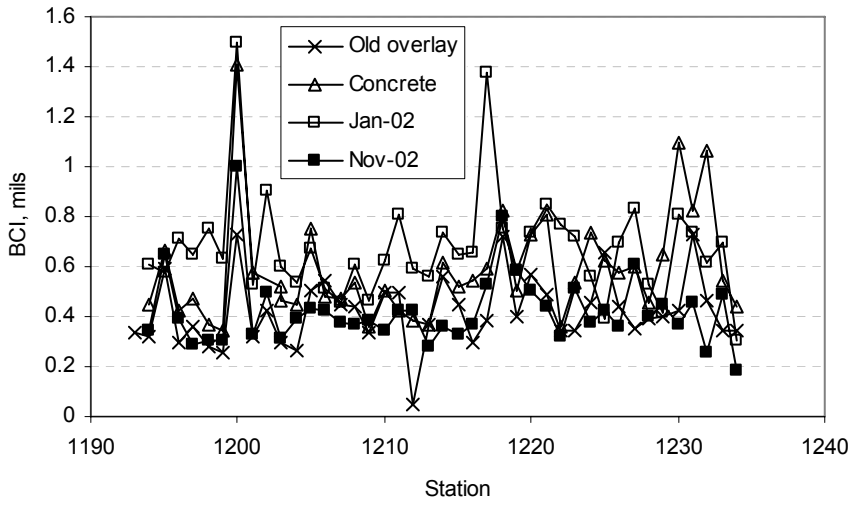

Figure E.32 Section 8 normalized BCI

Section 9

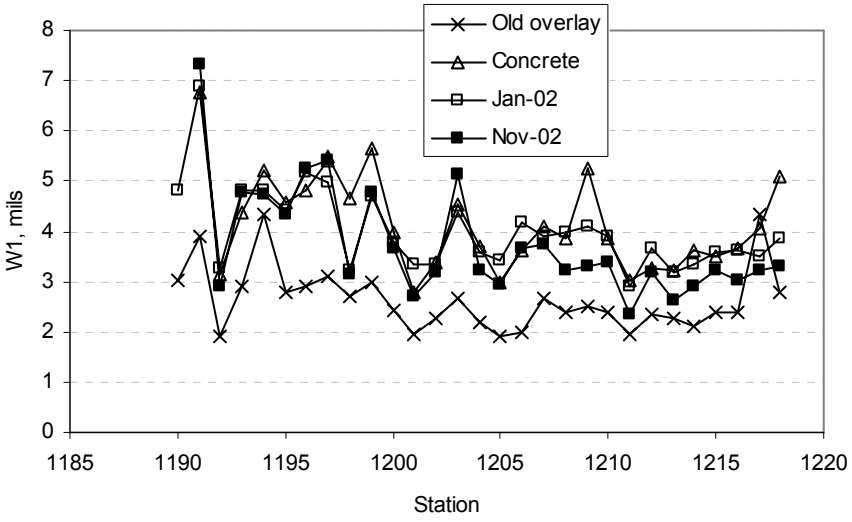

Figure E.33 Section 9 normalized W1 deflections

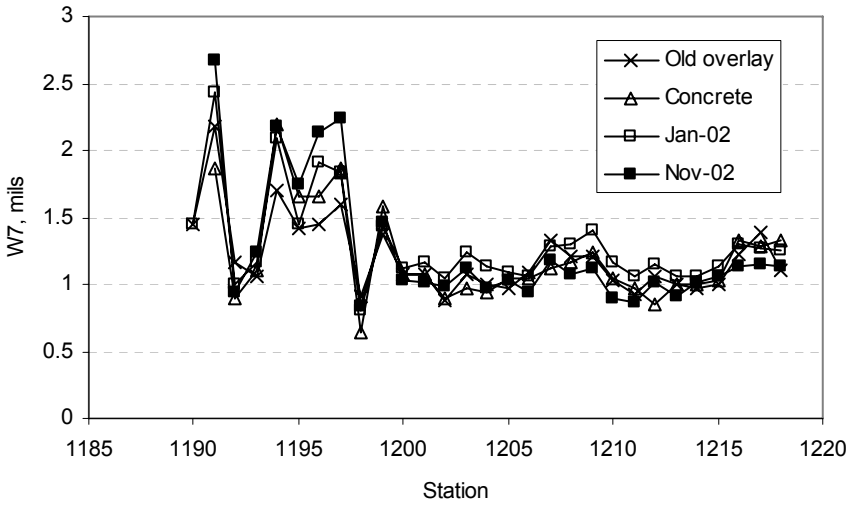

Figure E.34 Section 9 normalized W7 deflections

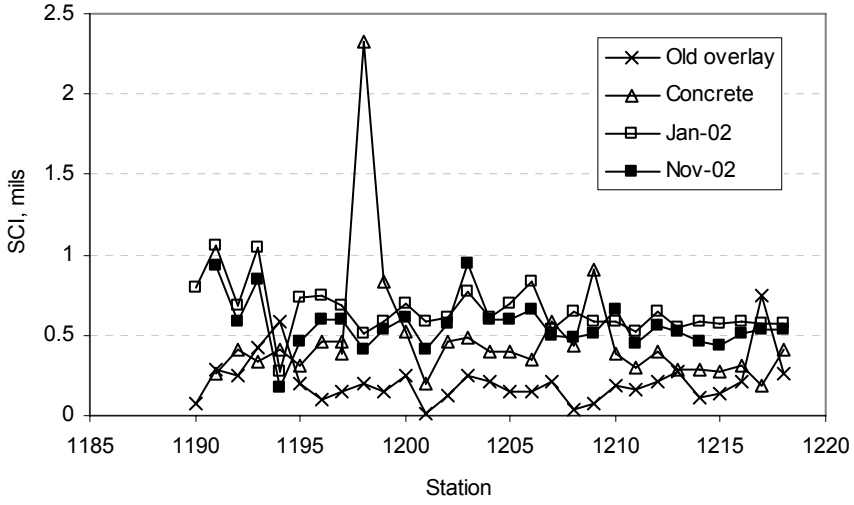

Figure E.35 Section 9 normalized SCI

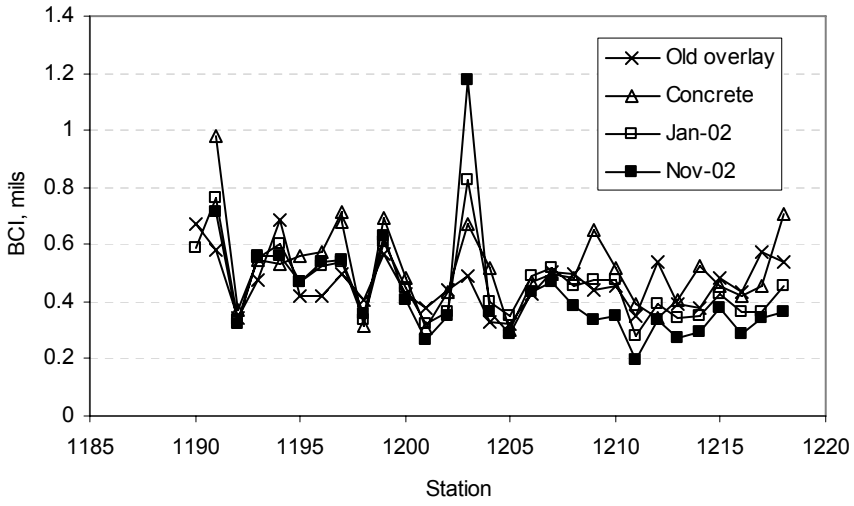

Figure E.36 Section 9 normalized B